Towards a rapid immuno-test for Tuberculosis: Immunochemical characterisation of a suitable mycolic acid antigen preparation.

By

Arthessa Ragavaloo

Submitted in partial fulfilment of the degree: MSc Biochemistry

Department of Biochemistry, Genetics and Microbiology

University of Pretoria

March 2020

UNIVERSITY OF PRETORIA

Declaration of originality

This document must be signed and submitted with every essay, report, project, assignment, dissertation and / or thesis.

Full names of student: Arthessa Ragavaloo

Student number: 10058100

Topic of work: Towards a rapid immuno-test for Tuberculosis: Immunochemical characterisation of a suitable mycolic acid antigen preparation.

Declaration:

1. I understand what plagiarism is and am aware of the University's policy in this regard.
2. I declare that this MSc dissertation is my own original work. Where other people's work has been used (either from a printed source, Internet or any other source), this has been properly acknowledged and referenced in accordance with departmental requirements.
3. I have not used work previously produced by another student or any other person to hand in as my own.
4. I have not allowed, and will not allow, anyone to copy my work with the intention of passing it off as his or her own work.

Signature of student: 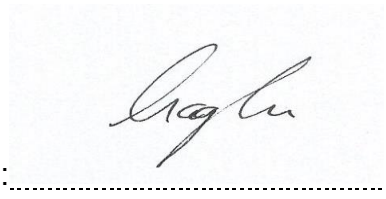

Acknowledgements

I hereby express my deepest gratitude to the following individuals and institutions for their support towards my MSc studies:

- My supervisor, **Prof Jan Verschoor**, for all his guidance, support and invaluable advice. Thank you for your patience and encouragement even when the road got tough. Without your persistent help, this dissertation would not have been possible.

- My co-supervisor at the Council for Scientific and Industrial Research (CSIR), **Dr Yolandy Lemmer**, for her invaluable contribution, guidance, and advice.

- **Mrs Sandra van Wyngaardt**: for her insightful technical assistance and always being there to lend a helping hand in the lab.

- To my colleagues **Ms Mosa Molatseli** for sharing all the trials and tribulations of this research and **Ms Heena Ranchod** for her mentoring and numerous helpful discussions.

- To the **National Research Foundation** for their financial support of this project.

- and finally, my family, friends and my parents, for their love and support.

Summary

Despite the immense amount of research, development, and implementation for new TB diagnostics, diagnosing TB in resource-poor countries remains a challenge, especially in children and people living with HIV. A delayed or missed diagnosis of active infection is one of the major causes of transmission and mortality. Major progress has been made in laboratory-based diagnostics, but point-of-care (POC) diagnostics that are critical in high burdened and resource-limited areas remain elusive. Blood based antibody biomarker tests are superior to sputum-based tests, but are compromised by HIV co-infection, which reduces the ability of the patient to produce antibodies or to contain the pathogen in the lungs. TB patients produce antibodies directed against *M. tuberculosis* mycolic acids (MA), a pathogen-derived lipid. Anti-MA antibodies arise without T cell help and are thereby not affected by HIV co-infection. They can therefore be used as biomarkers for detection of TB in patient sera. The Mycolic acids Antibody Real-Time Inhibition (MARTI) test has the potential to accurately detect patient low affinity anti-MA antibodies as biomarker for active TB. A point of care version of MARTI is envisioned to be a lateral flow immunoassay named Mycolic Acid Lateral-flow Immuno-Assay (MALIA). MALIA makes use of recombinant monoclonal antibodies (gallibodies) that are specific to MA to compete with patient biomarker antibodies for binding to the MAs on a test line to indicate TB. The aim of this study is to demonstrate proof of principle that MALIA is feasible, both in terms of function and affordability.

For affordability, the up scaled counter current distribution (CCD) purification of the most expensive element, MA, was attempted with success. However, quantification of the yield of MA post purification resulted in a 37% loss after acetone precipitation, even though MA has never been shown to be soluble in acetone. The probing of the acetone waste with gallibodies in ELISA confirmed the presence of antigenic MA. An immuno-blot test on silica TLC plates was developed, showing that the MAs lose antigenicity when separated by means of TLC. Whether this was due to separating mycolate from its organic counter-ion was investigated, but gave inconclusive results, but indicated that MA remains in acetone solution for hours after heating to 90 °C and cooling to room temperature The solubility limit of MA in acetone was determined to

be 0.25 mg/ml before falling out of solution after four hours of cooling. The discovery of acetone soluble MA overcomes the challenges of solvent compatibility in automated MA printing for MALIA, while simultaneously enhancing the antigenic conformation of MA on silica. Silica on TLC plate format proved to be a workable and affordable solid phase substrate for lateral flow immunoassay. Proof of principle of a workable and affordable MALIA for POC TB screening was thereby provided.

Table of contents

List of Figures

List of tables

Acronyms and abbreviations

AcF	Acetone filtrate
AIDS	Acquired immune deficiency syndrome
Ala	Alanine
APC	Antigen presenting cells
ATS	American Thoracic Society
BCG	Bacillus Calmette Guérin
BD	Becton, Dickinson and Company
CD4	Cluster of Differentiation 4
CD8	Cluster of differentiation 8
CCD	Counter current distribution
CF	cellulose fibre
CH	constant heavy domain
CH1-4	scaffold containing constant heavy domains 1-4
CH2-4	scaffold containing constant heavy domains 2-4
CLIA	Clinical Laboratory Improvement Amendments
CXR	Chest X-rays
dddH2O	Double distilled de-ionised water
EIS	Electrochemical Impedance Spectroscopy
ELISA	Enzyme-Linked Immunosorbent Assay

EMB	Ethambutol
ESI	electrospray ionisation
EtOH	ethanol
FIA	flow injection analysis
FM	Fluorescence microscopy
H_2SO_4	Sulphuric acid
H_3BO_3	Boric acid
HCW	Health care workers
HDMS	high definition mass spectrometry
HIV	Human Immunodeficiency Virus
HPLC	high performance liquid chromatography
HRP	horseradish peroxidase
ICS	immunochromatographic strip
IgG	Immunoglobulin G
IgM	Immunoglobulin M
IGRAs	T-cell-based interferon-ɣ release assays
INH	Isoniazid
KCl	potassium chloride
kDa	Kilodaltons
KH_2PO_4	di-hydrogen potassium phosphate
kMA	keto-MA
LAM	Lipoarabinomannan
LC	liquid chromatography
LFT	Lateral flow test

LFA	Lateral flow assay
LFIA	Lateral Flow Immunoassay
M. tb	*Mycobacterium tuberculosis*
MTC	*M. tuberculosis complex*
MA `	Mycolic Acid
MALIA	Mycolic Acid Lateral-flow Immuno Assay
MARTI	Mycolic acid Antibody Real-Time Inhibition
MDR	Multidrug resistance
MGIT	Mycobacteria Growth Indicator Tube
mMA	Methoxy-MA
MS	Mass spectrometry
NAAT	Nucleic acid amplification techniques
NaCl	Sodium chloride
Na_2SO_4	Sodium sulfate
$NaHCO_3$	Sodium bicarbonate
Na_2HP0_4,	di-sodium hydrogen phosphate
$Na_2B_4O_7$	Sodium tetraborate
PBS	Phosphate buffered saline
POC	Point-of-care
PZA	Pyrazinamide
OD	Optical density
QTOF	quadrupole-time-of-flight
RF	Retention factor
RIF	Rifampicin

scFvs	Single-chain variable fragments
SPR	Surface plasmon resonance
TB	Tuberculosis
TLC	Thin layer chromatography
TMB	Tetramethyl Benzidine
TST	Tuberculin Skin Test
UPLC	Ultra Performance Liquid Chromatography
WHO	World Health Organization
WMA	World Medical Association
XDR	Extensively drugs resistant
α	Alpha

Chapter 1: Introduction

1.1 Tuberculosis

“Just sleep and eat nutritious foods” (1) a common phrase used by medical practitioners in the 1800s towards patients burdened with Tuberculosis (TB), a disease that is brought about by infection with airborne mycobacteria, usually affecting the lungs. The term ‘’tuberculosis” came from the word “tubercle” used by Franciscus Sylvius to describe the characteristic nodules in lungs of TB patients in 1679 (2). This infectious disease is caused by the *Mycobacterium tuberculosis (M.tb)* species of bacteria and has affected the world for thousands of years (3). *M. tuberculosis* and its closely related mycobacterial species are known as the *M. tuberculosis* complex (MTC). The mycobacteria grouped in the MTC share 99.9% similarity at the nucleotide level and have identical 16S rRNA sequences (4), but differ in terms of their host tropisms, phenotypes, and pathogenicity. Of the MTC, *M. tuberculosis*, *Mycobacterium africanum* and *Mycobacterium canettii* are essentially human pathogens, *Mycobacterium microti* are rodent pathogens, whereas *Mycobacterium bovis* display a wide range of hosts, including humans, bovines and goats (4, 5). Clinically the *M.tb* is recognized for being the main cause of human TB. The infectious origin of TB was first speculated on in 1720 by the English physician Benjamin Marten, in his publication “A new theory of Consumption” (6); however, it was only in 1865 that the infectious nature of TB was demonstrated by the French military physician Jean-Antoine Villemin by inoculating rabbits with TB infected tissue. A milestone in the research towards TB came in 1882 when Robert Koch was able to isolate the tubercle bacillus from TB burdened guinea pigs. This discovery proved that TB is caused by an infection with the tuberculous bacilli that subsequently became known as *M.tb* (6). *M.tb* are defined as rod shaped, nonmotile, nonsporulating, weakly gram-positive, acid-fast bacilli. The waxy cell wall confers acid-fastness, extreme hydrophobicity, resistance to drying, acidity/alkalinity and many antibiotics, as well as distinctive immunostimulatory properties (7,8).

1.2 Pathogenesis of tuberculosis

M. tuberculosis enters the body by inhalation of bacilli that are released into the air in the form of droplets when someone with infectious TB coughs or sneezes (9)(10). The pathogen then enters the host respiratory pathway and invades the lungs. The infection begins when the bacteria are taken up by alveolar macrophages, which cause an inflammatory response. An innate host immune response recruits inflammatory cells to the lung as the initial stage of immune protection (11)(12) after spreading of *M. tuberculosis* to draining lymph nodes. In the lymph node, presentation of bacterial antigens by dendritic cells prepares antigen-specific T cells, which differentiate from naïve into effector T cells. The effector T cells migrate to the infected lung and, in combination with other leukocytes and B cells, stimulate the formation of granulomas around the sites of infection (11). The infected area now contains macrophages and lymphocytes, which together form the granuloma. The granulomas isolate the infection and hinder the pathogen's continued proliferation and spreading to the rest of the lung and other organs (13). The spread of infection occurs when the centre of the granuloma undergoes caseation and releases infectious bacilli into the airways. The spread of infection is due to a change in the immune status of the host, which is usually a consequence of old age, malnutrition, or HIV-co-infection (13). This leads to development of a persistent cough that facilitates the aerosol spread of the infectious bacilli, infecting any individual exposed to the aerosol. Therefore, due to an effective immune system response, an infected host might not become ill when the bacilli remain in the granuloma and the immune response controls and forces the infectious bacilli into an inactive state. This is referred to as a latent infection. When the infection cannot be contained at the site of first entry, the host might end up developing disease, which is referred to as active TB.

Approximately 10% of all infected people will develop active TB (14). Every year this percentage increases by 10% in immuno-compromised individuals, including more frequently those who are human immunodeficiency virus (HIV) positive (14). There are several exogenous factors influencing the rate of *M.tb* infection converting to active TB after exposure. These mainly include behavioural risk factors such as smoking, alcohol abuse, poor ventilation, and overcrowding of living space. Endogenous risk factors also affect the rate of the progression of TB from infection to active disease. These include circumstances that alter the immune response (Fig. 1). People from low

socioeconomic-status populations are also known to be of high risk of becoming infected and progressing towards active TB.

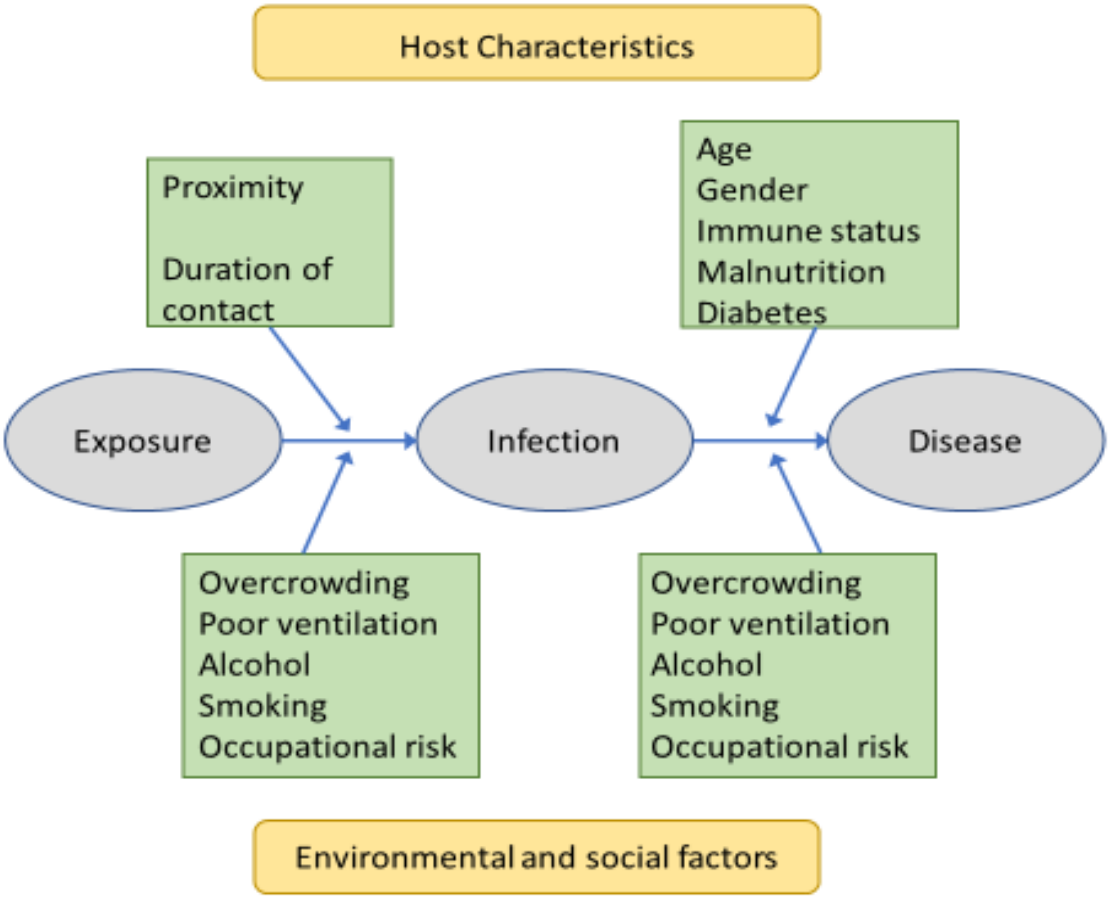

Figure 1: The risk factors for TB infection and disease **(15).**

1.3 Current Tuberculosis dilemma

The second deadliest infectious disease in humans, following HIV/AIDS is TB (16). It is a major health problem worldwide. The rise in the number of incidences is mainly due to emerging anti-TB drug resistance, but also by co-infection with HIV. The World Health Organisation (WHO) estimates that in 2017 there were 10 million new TB cases: 5.8 million among men, 3.2 million among women and 1.0 million among children. There were also 1.6 million TB deaths (approximately 1.3 million among HIV-negative people and 0.3 million among HIV-positive people) (17). Figure 2 illustrates the incidence rate of the people infected with TB worldwide in 2017. The number of

TB deaths is unacceptably high, especially in the southern African region, where it is enhanced by HIV co-infection. Of the overall TB cases in 2017, 9% were among people co-infected with HIV, where the highest proportion is in the WHO African Region, exceeding 50% in parts of southern Africa (17). The risk of developing TB in the population living with HIV is 20 times higher than the risk in the rest of the world population (17).

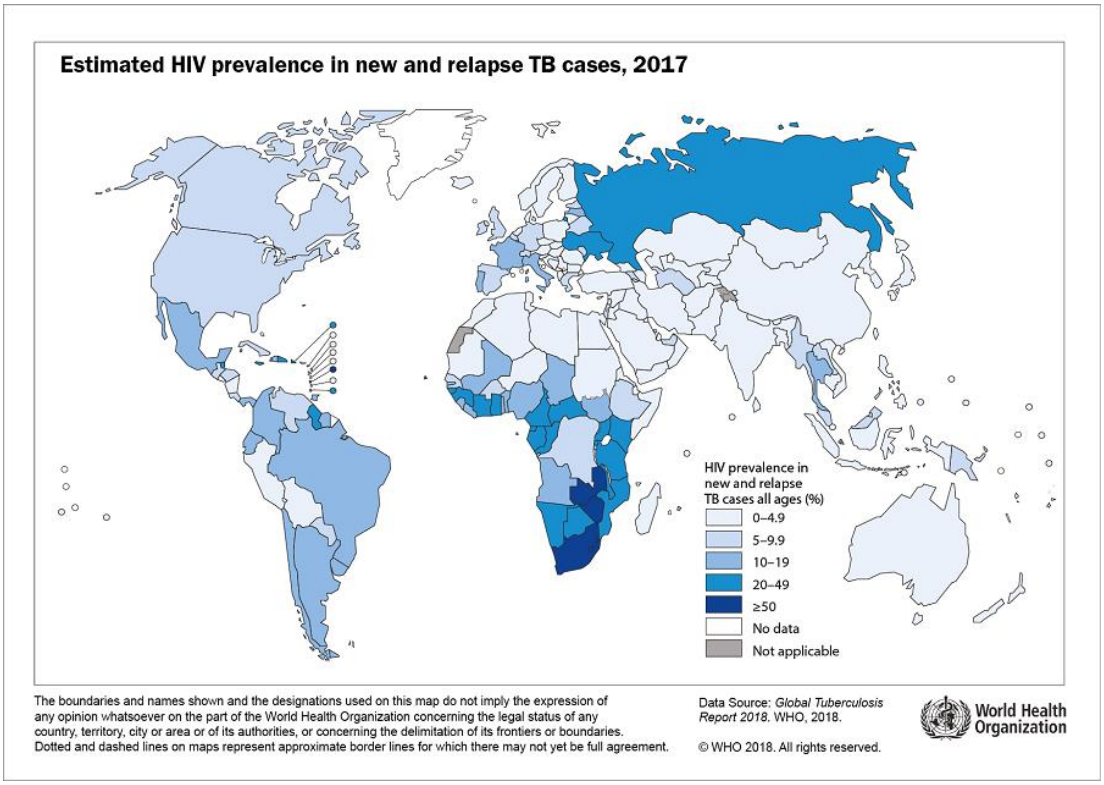

Figure 2: **World Health Organisation map of TB incidence by country, 2017** (17).

1.4 Socio-Economic burden of TB in South Africa

South Africa has one of the highest burdens of TB in the world, where transmission is favoured by the escalating poverty conditions. TB transmission occurs in households, public transport vehicles, mines and congregate community settings, such as prisons, schools and community halls where people are in close contact (18). People living with HIV, unvaccinated children and the elderly are considered high risk individuals. Poverty leads to a greater risk of TB infection by malnutrition and poor healthcare (19). Once infected, a patient's physical strength and ability to work is reduced ultimately worsening poverty due to the loss of income (20). A priority for the management of the TB epidemic is to ultimately reduce the impact of the cost of illness (20).

Due to a combination of economic decline, insufficient application of infection control measures and the HIV epidemic, TB incidence is on the rise, prevalence is high and remission very slow. The high prevalence of HIV infection has played a central role in increasing and maintaining the high burden of TB in South Africa. The HIV epidemic has impacted greatly on TB in South African health care workers (HCW). Up to 20% of HCW are living with HIV (21,22,23) and are five times more at risk of developing TB in the work place than HIV-negative HCWs (24,25). Nosocomial transmission or hospital acquired infection occurring from patient to HCW is normally due to inadequate infection control measures in clinics and hospitals. The province of KwaZulu-Natal in South Africa has one of the highest prevalence's of TB patients co-infected with HIV. A report from a study conducted in hospitals in KwaZulu-Natal indicated that one in five in-patients had active TB (25, 26). These results raise concerns about nosocomial transmission to healthy HCW and patients and should be of particular concern of the management and control TB epidemic.

To disrupt the ongoing cycle of TB transmission, its early detection, treatment and control must be implemented to reduce the duration of infectiousness and prevent transmission of new infections.

1.5 TB Control

Disrupting the chain of transmission is the fundamental objective of TB control. This can be achieved by prevention, detection and treating. Current health interventions for TB prevention strategies involve vaccination against TB, screening of high-risk groups, treatment of active or latent infection and prevention of transmission into communities and healthcare facilities (27).

The only WHO approved vaccine against TB is the Bacillus Calmette-Guerin (BCG) vaccine developed by Calmette and Guerin in the 1920's and is currently used to vaccinate neonates and infants. While the effectiveness of BCG against *M.tb* infection is > 80% in children it only protects against severe forms of paediatric TB and does not offer protection in adolescents and adults (28).

TB infection prevention and control is one of the components of the *End TB Strategy* (29). Effective TB control strategies also involve implementation of infection control measures in healthcare facilities and in other community structures (e.g. schools,

places of worship, congregate setting) involving administrative, environmental and personal infection protection. This policy emphasizes the need to reduce diagnostic delays and start treatment as quickly as possible. The WHO F-A-S-T strategy refocuses efforts on Finding cases Actively, and Separation until effective Treatment is started (29). FAST aims to shorten the time between transmission and treatment. Mapping of high-risk groups and carefully planning systematic screening, within or outside health services, can help improve early TB detection.

1.6 TB Treatment

TB treatment is aimed at curing and reducing transmission and can be characterised by three fundamental objectives: (1) reduction of the number of TB bacilli rapidly in order to reduce morbidity and disrupt transmission (2) to prevent worsening of resistant TB and the development of resistant strains; and (3) to prevent relapses after completing treatment (30,31).

TB treatment is further characterized in 2 phases, an initial intensive phase and a continuation phase. The initial intensive phase is intended to fulfill objectives 1 and 2 (31). In order to rapidly reduce bacilli reproduction multiple drugs are used in combination. This is due to the spontaneous mutations creating resistance against a single anti-tuberculosis drug. There are four first line drugs available for initial treatment of TB, i.e. Isoniazid (INH), Rifampicin (RIF), Pyrazinamide (PZA), and Ethambutol (EMB) (31) and thereafter RIF and INH for continuous phase treatment. Objective 3 should be achieved by prolonging treatment over time and using drugs with a sterilising effect that are capable of eliminating persistent bacilli, which seem to restrict their metabolic activity and which cause the relapses that occur following anti-tuberculosis treatment (31).

Patients with high risk of having TB should receive anti-tuberculosis treatment as soon as possible. Premature interruption of treatment, incorrect use of the drugs or inaccurate diagnosis can lead to drug resistant forms of TB. Drug resistance can extend to multidrug resistance (MDR) and extensively drug resistant (XDR). MDR-TB can be defined as TB resistant to INH and RIF. XDR-TB occurs when the bacteria develop resistance against all four of the available drugs, but also to at least one fluoroquinolone as well as an aminoglycoside (amikacin, kanamycin) or capreomycin

(31). Solutions to control drug-resistant TB are to cure the patient without disruption to the drug regimen, provide access to diagnosis, ensure adequate infection control in facilities where patients are treated and to ensure proper use of the drugs.

1.7 TB diagnostics

Due to the process by which latent TB becomes active, the highest priority should be to diagnose sick patients with active TB as early as possible, before irreversible damage is done to the lungs (32). Early diagnosis of TB would not only limit the spread of the disease, but also lead to a more successful treatment of patients.

An ideal test should have high sensitivity and specificity. Sensitivity is the ability of a diagnostic test to accurately identify the condition it is attempting to diagnose, in this case TB. The lower the sensitivity of the test the greater the chances that TB infected individuals will not be accurately identified by the test; this can lead to false negative results (in which TB is present but not detected). Specificity is the ability of a test to accurately rule out the condition the test is seeking to diagnose (33). The lower the specificity the greater the chances that people without a condition will be falsely diagnosed as having it (the test will detect TB, but is not present). Therefore, low specificity will lead to a greater number of false positive results (33). Accuracy of a diagnostic is important when identifying TB. Some tests have low accuracy, either as a result of low sensitivity (high false negative results) or low specificity (high false positive results).

1.7.1 Diagnosis of latent TB

A method that can sensitively detect when latent TB becomes active is dearly needed for screening people at high risk of exposure to TB infections. This includes HCW exposed to TB patients and individuals infected with HIV (34). A quarter of the world's population is estimated to be latently infected with TB. The standard screening test is the tuberculin skin test (TST). The TST is performed by injecting a small amount of TB purified protein derivative into the skin in the lower part of the arm. If the skin area reacts to the antigen within 48-72hours it is considered a positive reaction (35). TST, however, has certain limitations. BCG anti-TB vaccination leads to cross-reactivity and false-positive test results. TST gives false negatives when performed in immuno-compromised individuals. TST is not specific enough because the test cannot

distinguish between the different species of pathogenic mycobacteria that are the cause of infection nor can it distinguish between latent and active TB, or even just an excessive exposure to the TB pathogen as happens with clinical staff attending to patients at a TB hospital or clinic. Due to these draw-backs alternative screening methods involving interferon-gamma release assays [IGRA] are being used, but they have their own limitations. The major advantages of IGRAs are that they do not compromise the person undergoing the test with TB antigens. They can therefore be done repeatedly as a continuous screening method on the same patient. In addition, they are not influenced by prior BCG vaccination, as the antigens for use in IGRA exclude those used in vaccination (33). None of the screening tests mentioned can distinguish active TB from latent TB

1.7.2 Diagnosis of active TB

The best affordable diagnosis of active TB is done with clinical and microscopic examination, involving sputum smears (35). The most widely used TB diagnostic test is smear microscopy. It involves the examination of stained sputum. An observation is then made on the acid-fast stained bacteria that were obtained from the medium under a microscope to identify *M. tuberculosis*. However, it is a tedious test with moderate sensitivity (33). The sensitivity decreases with diagnosis in children, and individuals co-infected with HIV (37). The sensitivity of the test was improved by fluorescence microscopy (37). An acid-fast fluorochrome dye with an intense light is used. Fluorescence microscopy (FM) has been shown to have 10% more sensitivity than conventional microscopy, but conventional microscopy is preferred, because it is inexpensive when compared to FM (37, 38, 39).

Culture of *M. tuberculosis* is a well-known gold standard method because it is the most sensitive bacteriological method available (40). The major drawback is the slow growth of the bacillus, so there is a delay of up to six weeks for obtaining results. In addition, extrapulmonary TB does not get ruled out by a negative culture. The method is also tedious and requires specialised laboratory infrastructure and equipment. To solve this time delay and limit technician contact time, automated systems such as the BACTEC™ 460 TB and Mycobacteria Growth Indicator Tube (MGIT™) 960 system have been developed (41). One of the disadvantages of the BACTEC 460 TB System is the use of ^{14}C-Labeled radioactive substrate (41). Because of the strict regulations of handling and waste disposal of radioactive material, it became necessary to develop

a non-radiometric technique for mycobacterial culture and susceptibility testing. Becton, Dickinson and Company (BD) developed a new system called MGIT™, which is non-radiometric and offers the same rapid, sensitive and reliable methods of testing as the BACTEC 460 TB System (41). The system contains a liquid culture medium (modified Middlebrook 7H9 broth), a growth supplement and a number of antimicrobials to prevent growth of contaminants (41). The culture is monitored for 60 minutes, thereby providing a short laboratory turnaround time when compared with conventional methods (41,42,43,44). However, a drawback to this system of mycobacterial growth in liquid culture is that contamination from other bacteria commonly present in patient samples can go undetected (45,46), thereby producing false positive results.

M.tb detection by nucleic acid amplification techniques (NAAT) eliminates the limitations of culture and microscopic methods. The WHO recently recommended GeneXpert as an initial diagnosis test for patients suspected to have HIV/TB co-infection and has also claimed it to be effective for diagnosing TB in children and adults (47). However, because it is sputum based, it cannot be very good in diagnosing children as children are seldom able to produce sputum of adequate quality (48). In children sensitivity is lower at between 65% and 76%, with specificity between 99% and 100%. There is also contradicting evidence on the sensitivity of GeneXpert of adults with extrapulmonary and sputum-scarce pulmonary TB, suggesting limited sensitivity in the context of less extensive disease or the non-respiratory samples used (25,49,50). Another drawback of GeneXpert machine is that it is electricity dependent requiring uninterruptable electricity as well as an air-conditioned laboratory facility, skilled technicians and regular maintenance (29).

Other commonly used diagnostic tests include chest X-rays (CXR). In patients with active pulmonary TB, lesions are often present in the lungs and are visible in CXR. Given its high sensitivity however, it is still a good method for ruling out TB, but not in diagnosing an active infection, as it cannot distinguish between lesions of active TB or from previous TB infections. An immuno-compromised person with a high risk of TB, such as a HIV-positive individual or, to a lesser extent, a person with diabetes, often shows atypical or abnormal manifestations in a CXR (51). Studies have shown that CXR is not specific and can misdiagnose TB as many other lung diseases have similar radiographic patterns to TB (52,53).

Many patients are being misdiagnosed mainly because of HIV co-infection, which is progressively in the increase. This makes diagnosis more difficult. These patients have a low $CD4^+$ T cell counts that correlate with inadequate quality of sputum samples, often leading to a false-negative result. Immune T cells with the CD4 marker play a crucial role in the ability to form granulomas. When these are impaired, diagnosis by X-ray chest radiographs become inaccurate (30,32). Many diagnostic tests that are based on the host response to *M.tb* infection, such as IGRA and TST, depend on active $CD4^+$ T cells and are impaired in patients with advanced immune suppression (16). Newer diagnostic techniques have been investigated in an attempt to overcome this inherent deficiency in the current state of the art of diagnosis of TB (54, 55).

1.8 Laboratory free TB diagnostic testing

Due to the absence of an effective vaccine, the control of TB still requires rapid diagnosis to reduce ongoing transmission (56). HIV diagnosis has paved the way for rapid diagnosis by the development of point-of-care (POC) or lab-free diagnostics suitable for field use, however the diagnosis of TB remains a challenge in resource-poor settings (57). Due to the limitation of the current diagnostics many individuals with active disease are misdiagnosed and fail to receive proper treatment leading to an increase in on-going disease transmission to family and community members. Improved POC diagnostics need to be developed to face these challenges.

It is estimated that 60 % of those who require assessment for TB do so in local/community health facilities, where sophisticated TB diagnostics is not available (Fig 3) (58). TB control programmes require a tiered network of laboratories in which different tiers use complementary diagnostic tools. Establishing, equipping and maintaining a laboratory network to ensure that there is timely access to quality-assured diagnostics is challenging, complex and expensive, especially in resource-limited or high-burden settings (58). As networks of TB laboratories develop and gain capacity, the need for human resources increases. Each laboratory will require trained and competent staff to perform the various diagnostic tests. Higher levels of skill and training are needed to perform advanced testing for drug resistance. More support staff are also required to assist with non-testing activities such as media and reagent

preparation, housekeeping and maintenance, waste management, data management, quality management, quality assurance activities and various administrative work (58).

Although laboratory TB diagnostics are available, the centre for continuous care may be some distance from the patient's home. Loss to follow-up or defaulting from care is a major problem in healthcare delivery in resource-limited settings (59, 60, 61). The ideal TB diagnostic is therefore a point-of-care test that allows patients to be diagnosed and receive appropriate care within hours of undergoing TB testing (62, 63). It is likely that POC formats will significantly reduce the loss to follow-up, but there are limited data available on the potential health impact of POC tests in resource-limited settings (64, 65).

The success of the TB diagnostic network depends on whether the general health system and diagnostic services work on functionality and efficiency. As diagnostic technologies have different infrastructure and biosafety requirements, only certain tests, seen in figure 3, can be positioned within the peripheral health-care services. Microscopy and Xpert MTB/RIF is primarily used. There are currently no POC TB diagnostic tests that are independently suitable for use in rural areas. New tests must be POC with rapid results available to both patient and HCWs.

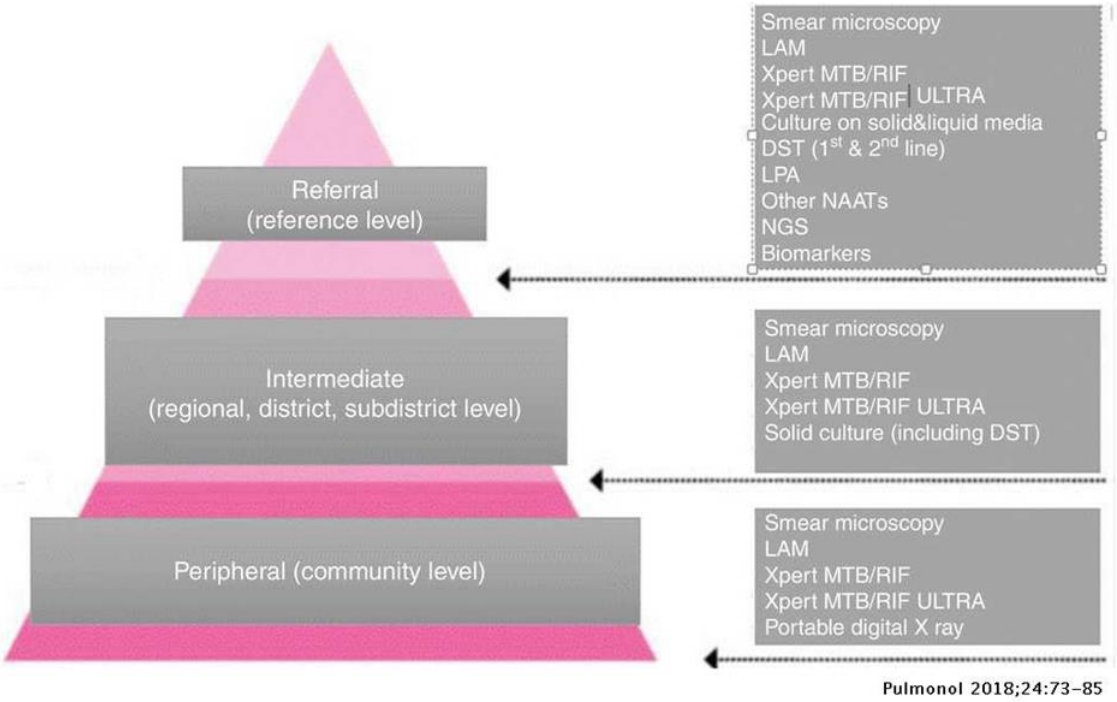

Figure 3: The three tiers of the network of TB laboratories: a representation of facilities where diagnostics may be implemented **(58).**

"Without diagnostics, medicine is blind." (66). Proper treatment to illnesses cannot be made without diagnosis. Sensitive, specific and rapid diagnostic testing not only paves the way toward effective treatment but also plays a critical role in preventing the transmission of infectious diseases.

1.9 Towards the development of a POC TB diagnostic

Despite existing technologies and advances over the last few decades, development of a simple and rapid POC test is still challenging in the current pipeline of tuberculosis diagnostics (67,68). In addition, novel diagnostic tools and reliable biomarkers are required to provide better performance in diagnosing TB.

Blood is an attractive sampling option for the detection of TB, especially in HIV-infected patients. Blood is easier and more reliable to sample than sputum because the invasiveness of sampling is neglectable (just a finger prick of blood). Sputum sampling is also inadequate to diagnose extrapulmonary TB, TB in children and TB in HIV-co-infected individuals. Blood sampling should be better able to overcome these limitations. Many serological tests have been proposed in the past for TB diagnosis. Serological tests include Enzyme linked immunosorbent assay (ELISA) or lateral flow

immunoassays (LFIA) to detect the humoral antibody response to *M.tb* antigens by measurement of antigen-antibody interactions (70). Serological tests have the potential to be suitable and improve diagnosis in resource-limited areas (69), because they are simple and offer the potential of low cost, rapid diagnoses with minimal training requirements (71, 72).

Antibodies or immunoglobulins are proteins produced by the B cells that defend a host against foreign agents such as viruses and bacteria (73). Antibody-based immunoassays are commonly used in diagnostics (74). They are based on the avidity and specificity of antibodies to bind and recognize the antigens. IgG is the major blood antibody of the secondary immune response associated with prolonged immunity whereas IgM is the predominant early blood antibody seen in the immune response to infectious diseases (70), but usually with short-lived memory. Immunodiagnostic assays based on detection of patient IgM and IgG against pathogen related antigens in patient sera with active TB disease is an attractive approach for rapid POC diagnosis or screening.

Studies towards the identification of new biomarkers for TB diagnosis have increased in the recent years (75). A good antibody biomarker should be highly specific to a disease, easily detectable by standard antibody detection methods and have the ability to distinguish between latent and active stages of *M. tuberculosis* infection (76). The early detection of TB is another important aim in biomarker research, as well as those that indicate risk of contracting or relapsing to active TB (77). As indicators of disease, antibodies are well suited for use in diagnostics because of their renowned properties of sensitivity and specificity. The advantage of detecting antibodies, rather than pathogens and their traces, is that antibodies are freely available in serum, whereas microorganisms can evade detection by shielding themselves within native cells in different organs of the body (78).

Previous work in our group suggests that antibodies to the *M.tb* antigen mycolic acid (MA), the unique lipid antigens of mycobacteria, could serve as an ideal biomarker for active TB diagnosis. This is because these antibodies are produced independent of T-helper cells and so are unaffected by HIV co-infection (79). Furthermore, work by Ndlandla (25) using a guinea pig TB infection model indicated that anti-MA antibodies are produced early upon infection, are short lived and will therefore diagnose active

TB independent of previous vaccination and even under the condition of HIV co-infection.

Human patient anti-MA antibodies have been considered before as a biomarker for active TB diagnosis with the potential of being detectable by means that are appropriate for POC TB testing. This idea was explored by Schleicher *et al.* (79), using an ELISA assay and MA as antigen to detect anti-MA antibodies found in patient sera (80). The results showed that there was a larger amount of anti-mycolic acid antibodies present in TB positive patients compared to TB negative. Due to this result, further experiments are being conducted to produce a diagnostic test that uses mycolic acid antigen and anti-mycolic acid antibodies to detect active TB (81). The Mycolic acid Antibody Real Time Inhibition (MARTI) assay was developed from this concept (81). MARTI makes use of immobilised liposomes (carrying MAs) on sensor surfaces to monitor the binding of anti-mycolic acid antibodies (80). The use of biosensor-based technology for TB diagnosis has been demonstrated well in wave guide (81) and SPR (82) evanescent field biosensors, while proof of principle has also been demonstrated in electro-impedance immunodetection (EIS) (83). The proposed MARTI test showed positive results for detection of TB using this principle. However, it was shown that the biosensor technique is very difficult and expensive to perform in the laboratory and that the above mentioned technologies are still too advanced to be used in a POC setting for screening large numbers of patients' sera. This led our group to expand the research into developing a new lateral flow diagnostic test for POC TB diagnosis. The test, to be called the Mycolic Acid Lateral-flow Immunoassay (MALIA) test, was developed from the MARTI test concept (84). MAs are used in the test to indicate the presence of active TB in a patient with the aid of monoclonal chicken antibodies (gallibodies) that are mono-specific to MA. These antibodies are used to compete with patient sample biomarker antibodies for binding to the MAs on a test line to indicate TB.

The work on this project began with Beukes *et al*. (85) who were able to successfully pan for MA-specific antibodies from a recombinant chicken antibody gene library. While the team could successfully isolate both cholesterol cross-reactive and non-cross-reactive anti-MA phage antibodies, their stability could not be retained over time. Ndlandla (25) was then able to select a new set of anti-MA phage antibodies, using a similar approach, by selecting for thermally stable scFvs. These scFvs were

recombinantly converted to IgY chicken antibodies (gallibodies) by Ranchod (86). These custom developed gallibodies were used for the development of the proposed MALIA test in this MSc study. MALIA, will serve as a negative predictor test (to exclude the possibility of active TB) and will take the form of a lateral flow immunoassay.

1.10 Problem statement

Many TB diagnostic tests used today are good but have limitations due to their poor sensitivity (especially in children or HIV infected patients), and inability to distinguish between latent and active TB. New methods are therefore being explored, which will have the potential to detect TB, even in HIV burdened populations. TB patients produce antibodies directed against *M.tb* mycolic acids (MA), a pathogen-derived lipid. Anti-MA antibodies can therefore be used as biomarkers for detection of active TB using patient serum samples. The Mycolic acids Antibody Real-Time Inhibition (MARTI) test has the potential to accurately detect patient low affinity anti-MA antibodies as biomarker for active TB. Although this method has been successful, the biosensor equipment requires highly-skilled staff for operation and costs of the unit are relatively high; thereby making this system not feasible for POC diagnosis. A new device needs to be developed that employs the use of MA and anti-mycolic acid antibodies in a simple process that can be used with minimal effort in a point of care (POC) environment. A POC version of MARTI can be a lateral flow immunoassay format test named “Mycolic Acid Lateral-flow Immuno-Assay” (MALIA). MALIA makes use of monoclonal chicken antibodies (gallibodies) that are mono-specific to MA. These antibodies are used to compete with patient sample biomarker antibodies for binding to the MAs on a test line to indicate TB. The problem is that a lateral flow test for anti-MA antibody biomarker detection cannot be done by means of the standard approach used for protein antigens to detect high avidity binding patient antibodies. Initial attempts at MALIA were challenged by the limited solubility of MA in lateral flow compatible solvents. In addition, it may be necessary to enhance the avidity of monoclonal antibodies to MA. This project explores the scope for a workable model of MALIA.

1.11 Hypothesis

Recombinant, monoclonal anti-MA gallibodies can be applied in a lateral flow immunoassay as a basis for the development of a MALIA point of care TB diagnostic.

1.12 Aims

1. Upscale purification of MAs from crude extracts of M. tb strain H37Rv by means of countercurrent distribution (CCD).
2. Application of monoclonal anti-MA gallibodies for:
    I. Monitoring the presence of MA in all fractions during purification.
    II. Characterising the antigenicity of MA in various fractions by immuno-blot test and TLC.
    III. Characterising the solubility of MA in different solvents.
    IV. Characterising the antigenicity of immobilised MA in MALIA

1.13 Chapter summary

The work done on this project has been described in three chapters with a concluding discussion.

Chapter 2 will introduce Mycolic acids as an antigen and the isolation and purification thereof (Aim 1&2-i).

Chapter 3 will introduce monoclonal antibody detection of Mycolic acids in various formats i.e. ELISA and blot tests (Aim 2-ii & -iii).

Chapter 4 will introduce Lateral flow test (LFT) in the form of a MALIA test for the diagnosis of TB and further describe a new principal in a lateral flow assay format (Aim 2-iv).

Chapter 5 will be a concluding discussion of the overall findings of this work.

Chapter 2: Improved Mycolic acid purification with CCD

2.1 Introduction

A dominant feature of *M.tb* and other pathogenic mycobacteria is the cell wall envelope, specifically in respect of its structure of lipids and sugars (87). The physiochemical properties of the cell surface contribute to the intracellular survival of *M. tb*, as with the other pathogenic mycobacteria (88). Figure 4 depicts a simple visual representation of the *M.tb* cell wall built upon a layer of peptidoglycan and arabinogalactan surrounding the cell's basic lipid bilayer. *M. tb* is unique among bacterial pathogens in that it displays a wide array of complex lipids and lipoglycans on its cell surface (88, 89). Cell envelope lipids constitute 40-60% of weight of mycobacteria. It was found by Goren and Minnikin (90, 91) that long fatty acids of mycobacteria include tuberculostearic, mycoserosic, phtheinoic and mycolic acids (MA) (92). MA is found in all the species of mycobacteria. It comprises a number of different high molecular weight α-alkyl, β-hydroxy fatty acids that can have up to 60–90 carbons (93, 94). Studies have shown that the cell wall MAs contribute to the virulence of *M.tb* (95), including a role in regulating the complex process of immunological response/s of the human body to the infection with *M. tuberculosis* (96). It has become apparent in recent years that MA is secreted in free-form during the course of mycobacterial infection (97,98).

The work described in this chapter will introduce *M.tb* mycolic acids as an antigen and the isolation and upscaled purification thereof for further use in this study.

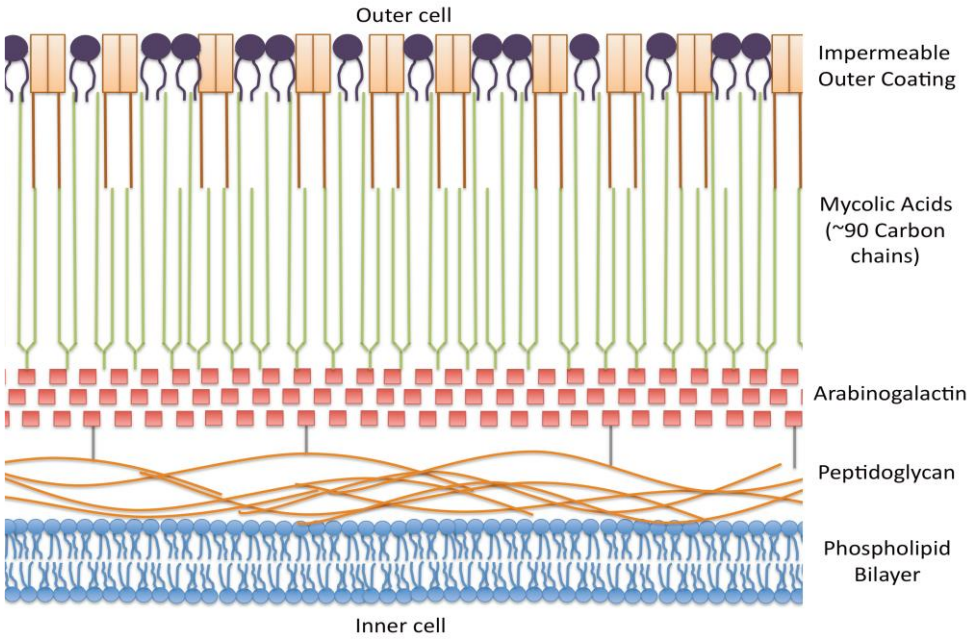

Figure 4: Basic structure *of M. tuberculosis* cell wall. The cell wall of *M.tb* is comprised of four layers; an outer layer of mycolic acids surrounded by inner layers of arabinogalactin and peptidoglycan. These surround the phospholipid bilayer of the cell (89).

2.1.1 Serodiagnosis of TB

Cell-mediated immunity is essential for control of *M. tuberculosis* infection. Activation of both CD4+ and CD8+ T cells is seen in active TB in humans (99). CD4+ T lymphocytes of T helper cell type 1 are thought to be most critical (100). Protein antigens recognized by the T cell receptors are presented on major histocompatibility complex proteins. CD4 T cells function in facilitating cellular and humoral immunity, while CD8 T cells function in killing target cells. The CD4 and CD8 responder T cells are responsible for cell mediated immunity that plays a critical role for TB protection. However, CD4 T cells are gradually destroyed during HIV infection, leading to corruption of T-cell control and altered activity of cytolytic CD8+ T cells. Therefore, TB co-infection with HIV may impair both the cellular and antibody response to protein antigens (70).

Arloing, 1898 described the first serodiagnostic test for tuberculosis (TB), which used hemagglutination (101). However, its sensitivity and specificity were not accepted in the diagnostic field of tuberculosis. In 1972, Engvall and Perlmann (102) described a

simple, highly sensitive, reproducible, and inexpensive technique using an enzyme-linked immunosorbent assay (ELISA). Many antigenic materials have been subsequently employed in the ELISA method in an attempt to improve both the sensitivity and specificity. Various antigens of mycobacteria have been applied in antibody-based serodiagnosis of TB, by using either protein or lipid antigens. A large number of native and recombinant antigens of *M. tb* such as purified protein derivative (103, 104), *Mycobacterium* glycolipids and 38 kDa antigen have been assessed, contributing substantially to the progress for the serodiagnosis of TB (105). The overall sensitivity of these methods ranges from 45 to 95%, and their specificity ranges from 90 to 100% (91).

2.1.2 Antigens used for biomarker antibody detection

Proteins of *M.tb* are not good antigens for TB biomarker antibodies, as antibody production to these antigens are paralysed by HIV co-infection, giving rise to false-negative results in this important cohort of people at risk of contracting TB. An alternative is the glycolipid, lipoarabinomannan (LAM). LAM is a cell wall component of mycobacteria and is detectable in the urine of patients with active TB infection. Purified LAM from *M.tb* was first used for serodiagnosis of leprosy (106, 107), however it was only evaluated as a potentially useful antigen for the serodiagnosis of tuberculosis in 1990 (108). The MycoDot assay is a commercially available rapid assay specific for TB, which detects anti-mycobacterial antibodies to the LAM antigen (109). Several researchers evaluated the assay and achieved a high degree of specificity (84–100%) but a low sensitivity (16–56%) (110-114). A low degree of sensitivity was mostly seen in patients infected with HIV (70, 112, 114). A low degree of sensitivity does not support its use in the diagnosis of TB, especially in HIV-infected patients (109). Other lipid antigens were explored such as 2, 3, 6-triacyl trehalose (TAT) by an ELISA assay and whole glycolipid (carbohydrate-attached lipids) antigens by a liposome agglutination assay. Results reported a sensitivity and specificity for TAT at 76% and 96% respectively (115,116) and whole glycolipids at an overall sensitivity and specificity of 94% and 98.3%, respectively (117,118). These results however have not been validated for implementation and comparison between different antigens can be difficult since the patient populations as well as diagnostic methods employed in studies differed significantly (89)

2.1.3 Mycolic acids

Mycolic acid (MA) is a unique pathogen-derived lipid, which is known to act as a fingerprint molecule for the particular mycobacterial species that infects (55). The name “Mycolic acid” was first proposed by Stodola *et al.* who described it as wax fractions containing active hydroxy acids of high molecular weight of tubercle bacillus and acid-fast bacteria (118). From that point onwards the structure of these lipids became of interest to researchers. Mycolic acids and their homologs are long chain β-hydroxyl, α-branched fatty acids found mainly in the genera *Mycobacterium*, *Nocardia*, *Rhodococcus*, and *Corynebacterium* (119). MA was first isolated by Anderson in 1938 and thereafter structural studies were performed by Asselineau in 1950 (120). Since then a number of MAs have been isolated and characterized. They have shown to have the basic structure of $R^2CH(OH)CHR^1COOH$, where R^1 is a C_{20} to C_{24} linear alkane branch and R^2 an alkyl chain C30-C60 containing various functional groups such as carbon-carbon double bonds and/or cyclopropane rings, methyl branches and oxygenated ketones, methoxies or hydroxyls (96,121).

MA are present in many forms and are secreted as free MAs or bound to sugar molecules on the cell wall such as penta-arabinose tetramycolates, or as extractable esters with trehalose, glucose or glycerol (122). Three main *M.tb* MA classes exist (Fig 5). These three classes are differentiated by the presence of different chemical functional groups on the main hydrophobic chain of MA, called the mero-chain (123). The most abundant are unoxygenated α-MA (αMA), the less abundant oxygenated methoxy-MA (mMA) and the least abundant keto-MA (kMA) (124). These classes of MA also differ in orientation on the main hydrophobic chain of MA: αMA contains cyclopropanes in mainly a *cis* configuration and is found in greatest abundance, whereas mMA and kMA contain cyclopropanes in either a *cis*- or *trans*-configuration (125, 126). Of total MA, around 50% is αMA, while the amount of the oxygenated MAs varies with methoxy at 32–40% and keto at 7–15%, depending on the growth stage of the bacilli (127).

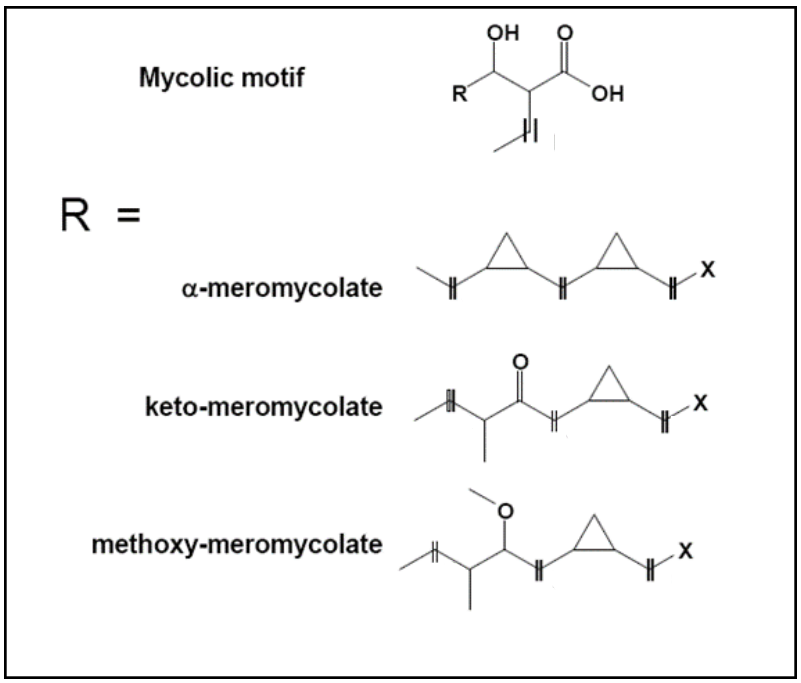

Figure 5: Graphical representation of the structures of mycolic acids and subclasses found in *M. tb*. X represents the mycolic acid motif (140).

The various structures of MA have been shown to play a major role in the virulence of the pathogen as well as having interesting biological activities, such as cholesteroid like properties (124). These MAs elicit an immune response owing to their lipid nature (79,122). The polar carboxylic acid and hydroxyl groups of the mycolic motif are proposed to be presented towards the outer surface of CD1b on APCs for interaction with T cell receptors (127, 128). Accordingly, tuberculosis patients produce antibodies directed against *M. tuberculosis* MAs (54). These antibodies were detectable by ELISA (129, 130). This may lead to the production of anti-MA antibodies which we exploit as a biomarker for TB diagnostics. (131). The anti-MA antibody biomarker can indicate active TB disease regardless of the HIV status of the patient, because the anti-MA antibodies levels are maintained even though the CD 4 T cells are declining (79).

2.1.4 Isolation and purification of mycolic acids

Butler (1985) (132) first purified MA from sonicates of *M.tb* strain H37Rv by extraction with chloroform and methanol. This method was not specific for MA as it also extracted fatty acids, lipids and other chloroform soluble components. This was solved by further purification by column chromatography. Due to the cost and limited capacity of column

chromatography, alternative methods for purification and characterizations of large amounts of pure MA was required.

Countercurrent distribution (CCD) was an alternative purification method for large amounts of mycolic acids. Glick (133) described liquid-liquid extraction as a common method for separation of chemical substances. It is usually carried out in a single separation funnel for substances with different partitioning properties. To exploit small differences in partitioning properties for purification, extraction must be carried out in systematic repetitive fashion over many partitioning stages. This type of sequential extraction was named counter current distribution (CCD). Separation power of a chromatographic column is expressed as the number of theoretical plates that it can achieve. One theoretical plate can be described as the separation that is achieved by one transfer cycle of CCD. The more cycles, the better separation is achieved. In column chromatography, the separation provided by its theoretical plates is not fully utilised when the flow rate does not allow enough time for equilibration of the solutes between the solid and mobile phases. In CCD the full separation potential of each tube/ transfer or cycle is utilised by allowing long enough equilibration times between each cycle.

The underlying principle in the separation of mixtures by CCD is the selective transport of solutes. For MA purification, a suitable CCD method was established by Goodrum *et al*. (92). In it, Siko (134) reported his improved biphasic, ternary solvent system consisting of 42% chloroform, 39% methanol and 19% 0.2 M NaCl. This solvent composition was obtained by titrating different ratios of chloroform and 0.2 M NaCl with the fully miscible methanol to develop a phase diagram (Fig 6) (134).

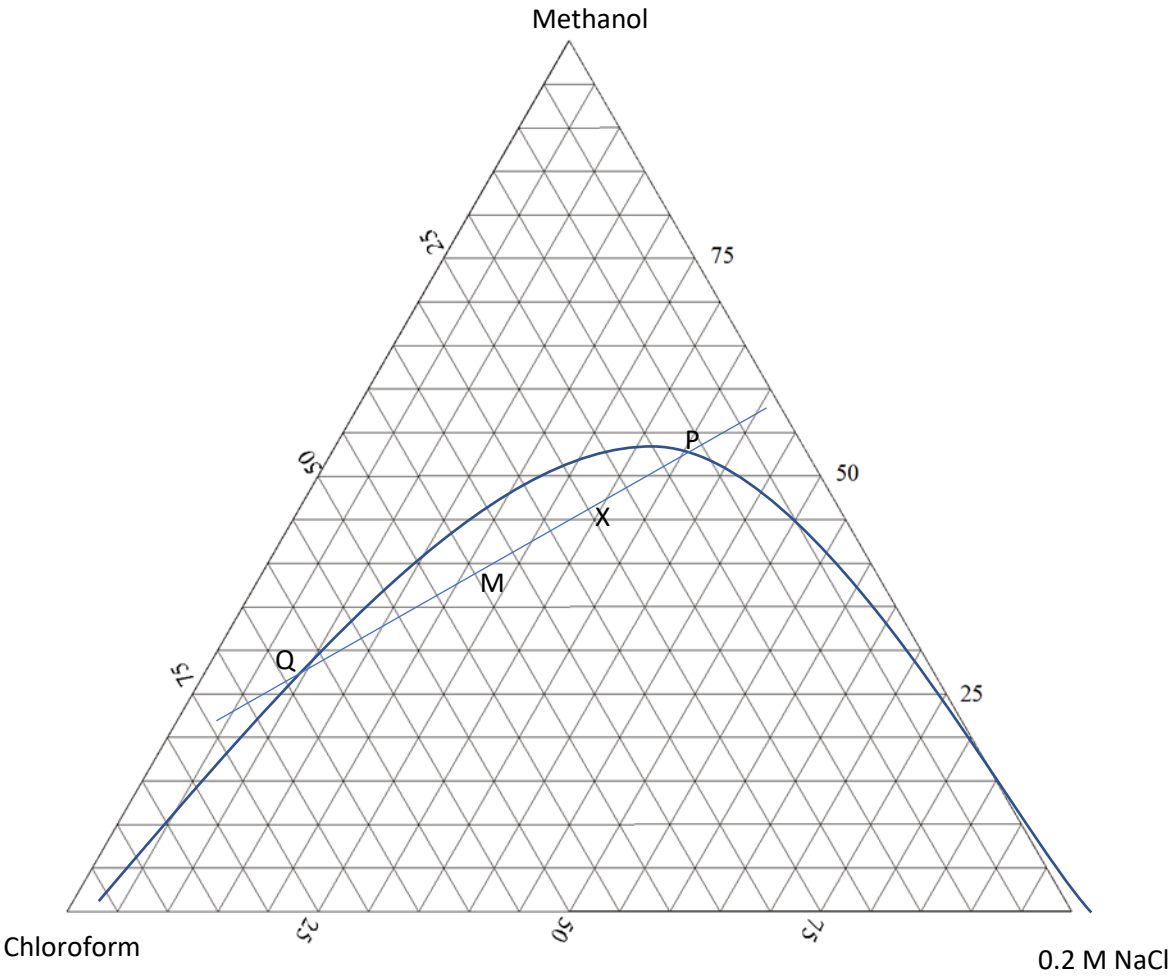

Figure 6: Phase diagram of the CCD ternary solvent system of chloroform, 0,2 M aqueous NaCl and methanol that was used to purify mycolic acids. Point M was obtained by drawing a line PQ pivoting over X such that PX: QX correlates with the volume ratio of lower and upper phase obtained by mixing composition X. The point M is the mid-point of line PQ, such that when making up composition M, upper and lower phases of equal volume are obtained, with the upper phase consisting of Composition P, and the lower phase of Composition Q. Thus, M is a composition ratio of 42% Chloroform, 39% Methanol and 19% 0.2 M NaCl (134**).**

The CCD method of purification of MA involves subjecting a crude extract of saponified *M.tb*, dissolved in the bi-phasic solvent system described above, to a counter current liquid/liquid separation. Previously, this method yielded 5.8 to 7.8% of purified mycolic acid from the dry weight of the crude cellular extract (92).

The first step is saponification and extraction. The saponification step is necessary to release the lipid component from the rest of the cell skeleton and to release the free

fatty acid salt from any ester form. The extraction step is necessary to remove the saponification agents from the cell wall component.

The crude cellular extract obtained from the large-scale saponification and extraction process is dissolved in the lower phase of the bi-phasic solvent system and an equal volume of the upper phase of the bi-phasic solvent system is added. This solution is then subjected to CCD through a series of approximately 25 cycles; each cycle comprising a mixing of upper and lower phases, a separation of the phases and a transfer of the separated phases to clean upper and lower phases (96). The CCD-separated material is then withdrawn from the tubes. The mycolic acids fraction, even after being purified by CCD, still contained traces of contaminating material. Adding acetone to the purified sample was found to selectively precipitate the mycolic acids, while simultaneously extracting these impurities.

When using water, rather than 0.2 M NaCl solution in the CCD solvent system, the various fractions of fatty acids and lipids from the cell-wall could be identified in the various tubes by their emulsification patterns in the lower or upper phase. The mycolic acids fraction, for example, was easily recognised by its emulsification pattern mainly in the lower phase within the first few tubes. When water was substituted by 0.2 M saline, the emulsification patterns collapsed and the mycolic acid fraction had to be confirmed by means of TLC (unpublished work).

The current method involves subjecting a crude extract of *M.tb* cell-wall components, dissolved in bi-phasic solvent system, described above, to a counter current liquid/liquid extraction to purify MA, but still on a comparatively small scale. Using this same method of purification, it was deemed possible to load more concentrated MA crude extract in the CCD to upscale the yield of pure mycolic acids per run. This would also better suit the monitoring of the purification process by TLC, while simultaneously reducing the reagent cost of mycolic acids for use in TB diagnostics. This hypothesis was tested in this experimental chapter.

2.2 Materials and Method

2.2.1 Materials

Silica plates: Thin layer chromatography (TLC) silica gel 60 F_{254} 20 x 20 cm plates (Merck, Kenilworth, New Jersey, USA).

Schott bottles (Sigma-Aldrich, St. Louis, USA)

Tank: Rectangular TLC developing tank (Sigma-Aldrich, Missouri, USA).

Desiccator: Duran desiccator with flat flange and knobbed lid (Merck, New Jersey, USA). Blue Silica gel as the drying agent. (Merck, New Jersey, USA)

2.2.2 Reagents

M. tuberculosis cell pellets: Self cultured by Heena Ranchod according to conditions established by Ndlandla *et al.* (123)

Purified MA: Previously purified MAs on 19/01/1998 by Van Wyngaardt purified using the CCD method described by Goodrum *et al.* (92)

Acetone (Sigma-Aldrich, Missouri, USA).

Chloroform (Merck New Jersey, USA)

Diethyl ether (Sigma-Aldrich, St. Louis, USA)

Hexane (Sigma-Aldrich, St. Louis, USA)

Hydrochloric acid (HCl) (Merck New Jersey, USA).)

Methanol (Merck New Jersey, USA)

Phosphomolybdic acid (Merck, New Jersey, USA)

Potassium hydroxide (KOH) (Sigma-Aldrich, St. Louis, USA)

Sodium chloride (NaCl pellets, Merck, New Jersey, USA)

Reagent A: KOH (25% (m/v)) dissolved in methanol-water in a 1:1 volume ratio

Reagent B: HCl, (32% (v/v)), dissolved in triple distilled water (dddH_2O) in a 1:1 volume ratio

Upper phase and lower phase solvent without saline: Chloroform, methanol and dddH_2O in a ratio of 42:39:19

Upper and lower phase CCD solvent with saline: Chloroform, methanol and 0.2 M Sodium Chloride in a ratio of 42:39:19.

TLC running solution: Diethyl ether (30 % (v/v)) dissolved in hexane

TLC developing solution: Phosphomolybdic acid 10% (m/v) dissolved in 99.9 % (v/v) ethanol. Stored at 4 °C until further use within 1 week.

2.2.3 Saponification of crude bacterial extract

To release mycolic acids from mycobacterial cell walls, homogeneous bacterial cell pellets obtained from were re-suspended in 300 ml of saline. After re-suspension the bacteria were allowed to sediment to the bottom of the Schott bottle, before 250 ml of the saline was removed. The bacterial cells were re-suspended in the remaining saline and divided into equal parts before centrifuging (Beckman Avanti J-25 preparatory centrifuge, California, USA) for 20 min at 1500 x g. The remaining saline was removed by decanting making sure not to disturb the bacterial pellet that now remains. The pellets were re-suspended in reagent A to obtain an optical density (OD) approximating McFarland standard 4, i.e. an OD of 0.837 at 486 nm measured using a spectrophotometer (UV-1600PC UV-VIS, VWR, Pennsylvania, USA).

Saponification was done using autoclavable 2.5 L tightly capped Schott bottles fitted with red caps and rings. The Schott bottles were wrapped in foil and incubated at 70ºC overnight in a water bath (FMH 110 electronics, Labotech, USA) covered in foil.

2.2.4 Crude extract of Mycolic acids

A funnel extraction was done on the saponified cell suspension in reagent A to obtain the crude MA extract. After cooling to room temperature, 1.5 ml of reagent B was added for each 2 ml of reagent A used. The cell suspension of reagent A and B was shaken carefully in a 2.5 L reagent bottle until no fumes were seen, then vigorously to ensure uniform mixing. The pH of the suspension was adjusted to 1 using reagent B to protonate all MAs for dissolution in chloroform. Chloroform (600 ml) was added before the suspension was vigorously shaken again for 10 min in tightly capped

reagent bottles. The crude MA extract was transferred to a separating funnel and allowed to separate into two phases at room temperature overnight. The lower phase, containing the crude MA extracts, was collected and evaporated at 60ºC in a pre-weighed round bottom flask on the rota-evaporator (Buchi Rotovapor RE 120, Gemini BV laboratory, Germany). Acetone (5-10ml) was added to allow complete drying of crude MA extract. This was repeated until crude MA extract was completely dried. The dried crude MAs was stored at 4ºC until further use.

2.2.5 Extraction of crude MA in the phase solvent without saline

Chloroform, methanol and water were mixed in a ratio of 42:39:19 in a 2.5 litre reagent bottle. The solvents were vigorously shaken and allowed to form 2 phases in a separating funnel. Both phases were collected and stored separately. The crude MAs extracts were reconstituted in equal volumes of lower phase solvent and upper phase solvent. The phases were mixed together and transferred to a separating funnel shaken vigorously and allowed to separate completely at room temperature. The lower phase extract was collected and evaporated at 60ºC in a pre-weighed round bottom flask on the rota-evaporator. Acetone (5-10ml) was added to allow complete drying of crude MA extract. This was repeated until crude MA extract was completely dried. The crude MAs were stored in a desiccator, with blue silica gel as the drying agent, overnight at room temperature to ensure removal of all water before weighing. Crude mycolic acids extract was stored at 4 °C till further use.

2.2.6 TLC analysis of Mycolic acids

Mycolic acid analysis by thin layer chromatography (TLC) has been employed worldwide as a fast method for identification of isolated mycobacteria. TLC is also a cheap, quick way to confirm the presence of impurities. For this study TLC is used to identify and determine the purity of MA.

In general, TLC was carried out as follows. MA samples (10 µl) were loaded on aluminum backed TLC silica plates by spotting using a Hamilton Syringe on a pencil line drawn 1 cm from the bottom of the silica plate. The spots were left to dry at room temperature. Once the spots were dry, the silica plate was placed in the TLC tank with running solution. This mobile phase is drawn up the plate via capillary action, until the

solution reached to about 2-3 cm from the top of the TLC. Subsequently, the plate was immersed in the visualization reagent container for 5 secs, in this case a developing solution using tweezers, placed on laboratory tissue paper and charred immediately using a heat gun (Bosch PHG 500-2, Midrand, SA). The plates were analysed and retention factor (Rf) values were calculated. (All solutions described above in section 2.2.2).

2.2.7 TLC analysis of previously purified MA

TLC technique was performed on previously purified MAs to determine the dilution at which the MAs would be detectable in the CCD. Samples of 1 ml MA were prepared in lower phase solvent to a dilution range of 4.8 -0.0048 μg/ml. From that solution, 10 μl was loaded on TLC plates. The TLC protocol (section 2.2.6) steps of developing and visualization was carried out as described above.

2.2.8 TLC analysis of crude MA extracts.

TLC was then performed to determine crude MA contaminants. A sample of 1 ml crude MA extract was dissolved in lower phase solvent to a dilution range of 5 -0.005 mg/ml. From that solution, 10 µl were loaded on TLC plates. The TLC protocol (section 2.2.6) steps of developing and visualisation were carried out as described above.

2.2.9 Purification of MAs by CCD

The phase solvent used for CCD was prepared by mixing chloroform, methanol and 0.2 M Sodium chloride in a ratio of 42:39:12. The solvent was allowed to form two phases in a separating funnel at room temperature. Each phase solution was retrieved and stored separately.

The crude mycolic acids extract was purified using the counter current distribution (CCD) method previously described by Goodrum *et al.* (92). The CCD instrument was built using an array of positions representing a chain of test tubes. The CCD instrument (Craig counter current train, New Jersey, USA) shown in figure 7 consists of four racks of interlinking glass tubes (Fig 7A) The principle is as follows: Each tube is filled with equal proportions of each phase (upper phase solution and lower phase solution). The

lower phase of the two-phase solvent system is the "stationary phase", whereas the upper phase is the "mobile phase". The process begins at tube 0 which contains the mixture of substances to be separated in the lower phase solvent and all the other tubes contain equal volumes of the same solvent. The upper phase solvent is added to tube 0, where equilibration takes place and the phases are allowed to separate. The upper phase of tube 0 is then transferred to tube 1 and fresh solvent is added to tube 0, after which the phases are equilibrated again. After each separation cycle, the clear upper phase moves along the tube rack from the first tube to the adjacent tube. Clean upper phase solution is added to the first tube at each transfer cycle, meaning that the initial volume of upper phase added to tube 0 will end up in tube 60 after 60 cycles.

Before purifying the crude MAs, the tubes of the CCD were cleaned by running the apparatus in wash mode sequentially with 1 L of 10% Contrad^{TM} solution, 2 L of dddH_2O to rinse out the Contrad solution and 1 L of 96% ethanol (Merck) to rinse the tubes. The machine was left upside down to drain all the liquid and to ensure it was completely dry before use. The apparatus was then loaded first with lower phase in each tube. The crude MA extract was loaded into the first tubes of the CCD apparatus. The crude MA sample flask was rinsed with lower phase with saline to ensure quantitative transfer of MAs into the CCD apparatus. The crude MA sample solution filled the first 2 tubes of the CCD and volumes were adjusted to exactly 10 ml in both tubes, using clean CCD lower phase solvent. Lower phase was added to first tube to equilibrate to the third tube and then re- adjustment to 10 ml and equilibration to 4th tube. In this way, the volume per tube was 10 ml for the first 4 tubes and approximately 5 ml was left over in the fifth tube after equilibration. CCD upper phase solvent (650 ml), enough for 60 cycles, was loaded to the large upper phase tank of the machine (Fig 7B). A volume of 10 ml of upper phase CCD solvent with saline was transferred manually to tube 0. Every second tube after the fifth tube was then loaded with 10 ml CCD lower phase solvent. The contents were mixed manually 20 times by shaking the machine and the contents were allowed to separate into two phases at rest position. This was the first cycle. Clean upper phase was transferred to the first tube to commence the second cycle and the routine was repeated until 60 cycles were done. In the first tubes initially, the upper phase would absorb some of the lower phase and the absorption was corrected by adding clean lower phase CCD solvent with saline to tube 0 at every cycle until it was no longer necessary. The volume of upper phase was

adjusted to exactly 10 ml by adjusting the rod that controlled the volume of upper phase entering the tubes (fig 7C)

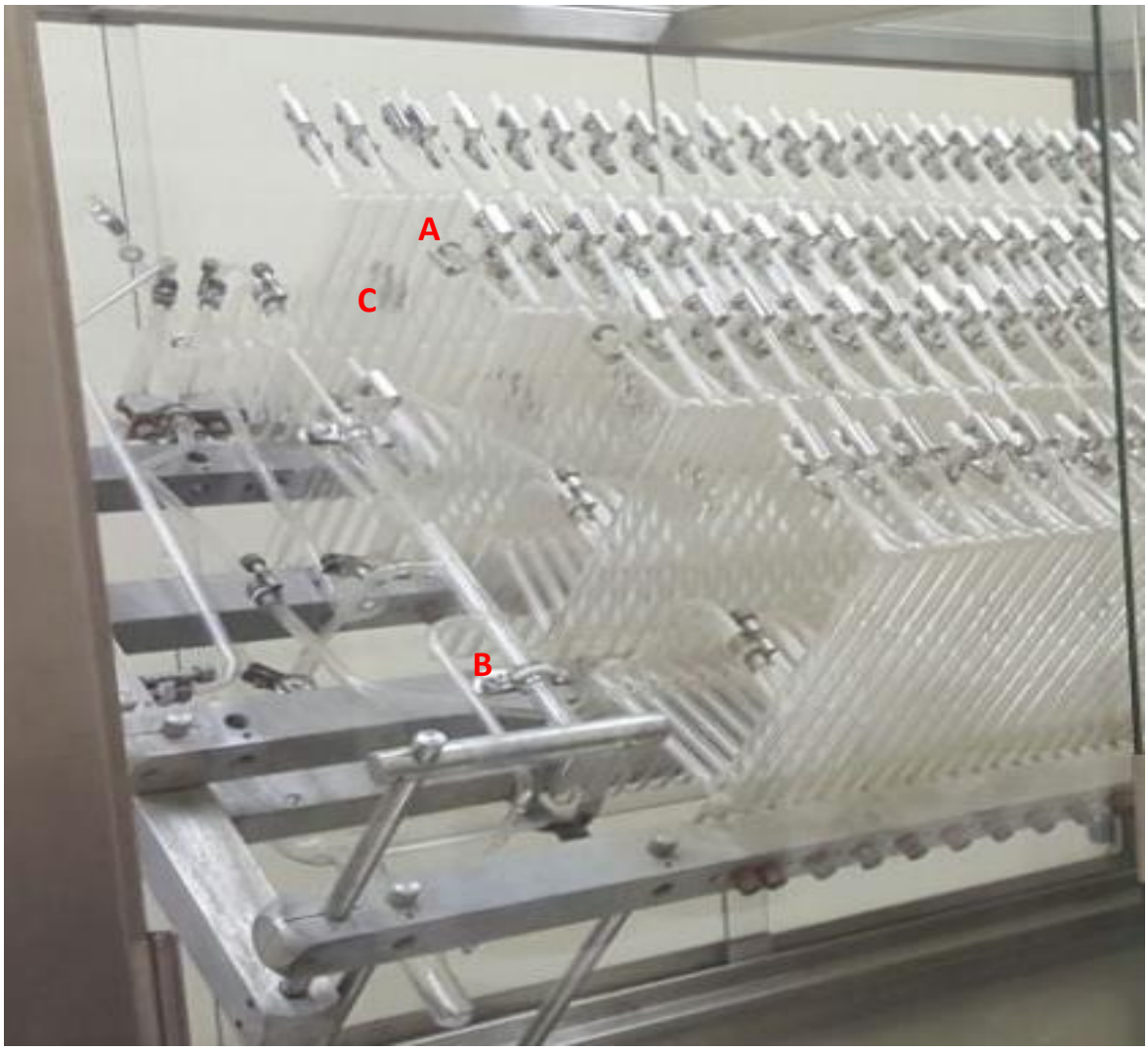

Figure 7: **Craig countercurrent distribution (CCD) train.** A – interlinking tubes, B – CCD upper phase solvent tank, C – Upper phase solvent adjustment rod

2.2.10 Analysis of CCD purified MAs using TLC

To analyse the purity and distribution of the MAs, 10 µl of lower phase and 10 µl upper phase samples of the same tube for every second tube of the 60 tubes were spotted on TLC plates. The TLC protocol (section 2.2.6) steps of developing and visualization was carried out as described above.

2.2.11 Acetone precipitation of CCD purified Mycolic acids

Firstly, the salt from the saline had to be removed in order to obtain correct yields of pure MAs. Both lower and upper phases of tubes 0-15 were drawn out from the CCD tubes, pooled and evaporated at 80ºC until mostly dry. The semi-dried MA was mixed in 2 ml chloroform and 1 ml water and shaken vigorously before transferring to a separation funnel allowing the mixture to separate into two phases at room temperature. The upper phase containing saline was discarded and the lower phase evaporated at 80ºC on the rota-evaporator. The saline removal process was repeated 3 times. Acetone (5-10 ml) was added to allow complete drying. This was repeated until MA was completely dried.

To remove contaminants that were attached or associated with CCD purified MAs, the dried MAs from the previous step were dissolved in 4 ml chloroform and concentrated to 1 ml at 85ºC on rota-evaporator. This was done for 5 min to ensure all MAs were dissolved. The addition of acetone was done to precipitate the MAs out of solution. To the MA extract, 20 ml of acetone were added and heated at 85ºC in a pre-weighed round bottom flask The MAs were allowed to precipitate from the acetone solution overnight at 4ºC.

Filtration through filter paper previously rinsed with chloroform and acetone was used to separate the MAs precipitate from contaminants. Cold acetone (10 ml) was used to rinse the MA precipitate on the filter paper. The precipitate was trapped onto the filter paper and the acetone filtrate filtered through into a round bottom flask labelled acetone filtrate/MA supernatant. This was repeated three times until the flask that contained the MA precipitate was completely clean. The precipitate on the filter paper was then rinsed in 10 ml chloroform three times into a pre-weighed round bottom flask labelled “MA precipitate” before it was evaporated at 60ºC on rota-evaporator until completely dried. The MA precipitation from contaminants was repeated a second time. Acetone (100 ml) and chloroform (4 ml) was then added to the MA precipitate recovered from the filter paper and heated at 85ºC for 5 min. The MAs were allowed to precipitate overnight from the acetone solution at 4ºC and recovered as before.

The MA precipitate and supernatant that were collected in round bottom flasks were stored in a desiccator, with blue Silica gel as the drying agent, overnight to ensure

removal of all water before weighing the flasks using an analytical balance (LABOTECH, USA).

2.2.12 Aliquoting MA precipitate and supernatant

Aliquoting into pre- weighed autoclaved brown glass vials (Note that these brown glass vials were not touched by hands, but were moved with sterile tweezers to prevent inaccurate weights) proceeded after collection of the weighed MA precipitate and supernatant.

The dried MA precipitate was dissolved in 25 ml ice cold chloroform and dispensed as 500 µl volumes into 40 pre-weighed 4 ml brown glass vials. The MA precipitate was rinsed with 20 ml ice cold chloroform and aliquoted into the vials as before. This rinsing and aliquoting was repeated three times. The chloroform was allowed to evaporate at 60^{o}C on a heating block (Reacti-Therm Thermo Scientific Pierce III, USA). The vials were capped and stored at 4^{o}C.

The dried MA supernatant was aliquoted as described above and stored at 4^{o}C.

2.3 Results

2.3.1 Countercurrent purification of mycolic acids

The method for MA purification by CCD was written up by Goodrum *et al.* (92) in which Siko (134) improved the method by substituting the water in the ternary biphasic solvent composition with saline solution. With water instead of saline, identification of the MA fraction on the CCD could be done by assessing the emulsion behaviour of the material in the tubes after separation. By substituting the water with saline, the separation went much faster due to improved equilibration times, but the fractions in the CCD train had to be identified by means of TLC.

Previous methods used HPLC to determine whether the MA collected from the CCD was pure, but because the molecular weight standards used in HPLC are no longer commercially available, reliance on TLC became crucial. It was therefore necessary to make sure that TLC functions optimally for the purpose.

TLC was performed on previously purified MAs to determine the concentration at which MAs would be visible after CCD purification shown by Figure 8.

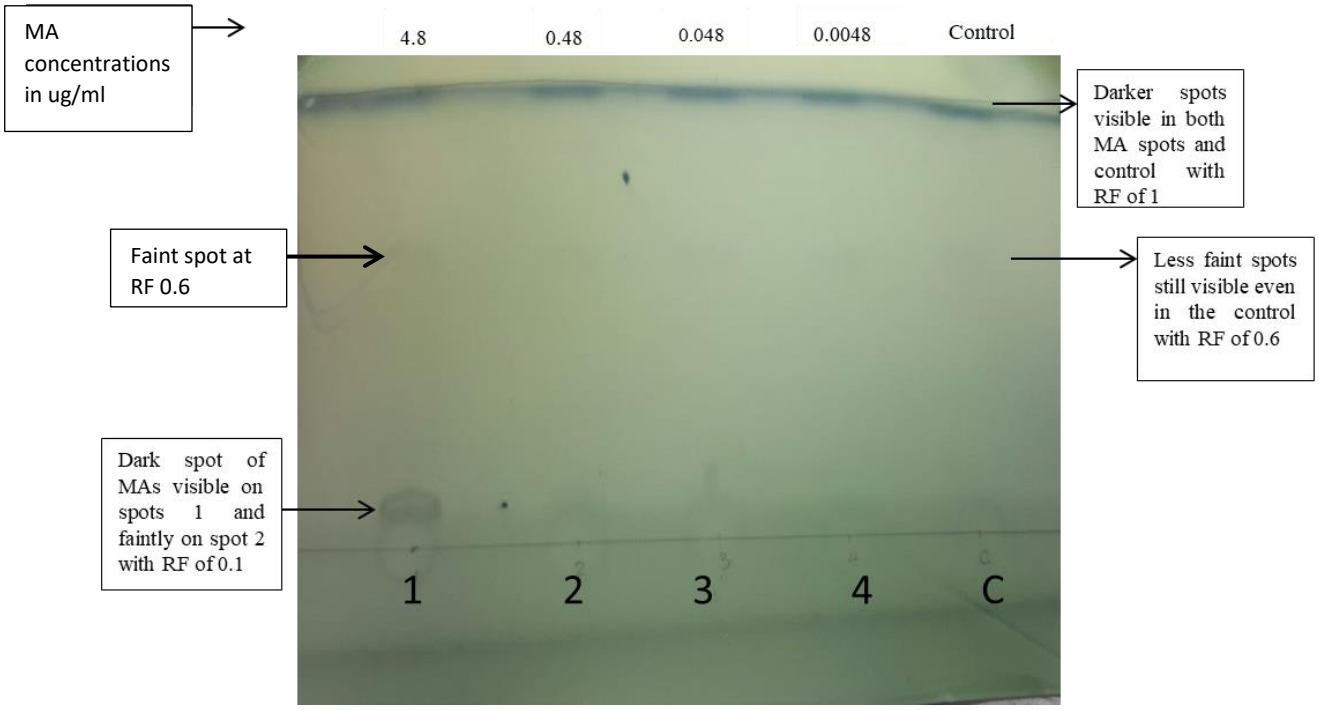

Figure 8: TLC analysis of previously purified MAs to determine at which concentration range MA would be visible after CCD purification. MA in a lower phase solution (Chloroform, methanol and 0.2 M Sodium Chloride in a ratio of 42:39:19) spotted on silica at 1:10 dilution range of 4.8 - 0.0048 µg/ml. Lower phase solvent spotted as negative control (C).

Upon observations of the TLC plate, a visible spot at Rf of 0.1 is seen at a MA concentration of 4.8 µg/ml (lane1). This spot represents MA and fades out at lower concentrations (lanes 2-4). Lower phase solvent was used as the negative control as MA distributes strongly into the lower phase during phase separation and CCD purification. For the negative control (C) a spot is seen as a line on the front at Rf 1, which is visible in all concentrations of MA. This therefore originated from, or is an artefact of the lower phase solvent, especially as it does not fade out with decreasing MA concentration. A faint spot is seen at Rf 0.6 for the control which seems to fade out with decreasing MA concentration and may therefore constitute a contaminant trace. Because this spot is also visible in the lower phase solvent control, it is a contaminant that is probably derived from the solvent system.

These previous purified MAs were purified at a lower scale according to Goodrum *et al.* (92) and the TLC is not as clear. When upscaling MA purification by increased loading concentration of MA crude extract on the CCD by 4 times, the higher concentrations of MA are anticipated to be more visible on TLC analysis pre- and post-CCD purification.

TLC analysis of crude MA extracts before CCD purification is shown in figure 9 where MA was spotted at a concentration range of 5 -0.005 mg/ml.

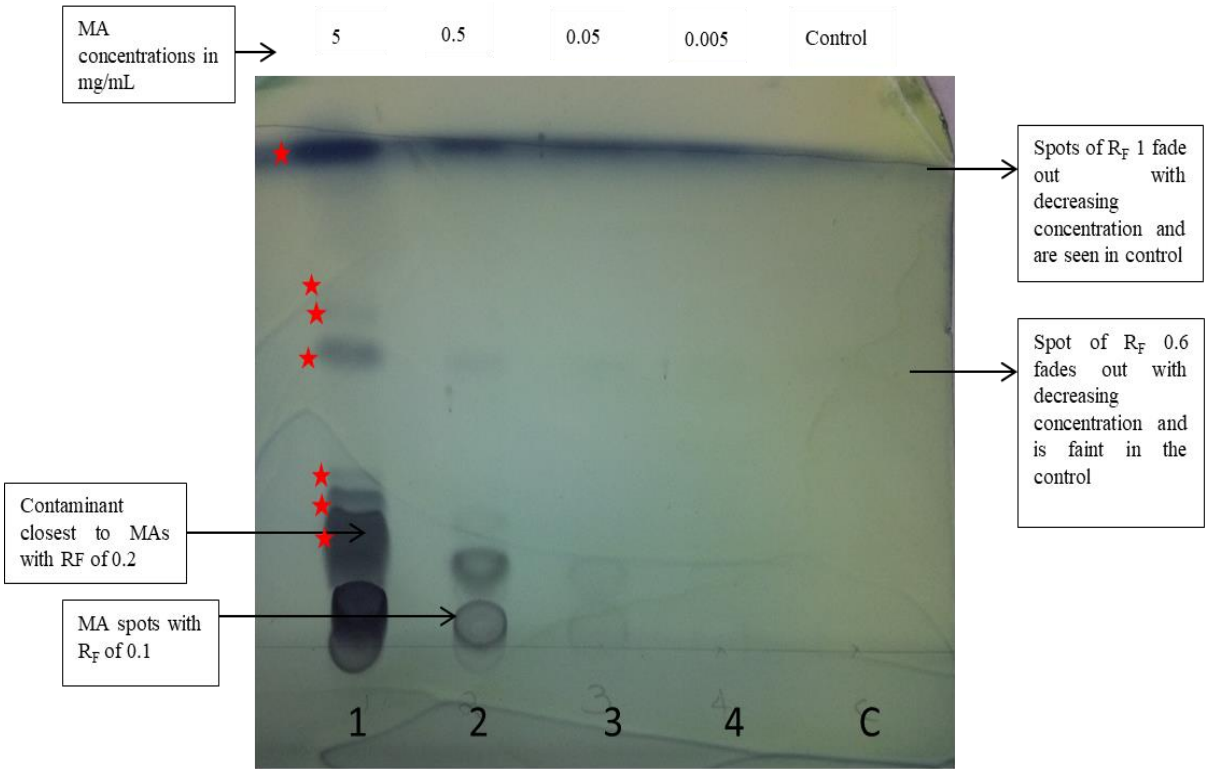

Figure 9: TLC analysis of crude mycolic acids before CCD purification. MA in a lower phase solution (Chloroform, methanol and 0.2 M Sodium Chloride in a ratio of 42:39:19) spotted on silica at 1:10 dilution range of 5 - 0.005 mg/ml. Lower phase solvent spotted as negative control (C). MA concentration = Crude MA concentration. Red stars = contaminants

As seen in figure 9, at a concentration of 5 mg/ml (lane 1), a spot for MA is seen as well as spots for various contaminants (red stars) in the crude extract that fade out with decreasing concentrations. The positions of the visible contaminants close to MA have a low Rf. It can be assumed that there might be more contaminants as some compounds might have the same Rf, thereby occupying the same position. The

negative control (C) showed faint spots of Rf 0.6 and 0.1 and are probably derived from the solvent system as seen before in figure 9.

Figure 9 shows that higher concentrations provide easier analysis as the MAs together with their contaminants are better visible without too much smear. The contaminants that exist at low concentrations in the crude MAs are visible only at the highest spotting concentration.

Based on the results of figure 9, a CCD purification of crude MA was done at a higher loading concentration than before. The loaded mass of crude extract was 1.7 g, loaded into the first 2 tubes and distributed up to the 5th tube by decantation through the transfer mode of the CCD apparatus. After that, 60 cycles of liqud-liquid extraction were done mechanically on the CCD apparatus. It was expected that the non-polar MA would remain in the lower phase of the first 5-7 tubes. However, with a higher loaded mass this increased to more tubes, due to absorption of some upper phase into the lower phase during the initial number of cycles. The shorter fatty acids are expected to move along the tubes as the extract proceeds to move and transfer from tube to tube in the direction of tube number 60. The method of CCD purification is described in section 2.2.9.

To analyse the distribution of MAs after CCD purification, TLC was performed from tubes 0-60 using both upper and lower phase, from every second tube starting with tube 1 to tube 15. The TLC results are shown in figure 10.

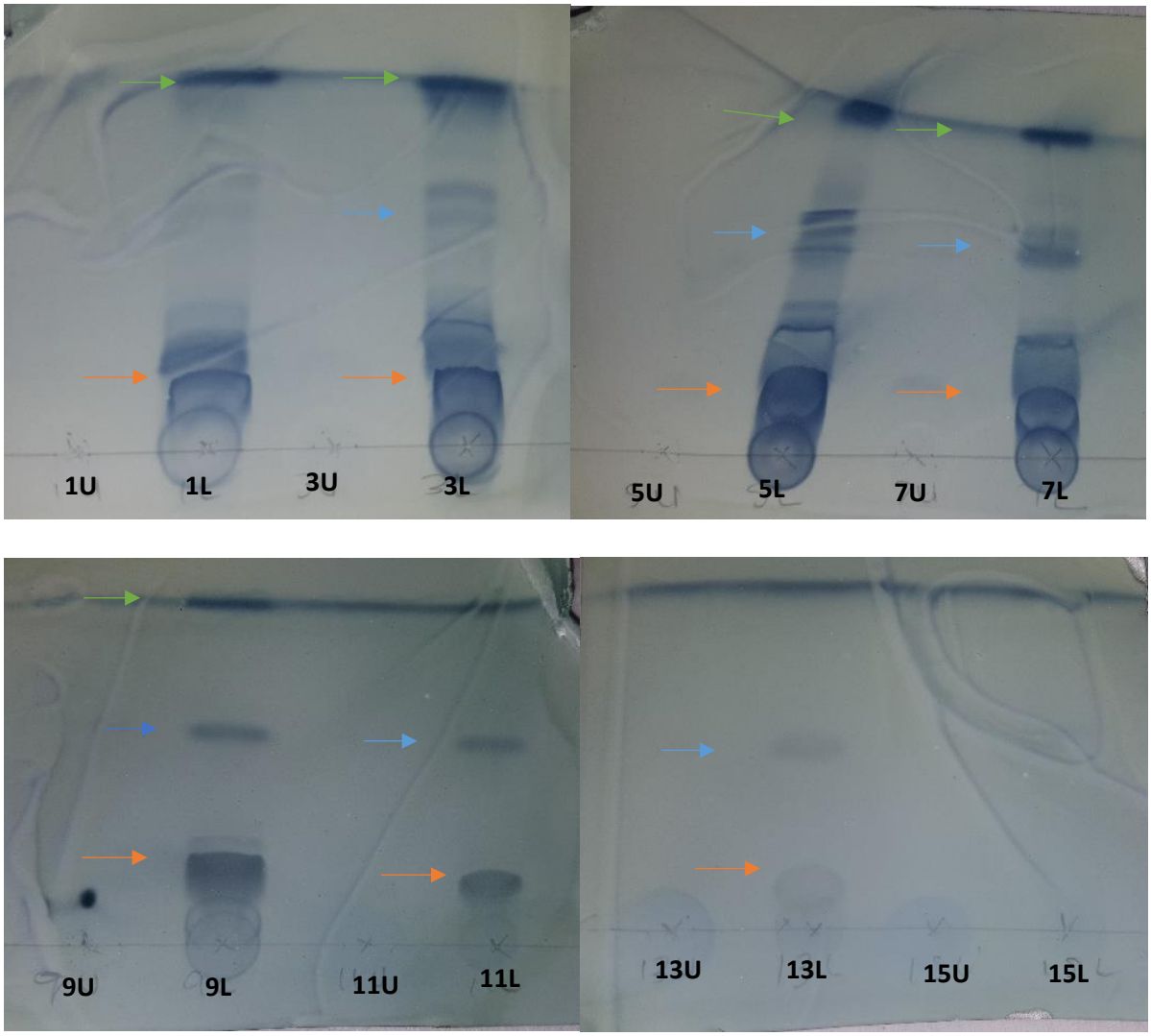

Figure 10: **TLC of fractions in the CCD tube train during purification of mycolic acids from crude extracts**. Blue arrow = compounds with Rf 0.6, Orange arrow = compounds with Rf 0.1, Green arrow = compound with Rf 1. Lane = Tube number/ CCD upper (U) or lower (L) phase solvent.

It can be seen from figure 10 that MA spots at Rf 0.1 were visible from tubes 1 to 13 and peaked in tube 5L. The compound with Rf of 1 also peaked at tube 5L and started to fade away as the MA spot started fading from tube 7L, showing an association with the MAs and also the lower phase solvent as seen in figure 8 and 9. The compound with Rf of 0.6 peaked in tube 5L and faded after tube 13L. As a similar spot was seen at the same Rf of 0.6 in the lane that only contained the lower phase solvent in figure 9, it was speculated to be originating from the lower phase solvent. The dark spot at the origin that peaked in tube 5L is speculated to be the ionized (more polar) form of MA. Nothing was seen in the upper phase of each tube, which therefore makes

chloroform the most probable cause for contributing the Rf 0.6 contaminant in the fractions that are harvested from CCD. The absence of material in the upper phase showed that most contaminants from the crude MA extract moved on. No spots for MA or contaminants were seen from tubes 15-60.

Figures 9-11 show that the MAs do not have high mobility on TLC, as they did not move far from the origin. Figure 10 depicts that MAs did not move along in the counter current tube train, but were retained in the first tubes, showing that they are extremely hydrophobic. More hydrophilic substances move further along the train of tubes. Even though Figure 9 showed only three compounds/contaminants excluding MAs, most of the contaminants of the crude MA extract seen in the TLC chromatogram of Figure 8 would have moved on down the rest of the tubes in the tube train. CCD purification at a lower scale had crude extract loaded in the first tube only and yielded MA enriched sample in tubes 1-10. Upon the up-scaling of the sample load of crude extract, the MA containing fraction was collected from tubes 1-15, due to the loading of the sample over 5 tubes, instead of one. The efficiency of separation therefore was not affected by up scaling CCD purification, while the improved MA detectability in the CCD tubes by TLC. of these compounds helped a lot to confidently identify the MA in the tube train after separation.

2.3.2 Parameters of purification of MAs by CCD

A few parameters are considered in CCD purification. Partition coefficients of compounds are important to determine how far along the train of tubes the MAs are distributed. These coefficients can also be used to determine the fraction of a substance in a particular tube. The width of neighbouring overlapping peaks are used to calculate the separation efficiency of the system and to determine the minimum amount of transfers to effect base-line separation between compounds. Baseline separation is achieved on CCD when two compound peaks are separated such that no solute mass can be found in the tube representing the bottom of the valley between the two peaks.

To determine the minimum number of transfer cycles to separate two compounds, the calculation strives toward a separation of peaks represented in the following idealised peak profile:

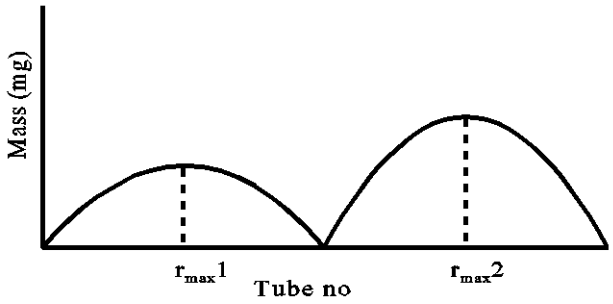

Width of a peak is described by $$W = \frac{6\sqrt{nK}}{1+K}$$

Where n is the number of transfer cycles and K is the distribution constant.

The partition coefficient of substances is given by:

Equation 1: $$K = \frac{r_{max}+1}{n - r_{max}}$$

Where r_{max} is the tube number (counting from tube "0") in which solute compound is most peaked or concentrated, which can be determined by TLC.

To achieve baseline separation, the width of the two peaks in the profile above

is calculated by Equation 2:

Equation 2: $$\frac{r_{max\,2} - r_{max\,1}}{1} = \frac{W_2 + W_1}{2}$$

The r_{max} values at complete separation are defined by

$$r_{max} = \frac{nK-1}{1+K}$$

which correlates with peak widths defined by

$$W = \frac{6\sqrt{nK}}{1+K}$$

Substituting the r_{max} and W equations into Equation 2 and simplifying the resulting equation, will give the number of transfer cycles required to base-line separate two compounds from one another by solving *n* in the quadratic equation 3:

Equation 3: $0{,}5n - 5{,}16\sqrt{n} + 0{,}5 = 0$

The partition coefficient for mycolic acids is calculated as:

K (mycolic acids) = $\frac{6+1}{60-6} = 0.129$

Because the partition coefficients for the two visible contaminants in the TLC profile of Figure 11 are the same as that for MA, these cannot be separated from one another by extending the number of transfer cycles to beyond 60 in an application of Equation 3. The remaining trace amounts of contaminants after CCD purification of MA crude extract was therefore removed by a completely different method, namely acetone precipitation of the MA (Section 2.2.11).

2.3.3 Analysis of MA post acetone precipitation

It is known that the mycolic acids fraction, even after being purified by CCD, was still found to contain some contaminating material. An amount of acetone was added to the purified sample and this was found to extract these impurities. In order to remove any residual impurities still present in the countercurrent-purified material, an additional extraction by acetone precipitation was done as described in section 2.2.11. Acetone containing the impurities ~~are~~ is filtered through the filter and what was left was pure MA essentially free from contaminants as shown by TLC in Figure 11.

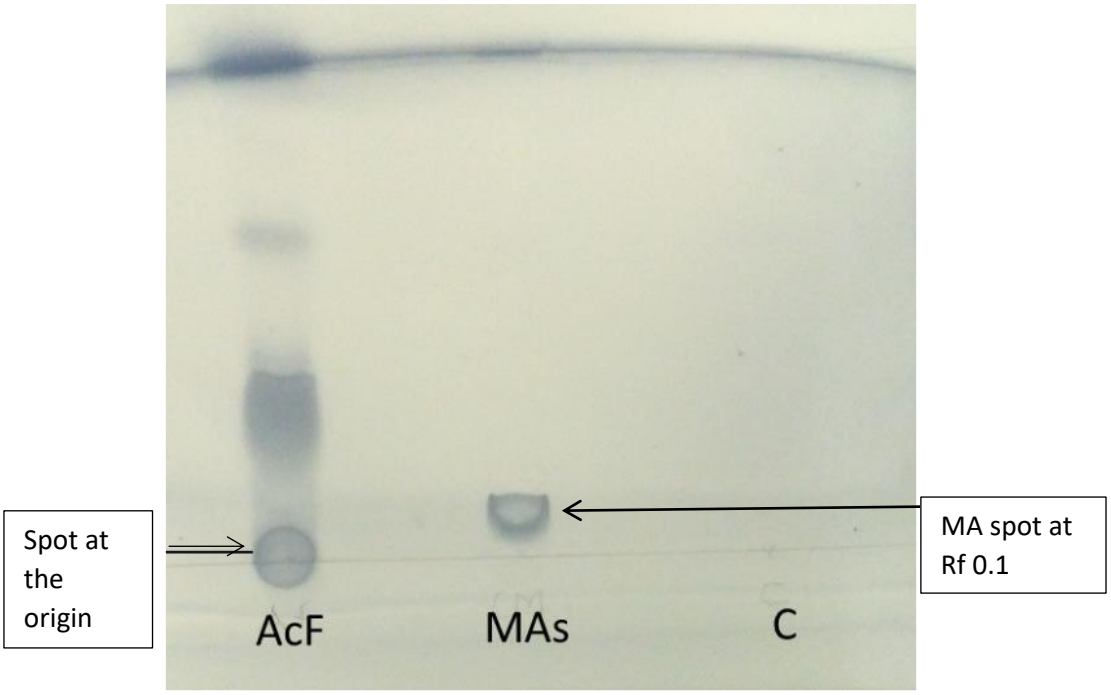

Figure 11: **TLC analysis of MAs supernatant and precipitate after acetone precipitation.** AcF = Acetone filtrate/ supernatant, MAs = precipitate. Negative control is lower phase solvent (Chloroform, methanol and 0.2 M Sodium Chloride in a ratio of 42:39:19) (C). AcF and MAs were both spotted at a concentration of 1 mg/ml. The negative control (C) is clean lower phase.

The MAs are visible at Rf 0.1 as compared to AcF that show four visible spots without any trace of the MA spot at Rf 0.1.

The spot at the origin of the TLC plate resulting from the MA-containing purified CCD fraction (Fig 10) appeared to be acetone soluble and was now found in the AcF fraction in Figure 11. There was no significant occupation of the Rf 0.1 locality in the AcF sample on TLC, whereas this characteristic MA spot was found practically pure in the acetone precipitated sample, as was anticipated based on previous work (2). From the results in Fig 11, there is therefore no TLC evidence of any significant loss of MA in the process of acetone precipitation.

2.3.4 Quantification of Mycolic acid yield as a percentage of mass

A mass of 1.7 g of mycolic acid enriched crude extract obtained from pre-purification through phase separation was loaded on the CCD. After 60 cycles separation was complete 979 mg of CCD purified mycolic acid was collected.

The CCD purified mycolic acids was then subjected to acetone precipitation where 453 mg of pure mycolic acid and 514 mg of contaminants was obtained.

The following formula was used to calculate the yield of MA:

$$\frac{Purified\ MA}{Total\ loaded\ crude\ extract\ mass}\ \text{X}\ 100$$

Estimated yield: $\frac{453\ mg}{1700\ mg}$ X 100 = 26.64% of the pre-purified crude MA extract

Siko (134) expressed the percentage yield in terms of the original crude extract, without the pre-purification that is done by funnel separation. He obtained 503 mg of funnel separated pre-purified MA extract from 2700 mg of original crude MA extract, which gives a 5.4 fold enrichment of MA by pre-purification calculated as follows:

$\frac{2700\ mg}{503\ mg}$ = 5.4 times

To compare the efficiency of the upscaled CCD purification with that obtained by Siko (134), the pure MA yield from pre-purified MA (26.64%, calculated above) needs to be divided by the times enrichment obtainable by pre-purification (5.4 times) as follows:

$\frac{26.64\%}{5.4}$ = 4.8% MA yield obtained by upscale of loading the CCD

A summary of MA yields from the original CCD purification method by Goodrum (135), the improved method by Siko (134) and the current upscale method is shown in table 1.

Table 1: **Comparison of yield of Mycolic acid post CCD purification according to Goodram (135) and Siko (134) methods.**

Parameter	Original Method (Goodrum)	Improved Method (Siko)	Upscale Method (this chapter)
Loaded Mass of mycobacterial crude extract	**31.1 mg**	**3.760 g**	**1.7g***
Mass of purified mycolic acids	**3.5 mg**	**218 mg**	**453 mg**
Yield	**5.3%-10%**	**5.8%-7.8%**	**4.8%**

*Obtained by pre-purification from a calculated 9.18 g of original crude MA extract

From the results obtained after acetone precipitation the CCD purification was successful in removing the remaining contaminants, however the MA yield is lower than the lower limit of the previous methods (table 1).

2.4 Discussion

Previous methods of isolating MA were explored by Beckman *et al.* (136), who isolated MA from *M.tb* by saponification, derivatisation and reverse phase HPLC, which only allowed small quantities of purified MA per column run (92). The counter current method removed this limitation. Counter current distribution (CCD) improved the ability to load and separate large amounts of extracted MA. This method resulted in baseline separation of MA from other components of the crude mycobacterial extract. The crude bacterial extract consists mainly of chloroform soluble products, fatty acids and mycolic acids. Goodrum *et al*. (92) and Siko (134) were first to describe a method for large scale purification of MA by CCD, without attempting to determine how much MA could in principle be loaded onto the CCD in a single run without compromising the separation efficiency. This chapter envisaged to scale up the CCD purification method.

It is important to determine the yield of any purification procedure. The original method by Goodrum *et al.* (92) reported a loaded mass of 31.1 mg crude MA extract after saponification and obtained a MA yield range of 5.3-10% upon several iterations of the

method (Table 1). Each CCD run required 3 days due to formation of emulsions in CCD tubes. The emulsions were a result of saponified lipids from the mycobacterial call wall complex. Siko improved the original CCD method by replacing water in the biphasic solvent system with saline to break emulsions forming during CCD purification and eliminated much of the time-consuming factor of purifying by CCD (134). The method of Siko obtained a MA yield range of 5.8 – 7.8% in several iterations (Table 1). The max potential yield of MA crude mycobacterial extract after saponification was reported to be 7.64%, based on HPLC analysis of crude extracts of *M.tb* (92). The methods of Siko (134) and Goodrum (135) therefore gave optimal MA yields.

Van Wyngaardt (unpublished data) sought to improve the purification method by using acetone precipitation for purifying MA but this was not fully investigated. It is known that MA has a low solubility in acetone and can be exploited to obtain biologically active MA by removing contaminants through selective acetone precipitation of the MA. This study further investigated CCD purification followed by acetone precipitation.

In the current study the total loaded mass of funnel pre-purified crude mycobacterial extract mass was 1700 mg, effectively a four times larger amount than previous methods mentioned above. CCD purification of the crude extract resulted in most contaminants being removed as seen in figure 10. However, three visible compounds were still associated with the MAs. The compound with a Rf of 1 is most non-polar (no bonding to the stationary silica or associating with its aqueous layer) whereas the compound of a Rf 0 is most polar and remained at the origin (137). The compound at the origin however, had a similarly low partition coefficient as MAs, tempting one to think of it as possibly another form of mycolic acid, e.g. its ionized form, i.e. the mycolate. Acetone precipitation should ideally remove all contaminants that the CCD could not eliminate. As seen in figure 11, acetone precipitation did successfully remove most compounds still associated with the MA after CCD purification. The MA yield obtained post acetone precipitation was 4.8% (Table 1). This represents a 37% loss of MA compared to the maximum potential MA content of *M.tb*.

This loss of yield could be due to scaling up of the loaded sample mass on CCD per run. Another possibility could be that because there was a larger mass of MA obtained, some of the MA could have been filtered with the acetone during the acetone

precipitation procedure It was never before explored whether any MA was retained in the acetone filtrate fraction after acetone precipitation of the CCD purified MAs. The recent development of anti-MA recombinant antibodies (section 1.9) made this possible in a simple immuno-assay approach. This is explored in the next chapter.

Chapter 3: Optimization of immune detection of mycolic acids

3.1 Introduction

The fact that anti-MA biomarker antibodies were detectable in TB patients irrespective of their HIV status demonstrated that the detection of anti-MA antibodies for TB diagnosis could be put to good use in HIV burdened areas (25). However, it was reported by Schleicher *et al*. that the ELISA method could not reliably distinguish between TB positive and negative patient sera, due to the interference of the ubiquitously present cross-reactive antibodies to cholesterol (79). Structural relatedness between MA and cholesterol was later demonstrated (85, 138) and confirmed that it was responsible for the low accuracy in the serodiagnosis of TB aimed at detecting anti-MA antibodies using the ELISA assay. It is well known that anti-cholesterol antibodies are present in all human sera (139). This is the probable reason for the background antibody activity to MAs in TB negative patients (140). Anti-cholesterol antibodies are elevated under conditions of AIDS and bronchitis due to the higher blood cholesterol concentrations (141). In addition, the cholesteroid nature of MA represents a three-dimensional phase structure of cholesterol packing that manifests at high cholesterol concentrations (25).

MAs have been demonstrated to be able to adopt folded conformations (W, U and Z-conformations) to give different antigenic or non-antigenic structures. Thus, a MA structure with a W-shape in two dimensions forms when the molecules fold at their proximal and distal functional groups giving four interacting folded arms (Fig 12). In the “Z” conformation three-arms fold to provide the three-dimensional, curved hydrophobic surface, while in the U-conformation folding occurs at only one functional group (138,142, 143). The existence of these conformations has been suggested by analyses of Langmuir monolayers which showed that the three major MA classes, discussed in chapter 2, can each adopt a folded conformation (140). A study using molecular dynamics predicted that the W-shape is the preferred shape for keto-MA (144).

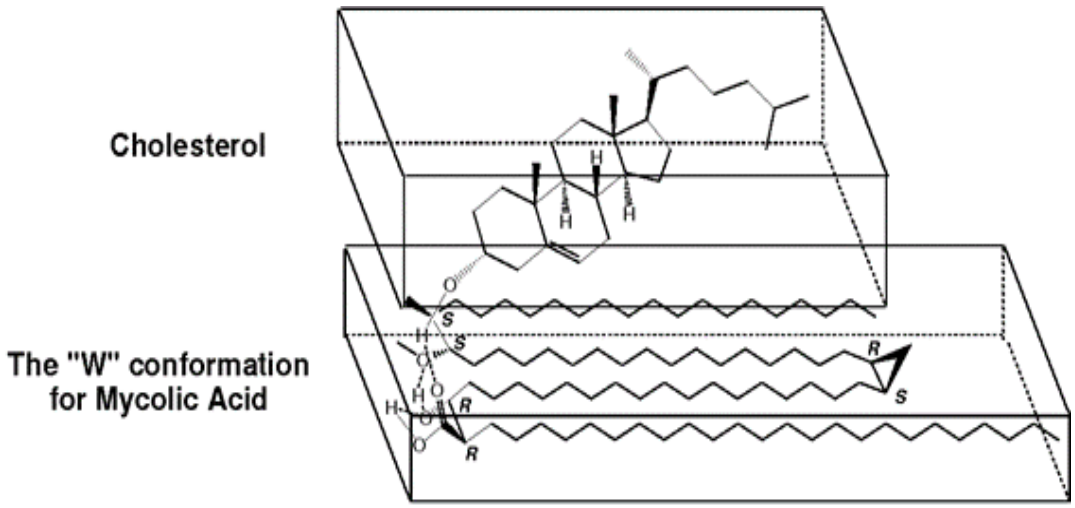

Figure 12: Graphical representation of mycolic acid folded to resemble a cholesteroid nature (138)

One possible way to overcome the problem of MA and cholesterol cross-reactivity is by using labelled monoclonal antibodies that are monospecific to MAs in lateral flow immunoassay. Chan *et al*. successfully produced such from a human antibody gene library (145). These monoclonal antibodies did not show cross-reactivity to cholesterol, but did show preferred binding of anti-MA antibodies to methoxy-MA.

MA extracted and isolated from *M.tb* is a combination of the 3 classes of MA mentioned in chapter 2. However, the percentage compositions of the major classes differ depending on growth conditions of the bacilli (25). Previous work done by our group showed that the most antigenic MA-antigen is the methoxy-MA class and that a combination of keto- and alpha-MA as capture antigen of anti-MA biomarker antibodies provide inadequately sensitive results for TB diagnostics (146). The natural combination of mycolic acid classes from a late culture of *M.tb* provided patient antibody signals that gave a sensitivity of detection that compared well with the best results that could be achieved with chemically synthetic methoxy MA (75). With Ndlandla *et al*. (123) having established a standardized MA antigen that is prepared, extracted and purified from late *M.tb* cultures, this was applied for MA specific antibody detection first by Truyts (147) and now in this MSc study as well.

As described in section 1.9 of chapter 1, this study is a contribution towards the development of a lateral flow immunoassay termed MALIA (Mycolate Antibodies Lateral flow Immunoassay) with the use of monoclonal antibodies as the bio-

recognition element (86). Beukes *et al.* (85) were the first in our research group to create and characterize such monoclonal recombinant single chain variable fragments (scFv's) that could recognize MA and/or cholesterol. One particular phage display clone from this study recognized cholesterol and MA equally well, while other clones recognized either MA alone or cholesterol alone. This confirmed the cross-reactivity between cholesterol and MA (85). Ndlandla (25) found that the scFv's from Beukes *et al*. (85) were not stably expressed. She used the approach by Jung *et al*. (148) to select three new stably expressing recombinant phage antibodies to mycobacterial mycolates from the chicken antibody gene library (25). These fragments were screened for their binding affinities against synthetic classes of MA and cholesterol. The clones were numbered 12, 16 and 18 (86). These clones were selected for their stability during prolonged storage and for their varying binding specificities. All clones recognize the natural mixture of MA. However, cross-reactivity with cholesterol was observed with clones 12 and 16, but not with clone 18. Clone 18 was also the only clone that did not recognize synthetic keto-MA. Clone 12 did not recognize synthetic alpha-MA, whereas clone 16 can recognized all the synthetic MA classes equally well. (86). These findings suggested that cholesteroid nature of the MA manifests towards the *trans*-keto MA subtype (86).

ScFv's are often of too low affinity to be useful in diagnostics. Thus, they are usually engineered into alternative forms to improve their affinity and stability (149). The scFv fragment gene codes from clones 12, 16 and 18 were excised from the phage constructs and expressed as monovalent scFv's. These scFvs were converted to divalent IgY chicken antibodies (gallibodies) by Ranchod *et al*., (86). Divalent IgY molecules were assembled and stabilised by disulphide bonds, which were then designated as ''gallibodies'. Generally, these scFv-IgY fusions can be immobilised on solid surfaces as well as stably conjugated to colloidal – gold (150). The anti-MA gallibodies from Ranchod were engineered into two types of bivalent IgY formats: one a theoretically flexible CH1-4 construct (fig 13a) and the other a truncated and hypothetically more rigid CH2-4 type as shown in figure 13b (86)

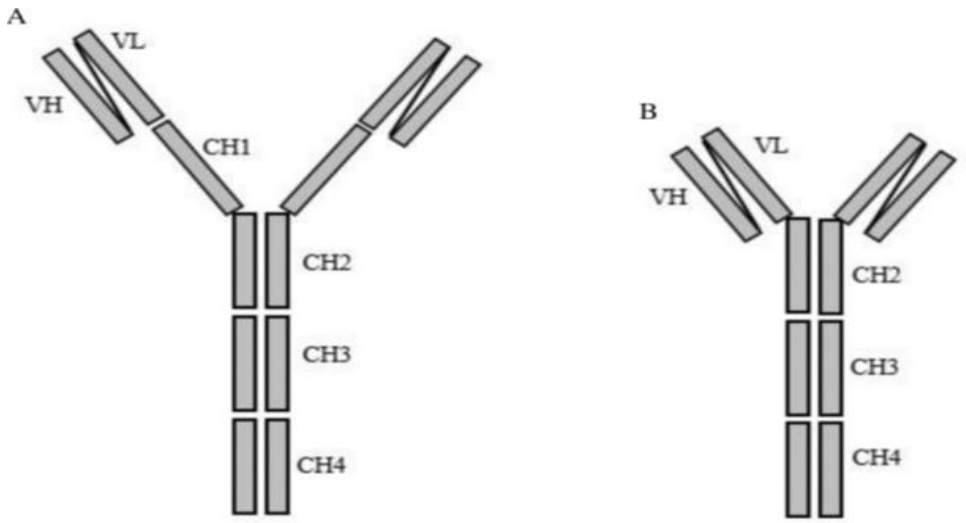

Figure 13: **Structures of the two types of Fc frames used for the gallibody engineering.** A: scFvIgY (CH1-4) and B: scFvIgY (CH2-4). Figure adapted from Greunke *et al*. (150, 86).

In this study, the gallibodies clone types are referred to by their number and their frame type as follows, for example: 12-1 refers to clone number 12, the CH1-4 frame, while 18-2 refers to clone 18, the CH2-4 frame type. Clones 12 and 18 were primarily used. For the purpose of this study it did not really matter which one of clones 12, 16 or 18 were used, nor whether they were assembled onto the CH1-4 or the CH2-4 gallibody frames, as they all had similar avidities for MA binding. Notably, only natural mixtures of MA were used as antigens in this study. Cross-reactivity with cholesterol was merely used when a control indicator of antibody activity was required when using clone 12.

3.1.1 Detection of anti-mycolic acid antibodies

In order to characterize anti – MA antibodies, a study was conducted by Ndlandla (25) using guinea pigs. Guinea pigs as animal models are preferred for studying TB infection due to the similarity to humans of infection by *M.tb* inhalation and expression of CD1 proteins required for lipid antigen presentation. In contrast, animal models such as mice and rats can only develop acute TB upon infection and do not express that class of CD1 molecules that present MA in primates and humans (25, 151). Ndlandla could detect anti-MA antibodies in guinea pigs within one week of experimental intratracheal *M.tb* infection. When guinea pigs were exposed to *M.tb* by inhalation of air extracted from TB patient wards in a TB hospital, they became latently infected and

no anti-MA antibodies could be detected. This ability to distinguish between latent and active TB is significant in order to improve TB diagnostics for purposes such as screening of health care workers against nosocomial infection and to assess the success or failure of treatment (25).

Anti-MA antibodies are natural antibodies of low avidity (131). This low avidity complicates sensitivity of detection (152). Previous research done within our group demonstrated the low avidity of anti- MA antibodies by means of ELISA (79, 86), thus failing to provide a clear and reproducible signal from anti-MA antibodies in human sera. This is because ELISA makes use of a wash step after antibody-antigen contact, which may remove the low avidity antibodies to the point of making them undetectable (131, 152). This problem was solved by Thanyani *et al*. (153) by using biosensor-based technology. It makes use of immobilised liposomes (carrying MAs) to coat the gold-plated sensor surfaces, which are then used to monitor the binding of anti-mycolic acid antibodies by optical biosensor technology (153). This test was named the Mycolic Acid Antibody Real Time Inhibition (MARTI) assay. The assay was evaluated with 61 patient sera samples spread across HIV positive, HIV negative and TB positive and TB negative patients. The overall specificity of the assay was initially calculated to be 48.4% and sensitivity was 86.7% (153), a number that was probably pessimistic due to the underestimation at that time of the number of false negative patients in the HIV positive cohort that were tested with mycobacterial culture from sputum. With the modern knowledge of 30% underestimation of TB positiveness by mycobacterial culture growth in HIV-co-infected humans, the assay was recalculated with this compensation in mind. This improved the specificity to 76.9% (153).

The MARTI test, however, only remains suitable for use in a TB reference laboratory. This is due to the requirement of highly skilled laboratory staff, equipment and an air-conditioned, dust free environment. Developments are being made in converting the biosensor method into a more user-friendly process using electro-impedance spectroscopy (EIS). The MARTI TB diagnostic process on evanescent field biosensor and EIS was patented by our group in 2005 and 2016 (154, 155, 156). The EIS method describes a process for coating the MA antigen onto a gold screen printed electrode and checking for the presence of MA by measuring a change in the cyclic voltammetry profile from uncoated to coated, followed by detection of antibody to MA by electro-impedance spectroscopy (155). There are still some challenges to overcome before

EIS can be implemented as a reliable POC TB diagnostic. These include reproducibility of electrode manufacturing and MA solvent compatibility for automated MA antigen immobilization on the electrodes (74). It would be desirable if the principles of the MARTI test could be expanded for reconfiguration in a simple format such as a lateral-flow immunoassay (84) that is better suitable for screening of large numbers of patients in POC settings, especially in rural areas (81). Recently a follow up study on the use of anti-mycolic acid antibodies for TB detection was published by Jones *et al.* in 2017 (157). In their study the authors made use of synthetic MAs linked to trehalose for detection of the biomarker antibodies, thereby illustrating that the sensitivity and specificity of the ELISA based test can be improved by using a range of mycolic acid antigens linked to trehalose. The promising results gained by the detection of biomarker antibodies to MA led our group to conduct further research into the antigen and its potential application for improving TB diagnosis.

3.1.2 Chapter outline

This study investigated how freshly produced and isolated MA can be optimally immobilized as antibody capture reagent in an immunoassay-based TB diagnostic. In chapter 2, it was found that the scaling up of MA purification resulted in a previously unknown quantity of MA remaining in the acetone waste after the last step of acetone precipitation of the MA to remove remaining impurities co-isolated by CCD. It was therefore appropriate to investigate the antigenic nature of the MA dissolved in the acetone filtrate (AcF) waste from the purification process with the use of anti – MA gallibodies. It is known that the strongly hydrophobic nature of MA makes them insoluble in water and water miscible organic solvents (85). Hitherto, there is no evidence to be found in literature that mycolic acids may be soluble in acetone.

3.2 Materials and methods

3.2.1 Materials

Gallibody purification column: Nickel-nitrilotriacetic acid agarose resin (QIAGEN®, Hilden, Germany)

Nunc MaxiSorp® ELISA flat bottom 96 well plates (Thermo Fisher Scientific, Massachusetts, USA)

Thin layer chromatography (TLC) plates: TLC silica gel 60 F_{254} 20 x 20 cm (Merck, Kenilworth, New Jersey, USA).

Desiccator: Duran desiccator with flat flange and knobbed lid (Merck, New Jersey, USA). Blue silica gel as the drying agent which turned yellow when saturated with water vapour. (Merck, New Jersey, USA)

3.2.2 Reagents

Phosphate buffered saline (PBS) 20X, pH 7.4: Prepared by dissolving 160 g of Sodium chloride (NaCl), potassium chloride (KCl, 4 g), di-hydrogen potassium phosphate (KH_2PO_4, 4 g) and di-sodium hydrogen phosphate (Na_2HP0_4, 28 g) in a total of 800 ml of autoclaved double distilled deionised (ddd) water (ddd H_2O) while stirring. The volume was brought up to 1 L and filtered through 0.2 µm cellulose acetate filters.

PBS (1 X) was prepared by adding 50 ml of 20 X PBS to 900 ml of autoclaved ddd H_2O. The pH was adjusted to 7.4 with 1 M HCl, after which the volume was made up to 1000 ml with ddd H_2O.

Lysis buffer (10X): Na_2HPO_4 was made to concentration of 0.5 M and NaCl to a concentration of 3M in ddd H_2O. Lysis buffer (1X) was prepared by adding 5 ml of 10X lysis buffer to 45 ml of ddd H_2O.

Elution buffer 1: NaCl (0.3 M), 0.05 M Na_2SO_4 and 0.01 M imidazole ($C_3N_2H_4$, Sigma-Aldrich, Missouri, USA) in ddd H_20.

Elution buffer 2: NaCl (0.3 M), 0.05 M Na_2SO_4 and 0.02 M imidazole in ddd H_2O.

Elution buffer 3 and 4: NaCl (0.3 M), 0.05 M Na_2SO_4 and 0.25 M imidazole in ddd H_2O.

Block buffer pH 7.4: Biochemical reagent casein (2% (m/v), Calbiochem, EMD Biosciences (USA)) dissolved in 1 X PBS pH 7.4.

Dilution buffer pH 7.4: Casein hydrolysate (4% (m/v)) dissolved in 1 X PBS pH 7.4 and 0.1% (v/v) Tween20 (Sigma-Aldrich, Missouri, USA).

Wash buffer pH 7.4: PBS 1X, pH 7.4 and 0.1% (v/v) Tween20.

Secondary antibody conjugate: Goat anti-chicken Fc: HRP diluted 1:1000 in 4% Casein hydrolysate/1 X PBS -0.1% Tween 20, pH 7.4 (AbD Serotic, Kidlington, UK).

Sulphuric acid (1 M H_2SO_4): In a fume hood, 1 ml concentrated sulphuric acid was added to 17 ml dddH2O while stirring continuously.

TLC developing solution: Phosphomolybdic acid (10% m/v Merck, New Jersey, USA) dissolved in 99.9 % (v/v) ethanol. Stored at 4 °C until further use.

Tetramethyl Benzidine (TMB) HRP substrate solution: Life Technologies, California, USA

Acetone: (purity 99.5%, Sigma-Aldrich, Missouri, USA).

Mycolic acids: Self purified (see chapter 2). Aliquotes of 1 mg stored at 4^{o}C and thawed just before use.

Gallibody purified from the 50 ml aliquots frozen culture media provided by Heena Ranchod (see chapter 2) and concentrated to 50 µl aliquots in 0.1 M Borate buffer pH 7.4. Stored at -20^{o}C, thawed once only for use.

Alanine: DL-Alanine (purity 99%, Sigma-Aldrich, Missouri, USA).

3.2.3 Purification of gallibodies

Gallibody clone types 12CH1-4, 12CH2-4, 16CH1-4, 16CH2-4, 18CH1-4 and 18CH2-4 were purified according to Ranchod (140) using nickel affinity columns. An amount of 5 ml of cell culture media containing the gallibodies was diluted with 45 ml 1X lysis buffer before being passed through the column. The eluent was passed through the column a second time, before discarding the eventual flow-through. The column was washed twice with 1 X lysis buffer and proteins retained in the column were eluted in 1 ml fractions using the elution buffers 1, 2, 3 and 4, in that order. Borate buffer was added in a 1:1 ratio to the purified gallibodies before concentrating by ultrafiltration-centrifugation at 3500 x g for 20 min using Vivaspin 10 000 MW PES centrifugation units (VivaScience, Satorius Group, United Kingdom. Protein concentration was determined by Bradford assay.

3.2.4 Enzyme-Linked ImmunoSorbent Assay (ELISA)

The ELISA is a method used in this study to detect and characterize gallibodies of interest by making use of MA immobilized by adsorption to the surface of a micro titre plate well. Indirect ELISA is a two-step process were the primary antibody binds coated antigen and are then detected indirectly via a secondary enzyme labelled anti-immunoglobulin antibody that binds to the primary antibody (86). In this project, only indirect ELISA was used. This process is outlined in Figure 14.

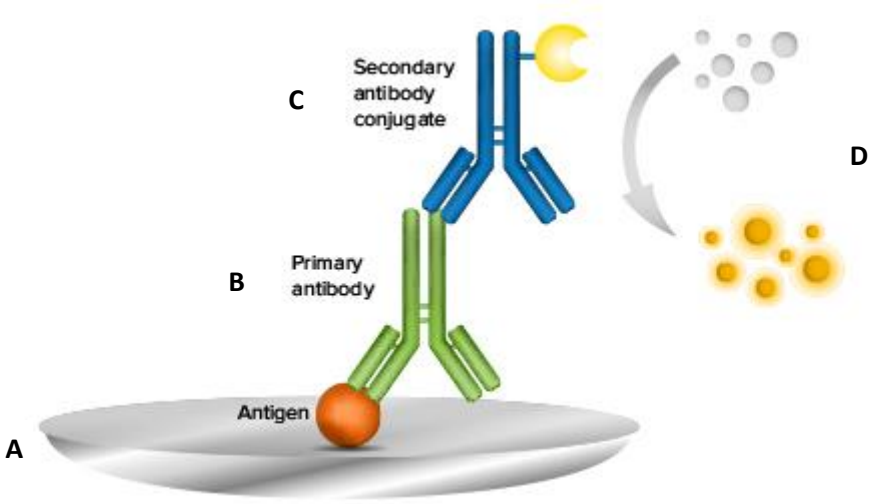

Figure 14: **Schematic of an Indirect ELISA.** (A) Coating of plate with antigen; (B) Binding of primary antibodies from serum; (C) Binding of secondary enzyme labelled antibody; (D) Enzyme reaction for conversion of substrate into coloured product at the end.

Standard ELISA protocol was performed as follows: ELISA plates were coated with a 0.25 mg/ml solution of purified MA in freshly distilled n-hexane or hexane alone as a background control (50 µl per well, using a glass Hamilton® syringe). Hexane was allowed to evaporate at room temperature, before the coated plates were stored at 4 °C until further use within one week. Non-specific binding sites of each well were blocked with 300 µl block buffer for 2 hours at room temperature and then washed three times with wash buffer. The wells were then incubated for 1 hour at room temperature with 50 µl of gallibody diluted in the dilution buffer. Unbound antibodies were removed by washing the wells with wash buffer as above. Secondary antibody conjugate solution was diluted in dilution buffer before adding 50 µl to each well and the plates incubated for 1 hour at room temperature. The conjugate solution was

discarded and the plates washed as above. The signal was developed by adding 50 µl of TMB to each well and then incubated at room temperature for 5 min. To stop the reaction, 50 µl of 1 M H_2SO_4 was added to each well. Plates were read at 450 nm (Thermo Electron Corporation Multiskan EX plate reader). (All buffers described above in section 3.2.2)

3.2.5 ELISA on MAs and AcF

An ELISA plate was coated with either 50 µl MAs (0.25 mg/ml) dissolved in freshly distilled hexane, 50 µl AcF (0.25 mg/ml) dissolved in hexane, 50 µl MAs (0.25 mg/ml) dissolved in hot phosphate buffered saline (PBS) at 80ºC or 50 µl AcF (0.25 mg/ml) dissolved in hot PBS at 80ºC. Hexane and PBS only were coated as negative antigen controls. The plate was incubated overnight at 4ºC to ensure complete coating. Because the PBS does not evaporate, the PBS coated portion of the plate was washed 3 times with wash buffer before adding block buffer and incubating at room temperature for 2 hours. Gallibody 18CH1-2 and 18CH2-4 diluted in dilution buffer to 0.25 mg/ml were selected as the primary antibodies. The steps of primary antibody and secondary antibody conjugate exposure followed by colour development with TMB solution and stopping of the reaction with sulphuric acid was carried out as described in Section 3.2.4

3.2.6 Immuno-blot test of AcF

Immunoblot tests are enzyme immunoassays, normally on a nitrocellulose membrane, but for the purpose of this study the immunoblot test was conducted on silica TLC plates. Antigens were immobilized on the silica plate. If antibodies specific to the immobilized antigen are present in the sample, they bind to the molecule on the plate. Visualisation of binding is achieved by a conjugated enzyme-HRP TMB substrate conversion to a colour product that falls out of solution at the site where the conjugate is bound to its immune complex on the plate.

A spotted concentration of 2 mg/ml of the AcF was separated by TLC as previously described in section (2.2.6), but without staining with phosphomolybdic acid and charring. On the same silica plate, but after TLC, 10 µl of cholesterol (2 mg/ml) dissolved in hexane, MAs (2 mg/ml) dissolved in hexane and AcF in hexane (2 mg/ml)

were spotted. The plate was immersed in block buffer and incubated for 2 hrs at room temperature.

The ELISA protocol (section 3.2.4) was then applied to the plate with the following changes: The immunoblot test was carried out in a petri dish instead of an ELISA plate. The plates were immersed in the buffer solutions enough to completely cover the plates. Gallibody 12CH1-4 and 12CH2-4 were separately diluted in dilution buffer to 0.25 mg/ml and applied as the primary antibodies. The buffers for developing the plates further are described in section 3.2.2, using the same number of washes in between as for ELISA. The eventual colour development on the silica plates was photographed using a mobile camera to record the results.

3.2.7 Gallibody concentration optimization

An ELISA plate was coated with 50 µl of MAs (self-purified) dissolved in distilled hexane to a final concentration of 0.25 mg/ml and distilled hexane only as a control.

Gallibody 12CH1-4 was chosen as the primary antibody and diluted in dilution buffer to concentrations of 0.5 mg/ml – 0.002 mg/ml.

The ELISA protocol (section 3.2.4) steps of primary antibody and secondary antibody conjugate exposure followed by colour development with TMB solution and stopping of the reaction with sulphuric acid was carried out as described with the following changes. biochemical reagent casein was used at 2% (w/v) as the blocking buffer. For the dilution buffer biochemical reagent casein was used at 2% (w/v) with 0.1% (v/v) Tween 20.

All buffers for ELISA/Immunoblot tests that follow have the biochemical reagent casein replaced with casein hydrolysate in the block and dilution buffers.

3.2.8 Comparison of commercial and self- purified MA

An ELISA plate was coated with 50 µl of MA (Sigma Aldrich, USA and self-purified) in freshly distilled hexane to a dilution range of 0.1 mg/ml – 0.5 mg/ml.

Gallibody 12CH1-4 was chosen as the primary antibody and diluted in dilution buffer to concentrations of 0.031 mg/ml.

The ELISA protocol (section 3.2.4) steps of primary antibody and secondary antibody conjugate exposure followed by colour development with TMB solution and stopping of the reaction with sulphuric acid was carried out as described.

3.2.9 Alanination of MA in acetone

To investigate whether the observed solubility of MA in acetone was due to ionisation of mycolic acid to mycolate, a 200 µl solution of 0.5 M alanine / 50% aqueous EtOH was added to 1 mg MA in a vial labelled **1**. For a control without alanine, 50% aqueous EtOH was added to 1 mg MA in a vial labelled **2**. Vials 1 and 2 were heated for 1 hr at 90^{o}C on a heating block (Reacti-Therm Thermo Scientific Pierce III, USA), while vortexing occasionally. After 1 hour, the vials were removed from the heating block. Once cooled to room temperature, 1.8 ml of dddH_2O and 2 ml of chloroform were added to both vials, vortexed (Velp Scientifica Wizard Advanced IR Vortex Mixer, Italy) and left standing at room temperature to allow for separation into two phases. Once a clear upper and lower phase was achieved in both vials, the alanine containing upper phase was removed by careful pipetting and 2 ml dddH_2O added to each of the two vials. This was vortexed and left to separate as before. This procedure was repeated 4 times. After the 5th water extraction, the upper phase was finally removed from each vial and the vials placed on the heating block at 80^{o}C were there was a flow of nitrogen gas to allow the chloroformic contents of the vials to evaporate to dryness. Both vials were stored in a desiccator overnight to allow complete desiccation before weighing.

3.2.10 ELISA Analysis of alaninated MA's

An ELISA assay was done on MA/Alanine and MA/non-Alanine samples described in section 3.2.9.

ELISA plates were coated with 50 µl pure MAs and MA/Alanine and MA/non-Alanine described above, dissolved in freshly distilled hexane with a decreasing two-fold dilution range of 0.25 mg/ml – 0.0625 mg/ml, calculated as if each vial still contained the original 1 mg of MA. Samples were coated in triplicate.

Gallibody 12CH1-4 was chosen as the primary antibody and diluted in dilution buffer to concentrations of 0.031 mg/ml.

The ELISA protocol (section 3.2.4) steps of primary antibody and secondary antibody conjugate exposure followed by colour development with TMB solution and stopping of the reaction with sulphuric acid was carried out as described.

3.2.11 Mass spectrometry of alaninated MA

Samples for mass spectrometry analysis (MS) were prepared as previously done in section 3.2.9: 200 µl solution of 0.5 M alanine / 50% aqueous EtOH was added to 1 mg MA in a vial labelled **1**. For a control without alanine, 50% aqueous EtOH was added to 1 mg MA in a vial labelled **2**. Vials 1 and 2 were heated for 1 hr at 90^{o}C on a heating block (Reacti-Therm Thermo Scientific Pierce III, USA). After 1 hour, the vials were removed from the heating block. Once cooled to room temperature the vials placed on the heating block at 80^{o}C where there was a flow of nitrogen gas to allow the contents of the vials to evaporate to dryness.

Samples described above were sent to Dr Lynne Pilcher to be analysed by LC-MS. The method is described below:

The samples were dissolved in ultra purity lc methanol (Romil-UpS™ Microsep, South Africa). Analysis was performed using flow injection analysis (FIA); the flow rate was set to 0.4 ml/min and the injection volume was 5 µl. Ultra purity methanol spiked with 0.1 % formic acid (Fluka® Analytical, Sigma-Aldrich, South Africa) was used throughout the 1 min run.

Compound detection was performed using a Waters® Synapt G2 high definition mass spectrometry (HDMS) system (Waters Inc., Milford, Massachusetts, USA). Samples were analysed using flow injection analysis (FIA). The system comprises a Waters Acquity Ultra Performance Liquid Chromatography (UPLC®) system hyphenated to a quadrupole-time-of-flight (QTOF) instrument. The system was operated with MassLynx™ (version 4.1) software (Waters Inc., Milford, Massachusetts, USA) for data acquisition and processing. An internal lock mass control standard, 2 pg/µl solution leucine enkephalin (m/z 555.2693), was directly infused into the source through a secondary orthogonal electrospray ionisation (ESI) probe allowing intermittent sampling. The internal control was used to compensate for instrumental drift, ensuring good mass accuracy.

The source conditions were as follows: the capillary voltage for ESI was 2.8 kV and 2.6 kV for positive and negative mode ionisation. The source temperature was set at 110 ºC, the sampling cone voltage at 25 V, extraction cone voltage at 4.0 V and cone gas (nitrogen) flow at 10.0 L/Hr. The desolvation temperature was set at 300 ºC with a gas (nitrogen) flow of 600.0 L/Hr.

Mass spectral scans were collected every 0.3 seconds. The raw data was collected in the form of a centroid profile. Mass to charge ratios (*m/z*) between 50 and 1 200 Da were recorded.

3.2.12 Determining the solubility of MA in acetone

To characterise the solubility of MA in acetone, 2 vials (**i** and **ii**) each containing 1 mg MA and 2 ml of acetone were heated for 5 min at 90ºC on a heating block (Reacti-Therm Thermo Scientific Pierce III, USA). Each vial was shaken by hand to mix and was left at room temperature to cool. After 1 hr the MA/acetone solution of the first vial (**i**) was transferred by pipetting to a clean brown glass vial (**iii**). After 4 hours the MA/acetone solution of the second glass vial (**ii**) was transferred to a clean brown glass vial (**iv**). The four vials were placed on the heating block at 80ºC where there was a flow of nitrogen gas to allow the contents of each vial to evaporate and dry. All vials were stored in a desiccator overnight at room temperature to allow complete desiccation before weighing.

ELISA plates were coated with 50 µl pure MAs and the residual MAs from vials **i-iv** from the previous step, calculated as if the original 1 mg of MA was still present in each vial. The residual MA in the vials were first dissolved in freshly distilled hexane to a decreasing dilution range 0.25 – 0.1 mg/ml. All samples of MA were coated in triplicate

Gallibody 12CH1-4 was chosen as the primary antibody and diluted in dilution buffer to a concentration of 0.031 mg/ml.

The ELISA protocol (section 3.2.4) steps of primary antibody and secondary antibody conjugate exposure followed by colour development with TMB solution and stopping of the reaction with sulphuric acid was carried out as described above.

3.3 Results

The scope of opportunity provided by the newly developed gallibodies for MA probing (86) is vast and goes far beyond its ultimate purpose of providing a labelled displacement marker for lateral flow immune detection of TB biomarker antibodies in POC TB diagnostics. We first interrogated their application in an analytical immunoassay method to monitor the efficiency of counter current distribution (CCD) purification of the natural mixture of MA from crude extracts of mycobacterial growth. Previously this was done with high performance liquid chromatography (HPLC) to determine where the MA activity resides during purification, but due to the discontinuation of production of the high molecular weight lipid marker and the high cost of running and maintaining HPLC facilities our group resorted to the fast and affordable, but much less specific thin layer chromatography (TLC) to monitor the purification. TLC worked great for confirmation of the presence of MA in fractions when the specific MA spot was previously confirmed of its identity by means of HPLC, but left a lot of guess work in complex fractions where the identity of the various overlapping TLC separated spots required fresh identification of the desired MA compounds. The ease, reproducibility and scale-up possibilities of manufacture of the anti-MA monoclonal gallibodies, combined with their proven analytical properties in immunoassay promises potential to have HPLC replaced by immunoassay for quantitative MA determination in the fractions obtained during and after CCD purification of MA. Moreover, by employing the gallibodies during the MA production and isolation processes, an additional quality check is gained by being able to ensure that functional MA antigenicity is retained during the purification process. This depends on the conformational folding of the merochain relative to the mycolic motif of MA, which HPLC cannot detect.

3.3.1 ELISA assay analysis of the ultimate CCD purification step of MA: acetone precipitation

As mentioned in chapter 2, it was never before directly explored whether any MA was retained in the acetone filtrate fraction after acetone precipitation of the CCD purified MAs. The recent development of anti-MA recombinant antibodies (gallibodies) made this possible. From the six available gallibodies that could be used for this purpose,

clone 18 derivatives were selected simply for their availability at the time, as any other gallibody clone would have served the purpose equally well. The first aim was to indicate if there was a significant amount of MA left in the AcF fraction after MA precipitation with acetone. AcF (acetone soluble MA purification waste) and acetone precipitate (purified MA) was coated from two different solvents: hexane - is the standard coating solvent used for ELISA assays in our research group - and hot PBS, which is a water-based solvent, but was shown previously to also work (79). The gallibodies 18CH1-4 and 18CH2-4 were used to probe the AcF and acetone precipitated MA obtained in section 2.2.11 of Chapter 2. Results of the ELISA are shown in figure 15.

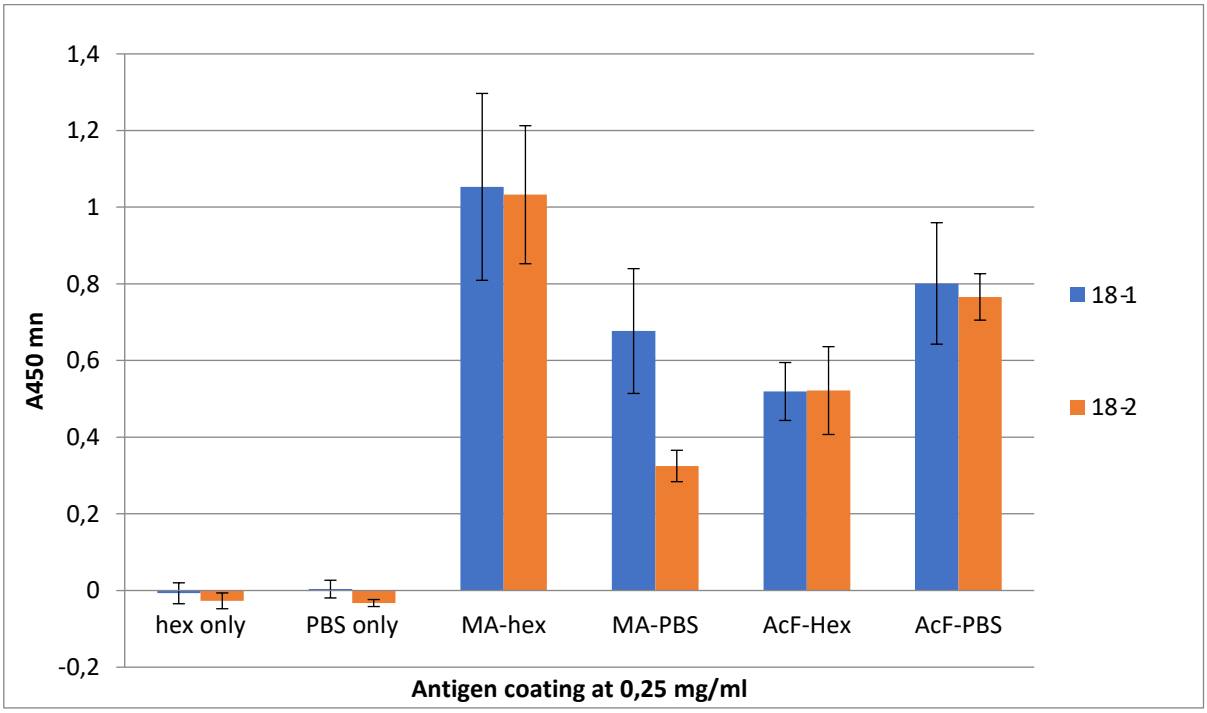

Figure 15: **Indirect ELISA assay to determine the presence of MA in AcF and acetone precipitate fractions in the last step of CCD purification of MA.** The ELISA plate was coated with MA and AcF samples described in section 3.2.5 at 0.25 mg/ml. Hexane (Hex) and PBS coated wells served as the background control. The MA was detected by either gallibody 18 CH1-4 or 18CH2-4. Error bars = Standard deviation, n = 4 (biological repeats).

Figure 15 shows that both AcF and acetone precipitated MA at a concentration of 0.25 mg/ml were able to bind to gallibody 18CH1-4 and 18CH2-4. The hexane and PBS negative antigen controls show no non-specific binding of antibody reagents used.

As anticipated, the two gallibody types did not differ much in their detection capability of MA. This is unequivocally the case where hexane was used as MA solvent, which also showed the anticipated stronger binding signal in the “pure” precipitated MA, compared to the “unpure” MA in the AcF. The same conclusion could not be drawn when hot PBS was used as MA solvent, demonstrating the reason why our group moved away from this method of MA coating with its inherent lack of reproducibility due to preliminary clotting of MA as it comes out of hot aqueous PBS solution during the coating procedure. The MAs in acetone precipitate present themselves better when coated in hexane (MA-hex) than when coated in hot PBS (MA-PBS). The opposite is true for the MAs in AcF. It is noteworthy that the AcF gives a high signal (three quarters of the signal given by MAs) even though it is diluted by other contaminants. It is probably these same contaminants that prevent MA from instant crystallisation out of the fast-cooling aqueous PBS solution during coating, making for more reproducible coating.

The conclusion, based solely on the immunoassay results from the better MA coating procedure from hexane, is that a significant amount of MA remains behind in the acetone supernatant fraction after acetone precipitation as the final step following CCD purification of MA. Provided that a reliable MA coating procedure is used, it seems clear that monoclonal anti-MA gallibodies can be used to identify MA in the purification steps of MA from a crude extract.

3.3.2 Immuno-blot test on AcF

A TLC analysis of MA and AcF after acetone precipitation was then done in order to determine which of the many spots of the separated AcF seen in figure 12 of chapter 2 contains MA. This was done by separating the AcF complex by TLC and probing it with gallibody. Non-separated MA, acetone supernatant and cholesterol were spotted as controls and simultaniously probed with gallibodies 12CH1-4 and 12CH2-4. The results are shown in figure 16.

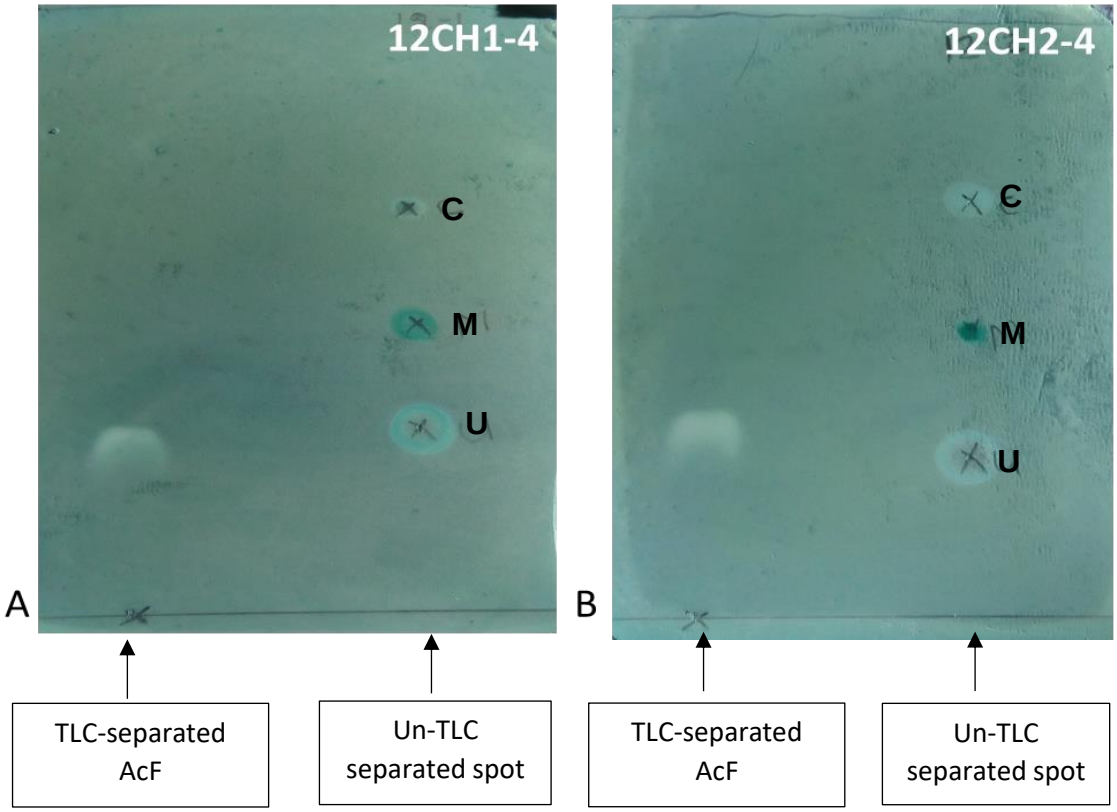

Figure 16: Immuno-blot test on TLC-separated and TLC-unseparated AcF. TLC plates spotted with MA (M), AcF (U) and cholesterol (C) as described in section 3.2.6. Immunodetection of the antigens were done with gallibody 12CH1-4 (A) or 12CH2-4 (B) at 0.25 mg/ml. The left-hand lane in A and B shows TLC-separated AcF whereas the right-hand lane in A and B represents TLC-unseparated immunoblot test spots.

Blue spots indicate the recognition by gallibodies and therefore specific binding. White spots indicate unrecognized water-repelling lipidic antigen and no binding to gallibody. The results of the immunoblot test show that MA spotted onto silica is antigenic at 2 mg/ml as seen by the blue spots at (M) on figure 16A and B. The unseparated AcF is positive for binding (U), but with less intensity compared to the blue spots seen at (M) on both A and B. Gallibody clone type 12CH2-4 is known to recognize cholesterol better than 12CH1-4 in ELISA (56), hence the lesser blue colour on the cholesterol (C) spot in Fig 16 (A) that was probed with 12CH1-4 compared to (B) that was probed with 12CH2-4 (140). When AcF was separated by TLC, it showed that the water-repelling white lipidic component was not stained in either (A) or (B) of Fig 16, meaning that antigenicity was lost by separating it from the other non-covalent complex components that co-purified from CCD.

TLC separation of the acetone filtrate caused the MA to become undetectable by the monoclonal anti-MA antibodies 12CH1-4 and 12CH2-4, while it was clearly visible in the unseparated acetone filtrate. The control spot probing worked out as expected, with both gallibody types binding both MA and cholesterol, as expected. The unstained white smudge seen when the AcF is separated by TLC could be MAs as this smudge is water-repelling lipidic in nature. The white smudge on its own however, is non-antigenic, because it failed to bind the gallibodies. Its antigenicity could have been lost due to a counter-cation that ionizes the MAs to be more polar, but is separated away from the MA during TLC on silica, which can pull apart the compounds through selective hydrogen bonding. The conclusion in this section is therefore that acetone soluble MA was found in the AcF fraction, but that its separation by TLC on silica from other compounds caused its loss of antigenicity. It could be possible that the association with the putative counter-ion is important for correct folding of MA into an antigenic fold. The hypothesis to be tested emanating from this conclusion is that acetone soluble MA could be the ionized carboxylate form of MA, while the free acid MA is precipitated by acetone.

3.3.4 Quantitative ELISA immunoassay with gallibodies and self-purified mycolic acids

Before the investigation into a putative ionized form of acetone soluble MA could continue, it was deemed necessary to first optimize the use of gallibodies in ELISA with an alternative blocking agent, as casein became in short supply due to import restrictions on bovine milk products into South Africa. A method from MSc student Alma Truyts was adopted (147), who reported that the bacterial culture media supplement, casein hydrolysate was shown to successfully replace biochemical reagent casein in the ELISA and was not encumbered by import restrictions. Gallibody type 12CH1-4 was therefore titrated at a decreasing concentration from 0.5 mg/ml – 0.002 mg/ml on a constant MA antigen coat at 0.25 mg/ml. The result is shown is shown in Figure 17.

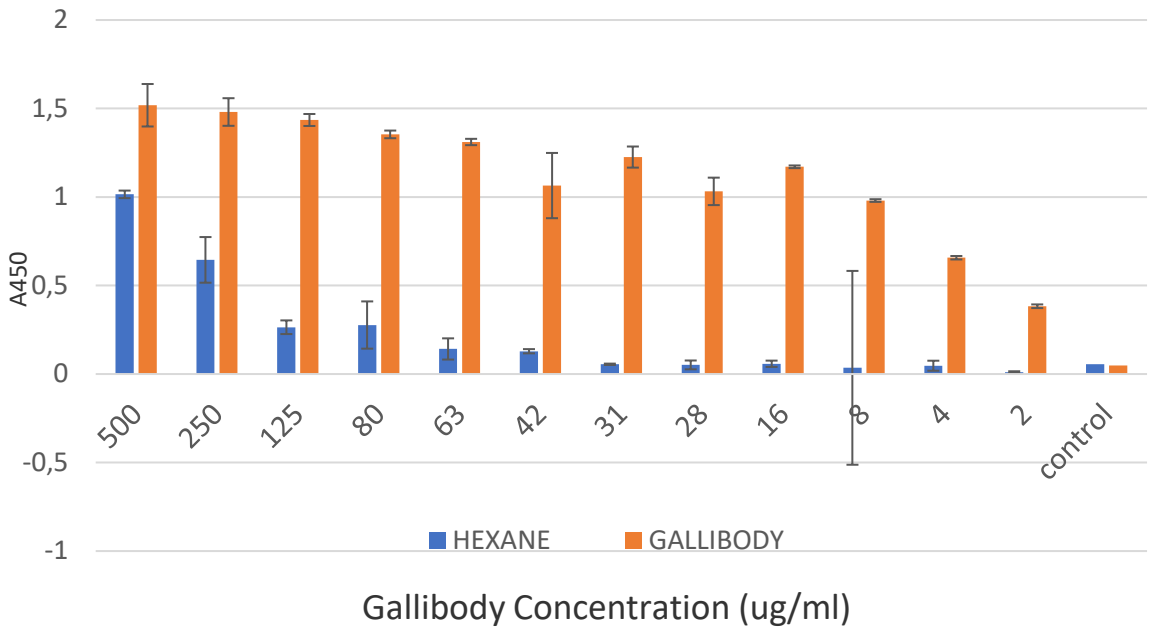

Figure 17: **Indirect ELISA assay to determine the optimum concentration of monoclonal antibody (gallibody type 12CH1-4) for immunoassay with casein hydrolysate as blocking agent.** Decreasing concentrations of gallibody 12CH1-4 incubated on coated MA in hexane (0.25 mg/ml) and hexane only. Coated wells were blocked with 4% casein hydrolysate. MA in hexane (orange bar) or hexane only (blue bar). Error bars = Standard deviation, n = 3 (biological repeats).

The results in figure 17 show that the MA binding signal of the gallibodies remains high at decreasing primary antibody concentration, more or less maintaining a plateau until about 8 ug/ml. Background signal becomes negligent at gallibody concentrations lower than 42 ug/ml. The titre point is at half-maximal signal, i.e. at gallibody concentration of 4 ug/ml. This suggests that a lower concentration of gallibody is preferable to avoid significant background signal when using casein hydrolysate as blocking buffer. From the results, the conclusion was that a safe, optimal 12CH1-4 concentration for quantitative immunoassay on MA antigen coated plates is around 31 ug/ml when using the casein hydrolysate blocking system.

It is known that self-isolated MA is chemically less pure (4% impurities) than commercially available Sigma MA, but gives comparable ELISA signals when using pure casein as a blocking buffer (40). The results obtained for our new batch of self-

isolated MA when using the optimal concentration of 12CH1-4 gallibody with casein hydrolysate as blocking buffer are shown in figure 18.

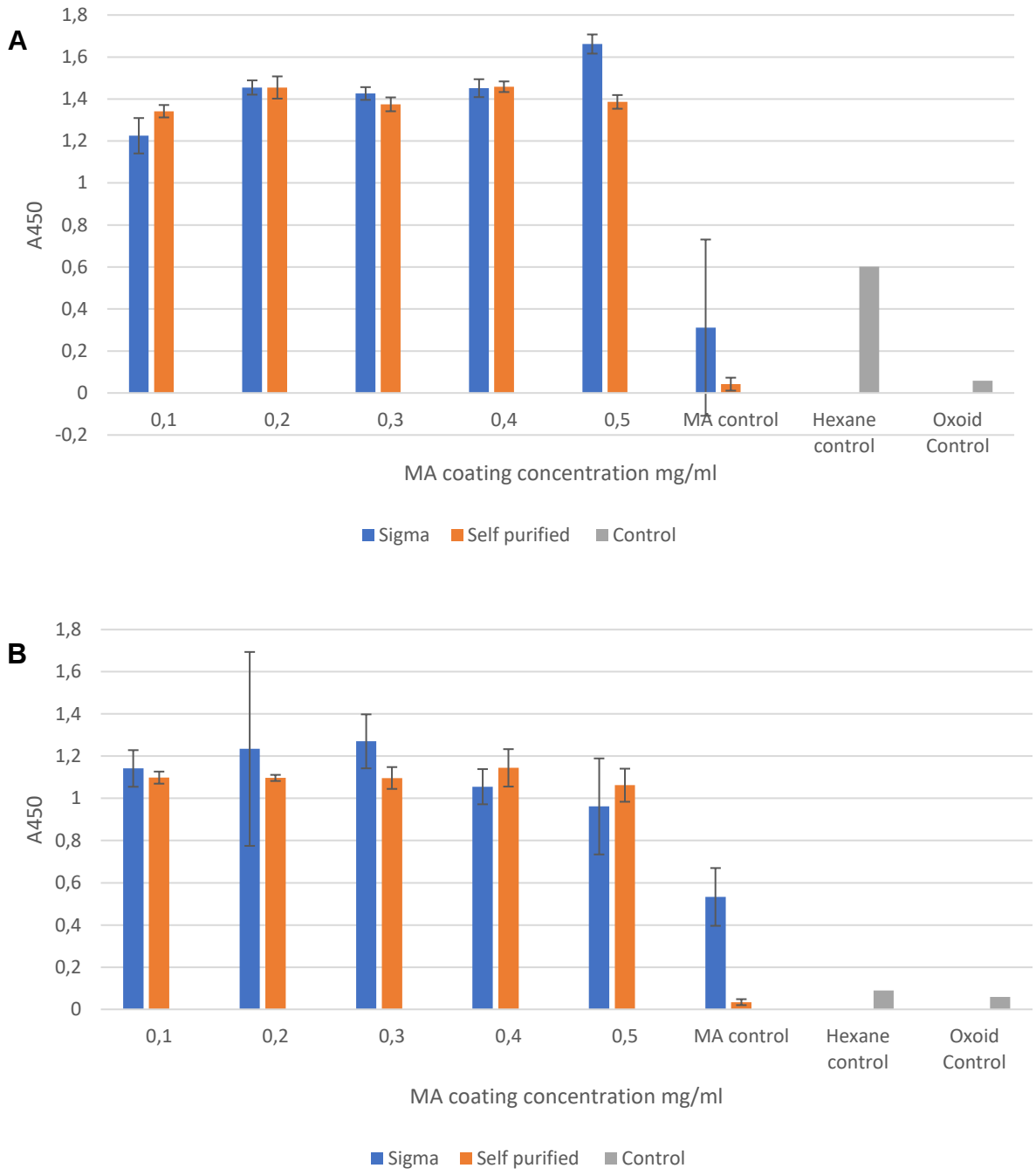

Figure 18: Indirect ELISA assay to compare the reproducibility of gallibody 12CH1-4 analysis of dilution ranges of self-purified and Sigma commercial MA with casein hydrolysate as blocking agent. Increasing coating concentrations of self-purified MA in hexane (orange bar) and commercially purified MA in hexane (blue bar) are shown here in duplicate (A and B) experiments. Coated wells were blocked with casein hydrolysate and incubated with gallibody 12CH1-4 at a concentration of

0.031 mg/ml. Coating with hexane served as negative antigen control. Coating with eitherhexane or MA, but gallibodies substituted with casein hydrolysate served as negative antibody controls and are labelled as Oxoid or MA controls respectively. Error bars = Standard deviation, n = 3 biological repeats.

Figure 18 shows the results of titrated MA coating concentration in a range between 0.1 and 0.5 mg/ml of both Sigma and self-isolated (SI) MA, with 1 well of each concentration incubated without gallibody and averaged as an MA control. The optimal gallibody concentration of 31 ug/ml was used for all. Hexane coated wells incubated with gallibody stand as the hexane control, while the oxoid control depicts hexane coated wells tested without gallibody. As seen in figure 18 A, there was no significant difference between Sigma and SI MA over the concentration range, but some unreproducible background is seen with the MA control for Sigma, and the hexane control. In the repeat of the experiment in figure 18B, no significant difference is again seen between Sigma and SI MAs over the concentration range, but the poorly reproducible background in the MA control of Sigma MA is again observed, while no high background value was obtained in the hexane control. Sigma MA appears to create a less well blocked surface to the secondary antibody-HRP conjugate using the casein hydrolysate blocking buffer. In these experiments the antigenicity of Sigma MA and SI MA is comparable, but the degree of variation tends to be higher for Sigma MA than for SI MA.

3.3.3 Towards generating an ionized mycolate with alanine as counter-ion

Results from figure 15 and 16 prove that there is MA present in the AcF after acetone precipitation of the upscale CCD purified MA (See Chapter 2). The MA in the filtrate possibly exists as the mycolate (more polar), while in the precipitate it is presumed to be the free mycolic acids (less polar). The counter-cation has to be small and organic to allow for hydrogen bonding to occur with the oxygenated functional group in the merochain, permitting the MAs to assume a structure recognizable by gallibodies. This normally happens with the unionized carboxylic acid group in the mycolic motif of MA. An amino acid counter-ion could free a carboxylate group in the vicinity of the mycolic motif to allow the keto- or methoxy group in the merochain to fold and hydrogen bond

to it, thus stabilising the antigenic conformation of MA. This was investigated using alanine as the counter-cation.

Non-covalent alanination of MA was attempted by exposing MA to an excess of alanine in hot ethanol-water to force a zwitter-ionic alanine to associate with its ammonium group to the α-carboxylate of MA within. Chloroform was then added and shaken to force all MA-containing material in the lower organic phase, while all the excess alanine material was forced into the aqueous ethanolic upper phase. The excess alanine was then removed by aspiration of the upper phase, followed by five times addition of water for liquid-liquid extraction of ethanol and free alanine. extracted and the MA dissolved in acetone under high temperature to dissolve the presumed alaninated MA product. This latter transfer of presumed alaninated MA from the reaction vial was repeated five times in order to affect a quantitative transfer of all alaninated and non-alaninated MA to the fresh vial.

Because the weighing of amounts smaller than 1 mg is not quite accurate, each vial was monitored for the presence of MA by solubilizing the content in a fixed volume of hexane (to effect 1 or 0 mg/ml of MA per vial if all or nothing was transferred) to coat ELISA plates. These were then immunoassayed by gallibody 12CH1-4, which would simultaneously then indicate the antigenicity of the residual MA in the vials. Results are shown in figure 19.

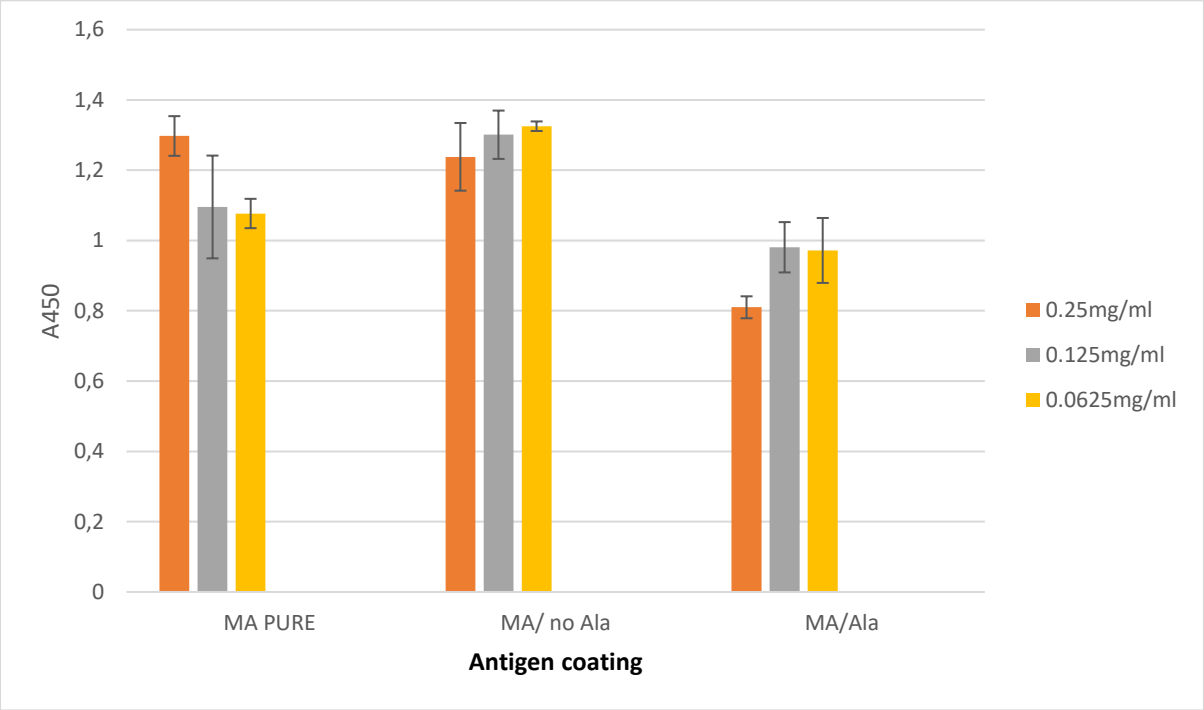

Figure 19: Indirect ELISA assay to evaluate binding and signal detection of a monoclonal antibody to MA/Alanine/acetone, MA/acetone, ELISA of MA/Alanine and MA/no Alanine. The MA coated plates were blocked with casein hydrolysate and probed with primary gallibody 12CH1-4 (0.031 mg/ml). Error bars = Standard deviation with n = 3 (biological repeats).

The p value (calculated using the student's t-test) between MA/Alanine and MA/non-Alanine for each concentration is smaller than 0.05 indicating that there is a significant difference between MA/Alanine and MA/non-Alanine (p value < 0.05). Due to the fact the titrations were not taken to limiting dilution of MA, there is no quantitative indication of the MA content having either alaninated or non-alaninated content. This result prompted the use of MS to determine whether the slight fall in antigenicity of MA/Alanine is really due to alanination of MA or not.

Alanination of MA was further investigated by Mass spectrometry (MS) analysis of alaninated MA compared to non- alaninated MA. Mass spectrometry, which is typically combined with liquid chromatography (LC), discriminates the molecules present in a biological sample according to their mass-to-charge ratio. Each of the peaks in the resulting chromatogram is associated with the characteristic mass spectrum of the metabolite allowing their identification (158). The mass peak for alanine is shown in

figure 20. From this we can identify if alanine is present in the alaninated MA sample. LC-MS analysis of MA samples with and without alanine described in section 3.2.9 was done by Dr Lynne Pilcher. Results are shown in figure 21.

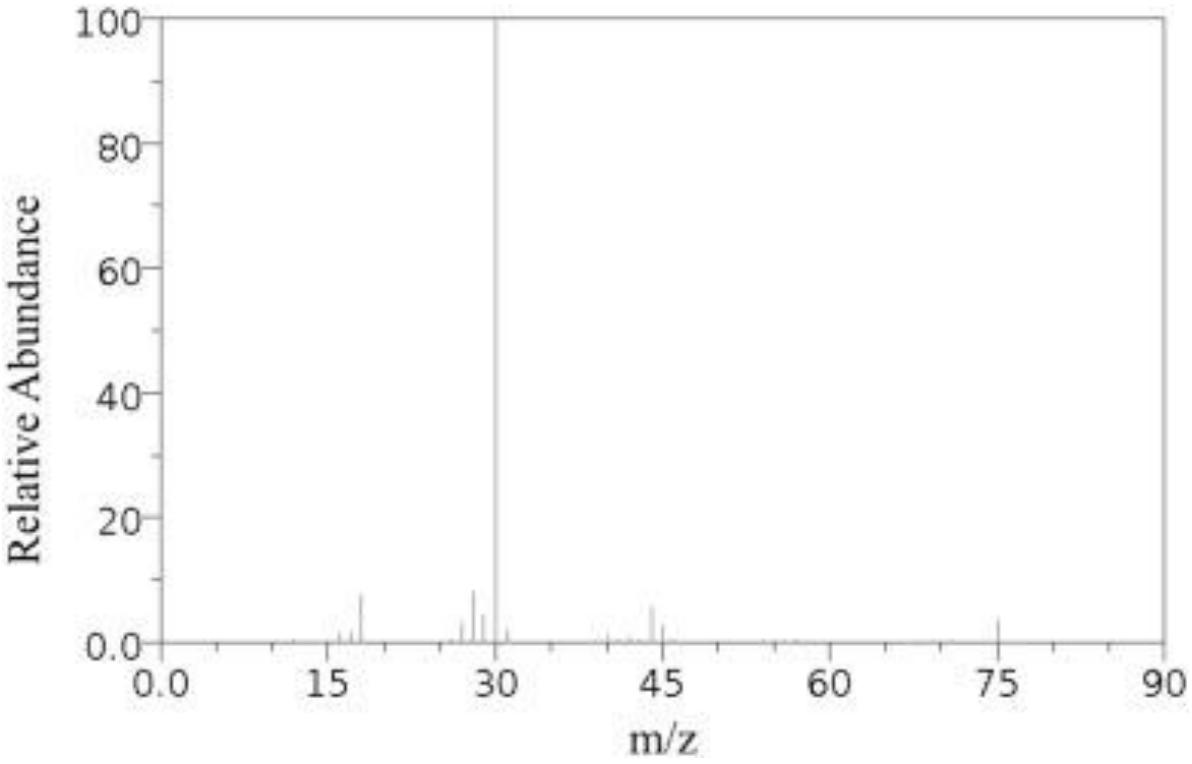

Figure 20: MS spectra of alanine (158)

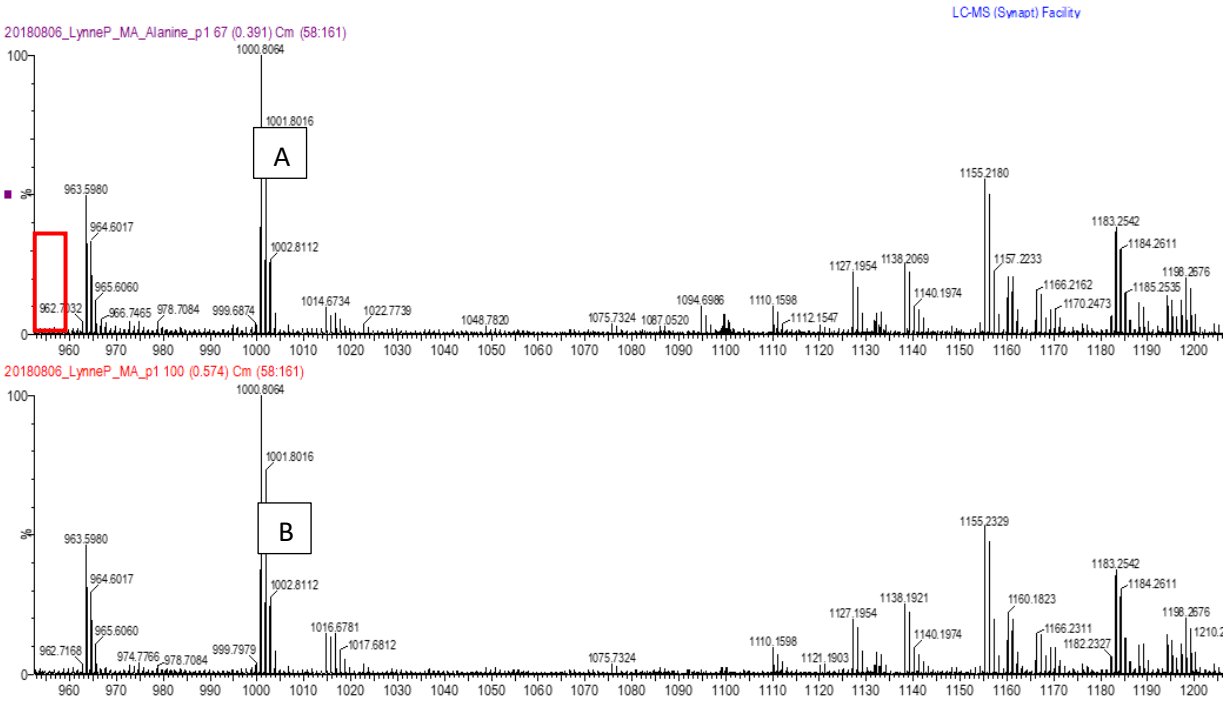

Figure 21: LC-MS chromatogram of the natural mixture of MA prepared with alanine compared with MA without alanine. LC-MS analyses of MA with alanine (A) and MA only (B) carried out in positive ion mode. Red box = position where alanine peaks should appear if present.

From figure 21 it can be seen that the MS profiles of 'alaninated' MA and non-alaninated' MA appeared essentially identical. No alanine peaks were visible, as indicated by the red box which is void of peaks in the "alaninated MA" sample. The LC-MS analysis of the 'alaninated' MA shows no significant difference from non-alaninated' MA and shows no sign of any alanine presence.

The conclusion from this experiment is that the attempt to alaninate MA did not succeed (Fig 21). There was therefore no expectation that acetone solubility of MA at room temperature before or after the alanine treatment was going to be found different. The hypothesis that acetone solubility of the mycolate ion is better than that of the free acid therefore remains untested. Nevertheless, acetone is a preferred solvent to hexane or chloroform for automated antigen printing on lateral flow substrates and screen-printed electrodes. It certainly is also a much more stable solvent than the dimethylformamide that was previously used for coating electrodes with MA for electro-impedance measurement of antibody binding (159). Because no one ever before formally investigated the solubility of MA in acetone, it was deemed useful to

launch a formal investigation into this, starting from hot acetone solutions of MA and allowing these to cool down to room temperature.

3.3.6 Determining the solubility of MA in acetone

To determine the acetone solubility of MA in acetone, the gallibodies were applied in quantitative immunoassay in order to confirm the gravimetric determination of the amounts of MA that can be transferred from a vial in which MA was solubilized in acetone under high temperature and then allowed to cool for a determined time before transfer to a fresh vial.

It is possible to envision the physiochemical properties of the functional groups of MA permitting conformational freedom of the long methylene units in the backbone of MA under high temperatures as it is known that in spite of their high molecular weight, mycolic acids have relatively low melting points and are highly soluble in organic solvents such as chloroform and benzene (149). It therefore stands to reason that the mycolic acids can be solubilized under high temperatures.

Two vials of MA (1 mg each) were set up, the MA dissolved in acetone (2 ml), heated at 90^{o}C for 5 minutes and left to cool for either 1 hour (vial 1) or 4 hours (vial 2). After cooling, the contents of vials were transferred into separate clean vials. These were put onto a heating block at 80^{o}C were there was a flow of nitrogen gas to allow the contents to be evaporated to dryness. The dry vial content was subsequently dissolved in hexane to be analysed by ELISA using gallibody 12CH1-4. Results are shown in figure 22.

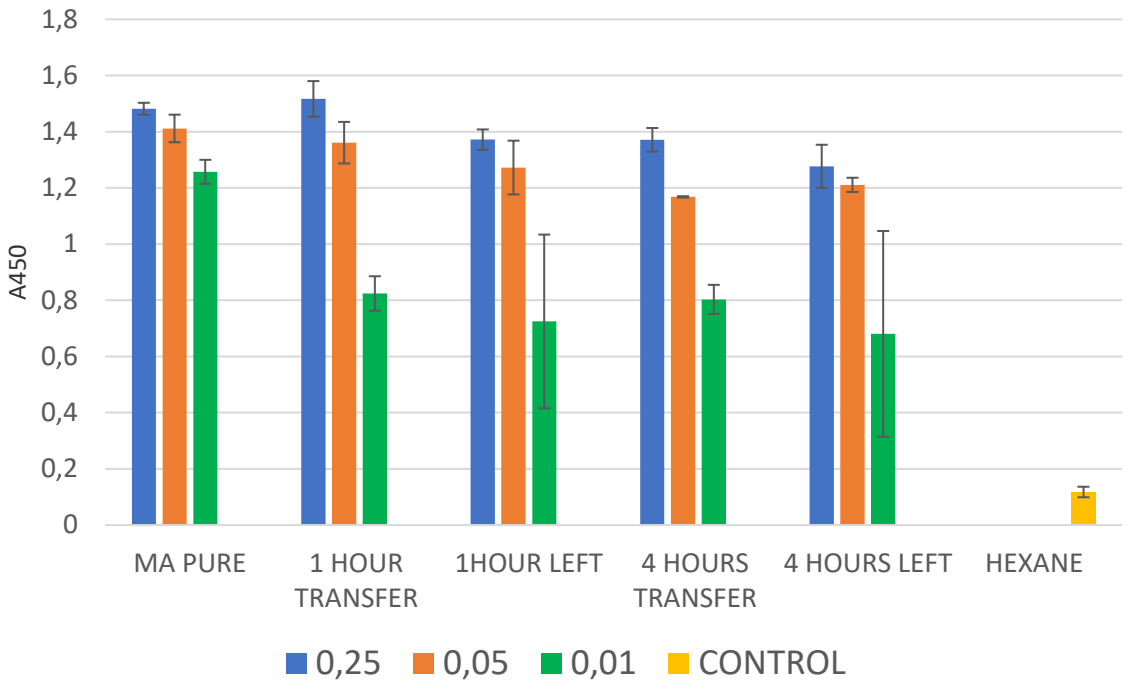

Figure 22: Indirect ELISA assay with monoclonal antibody to evaluate amount of MA remaining in acetone solution for 1hr vs 4hrs after cooling to room temperature, compared to pure MA of the same initial concentration. MA from donor and recipient vials after the indicated cooling time was coated by limiting dilution. These and hexane antigen controls were probed with gallibody 12CH1-4 (0.031 mg/ml) after blocking the antigen coated wells with casein hydrolysate. Error bars = Standard deviation, n = 3 (biological repeats).

From heating MA at 90^{o}C it was observed that MA remains in solution at 1 hour due to the clear solution that was observed. The solution became progressively opaque towards 4 hours after cooling, but the amount of MA that could be transferred remained at around 50% of the original content. The increasing opaqueness with time is most likely due to micellar MA dynamically growing bigger and eventually sedimenting to the bottom of the vial. This means that a solution of MA in acetone is not stable at saturating concentrations and should be applied within 4 hours after cooling, or used at a lower concentration.

From the results of figure 22 it can be seen that the amount of MA that could be transferred and the amount that was left behind was approximately the same for both 1 hour and 4 hours of cooling. This is also true for antigenicity as the ELISA signal is comparable and almost the same to pure MA at the same concentration.

From this one can conclude that MA can be dissolved in acetone at room temperature to a certain limit, of which the first indication is that it is at around 0.25 mg/ml, which would be the maximum, but unstable MA micellar solubility in acetone over a period of four hours after cooling.

3.4 Discussion

It is known that neutral solvents such as acetone removes free lipids because it is used to dissolve oils. Therefore, acetone can be exploited to separate MA from its contaminants. This was confirmed in chapter 2, where it was identified that acetone successfully removed contaminants from the MA precipitate after CCD purification (section 2.3.3). However, quantification of results indicated a 37% loss in MA yield post purification (chapter 2). It was therefore imperative to investigate whether any antigenic MA content could be detected in the acetone filtrate (AcF). If this was to be the case, it could be a possible reason for the MA loss that was observed in the acetone precipitated MA, which would then require retrospective re-assessment of the acetone precipitation step in upscale purification of MA by CCD.

Ranchod *et al*. (86) developed gallibodies that can be used as primary antibodies to detect MA using a horse radish peroxidase (HRP)-conjugated anti-chicken antibody immuno-assay approach (section 3.1). Gallibodies were used to probe the AcF for the presence of MAs. This chapter investigated the content of the acetone filtrate fraction after acetone precipitation of the CCD for the presence of antigenic MAs.

As was seen in figure 15, AcF indeed contained antigenic MAs, which presented themselves better in hot PBS, whereas the MAs in the acetone precipitate presented themselves better in hexane. It can be hypothesized that the culturing method for *M. tb* could therefore have resulted in two different types of MAs that are both antigenic but have different polarities, hence different separation and coating properties. Alternatively, the way that pre-extraction was done before CCD could have allowed more MAs to be converted to mycolate salts with organic cations, allowing solubility in acetone.

An immune-blot test followed to identify the antigenic compound(s). Figure 16 showed that when the compounds of the AcF are TLC separated, then antigenicity is lost,

compared to when merely spotted. The white smudge observed at low Rf on the TLC separation lane of AcF could be the hydrophobic MA, but in a non-antigenic state possibly due to loss of a putative counter-cation to the mycolate that may be required for antigenic folding of the mycolate. It is possible that the silica on the TLC plate is able to pull apart the compounds through hydrogen bonding, separating the lipidic mycolate from its counter-cation. This hypothesis was to be tested by creation of an alanine-mycolate and its antigenic characterisation. However, the ELISA results from figure 19 showed little, albeit a significant difference between MA exposed to alanine in acetone compared to MA not exposed to alanine. The inability to successfully create MA/Alanine was confirmed in figure 21 where a mass spectrometry analysis was done on an MA sample not exposed to alanine compared to sample that was. No traces of alanine could be detected in the putative MA/Alanine product. The hypothesis that a complex of mycolate and an amino acid counter-ion, in this case alanine, improves acetone solubility therefore remains untested.

Subsequently, the hypothesis was tested that mycolic acid in its non-ionized carboxylic acid state is in itself soluble in acetone to a significant degree. MA was dissolved in acetone at high temperature and then allowed to cool. The amount of MA staying in solution was investigated. Figure 22 portrays a quantitative result; MA was titrated down to where a decreasing signal was obtained; thus, indicating comparable MA amounts in the transfer vials and what was left behind as insolubilities in the original vial.

The MA was transferred from one vial to another by pipetting, suggesting that MA that stayed behind stuck to sides of the glass vial. The possibility that the transferred and remaining MAs after acetone transfer are not the same was not investigated. The MA that remain could, for instance, have longer wax chains. Mass spectroscopy could be done on residual MA remaining behind in vials from which MA is extracted and compared to that which is transferred in the first acetone transfer. but research time and budget did not permit a MS analysis at this stage.

It can be also hypothesized that the MA dissolves as dynamic micelles, the nature of which is to be determined in future. This chapter concludes that MA could be solubilized at high temperatures. The MA solvation method in acetone can be used as such within 4 hours after heating. MA solubility is 0.25 mg/ml, probably as a micelle

suspension that coagulates into a sediment after several hours at saturating concentration. The important discovery of solubility of MAs in acetone may overcome challenges in development of lateral flow test. The next chapter explores application of this discovery in an attempt to generate a workable prototype MALIA.

Chapter 4: Towards lateral flow immunodetection of anti-mycolic acids antibodies

4.1 Introduction

In a resource limited, poverty burdened community, proper healthcare is almost non-existent due to lack of transport mobility and access to clinics (160,161). Point of care (POC) testing can be a solution in improving healthcare in such settings. The first reported use of POC testing dates back to 1550 B.C., when ants were used to diagnose glycosuria in patients likely to have diabetes mellitus. As it was then, the goal of POC testing remains to provide immediate and convenient rapid medical testing at or near the site of patient care (162). Lateral flow or Lateral Flow Immunoassay (LFIA) technology is one of the most successful and simple rapid diagnostic testing systems. This form of rapid testing was derived from the latex agglutination test developed by Singer and Plotz in 1956 (161,163). The success of the human pregnancy dipstick test drove the development of early LFIAs. Rapid tests for infectious diseases such as human immunodeficiency virus (HIV-1 and HIV-2), TB and hepatitis B were initially introduced as a dipstick format in developing countries. In the late 1980s, the first immunochromatographic strip (ICS) lateral flow format was introduced for disease diagnosis (161). Since then, the use of LFIA has evolved from the medical field to veterinary, food and agricultural services. The LFIA has grown to become the most popular commercial POC device format with an estimated market size of US$18 billion predicted for 2016 (164,165,166).

However, despite the effort and financial resources that have been invested, POC diagnostics of adequate quality for TB have not yet materialised. A recent WHO/TDR report described and tested 19 commercialised diagnostic tests for TB that measured antibody responses to *M.tb* of which the report deemed all of these to be unsuitable for use due to poor sensitivity and specificity (167,168). The current global challenge is to develop and progress already identified biomarkers into diagnostics with a POC format. As described in chapter 1, employing the use of MA and anti-mycolic acid antibody biomarker in a workable model for diagnosis in a POC environment would fulfil a great need in the management of the TB epidemic.

This chapter will describe the work towards a workable LFIA device for TB diagnosis.

4.1.1 Principle of a lateral flow immunoassay

A LFIA involves the migration of an analyte containing aqueous sample, e.g. blood or serum, by capillary action through a porous substrate over test and control lines/ spots where the binding of the analyte is made visible. Substrate types include nitrocellulose, polymer, paper, or other composite sheet-like materials that facilitate the separation, capture, and detection of the analyte(s) of interest (161, 164). Due to capillary action of flow in a LFIA, no external force such as pumps are required for movement of sample towards the detection zones. Interactions occur from the binding of labelled analyte at specific detection zones containing immobilized antibodies or antigens to produce a signal that can be visualized by colour development (169), fluorescence (170), chemiluminescence (171), electro-magnetic signal generation (172) or optical detection (164).

4.1.2 Components of lateral flow immunoassays

LFIA devices, seemingly simple, consist of vital components, each of which must be fully considered before construction and assembly (164). The high selectivity of the biorecognition element is key for the performance of the assay. Antibodies used in LFIA can be monoclonal, polyclonal, or both, but recombinant monoclonal antibodies are increasingly being used. It is essential that these comply with adequate affinity and specificity (161). Monoclonal antibodies have high specificity, which helps in decreasing false positive reactions by cross-reactivity, while polyclonal antibodies are able to recognize multiple epitopes on a single antigen (161), which increases the sensitivity of the assay. LFIA require antibodies for binding specifically to the target antigen, carrying the label for visualisation. More than one antibody might be used in a single assay, due to the necessity for an adequate antibody control (161). LFIAs are generally composed of four main components: a lateral flow substrate, sample pad, conjugate pad and absorbent pad (wick), which are all assembled onto a backing card for support (Fig. 23). Typically, hydrophobic nitrocellulose (high protein binding), glass fibre (non-protein binding), or cellulose acetate (low protein binding) substrates are used for LFIA (161). Nitrocellulose substrates are the most widely used LFIA

substrate. Factors ascribing to this, besides high affinity for adsorption of proteins, include the variety of pore sizes, ease of wetting, lack of interference with test and control reactions, relatively low cost, commercial availability, good capillary flow characteristics and ease of handling (161, 164). The sample pad is commonly composed of cellulose. The major role of the sample pad is to allow continuous uniform transport of the sample to the conjugate pad (174). The conjugate pad is generally composed of glass fibre and facilitates drying and stabilization of detector agents until test use. These detector agents typically are labelled biorecognition molecules. Labels such as latex beads, colloidal carbon, colloidal gold, fluorescent tags, enzymes, streptavidin, or gold nanoparticles are conjugated with an antibody or an antigen (174). Requirements for a good label are that it should be detectable at very low concentrations and it should retain its properties upon conjugation to antibodies (169). Nowadays colloidal gold is the most widely used label. It is stable, has an intense colour and no development process is needed for visualization (169). An absorbent ‘‘wicking” pad, usually composed of cellulose or cotton, is at end of the test strip and terminates sample flow by having an absorption capacity greater than the sample volume (164). It also helps in maintaining flow rate of the liquid over the substrate and stops back flow of the sample. All these components are fixed or mounted over a backing card (174). A lateral flow device also includes at least two reaction sites, one that responds to the compound to be detected (test line), and a second that is used as a control to ensure correct operation of the device (control line) (174, 175).

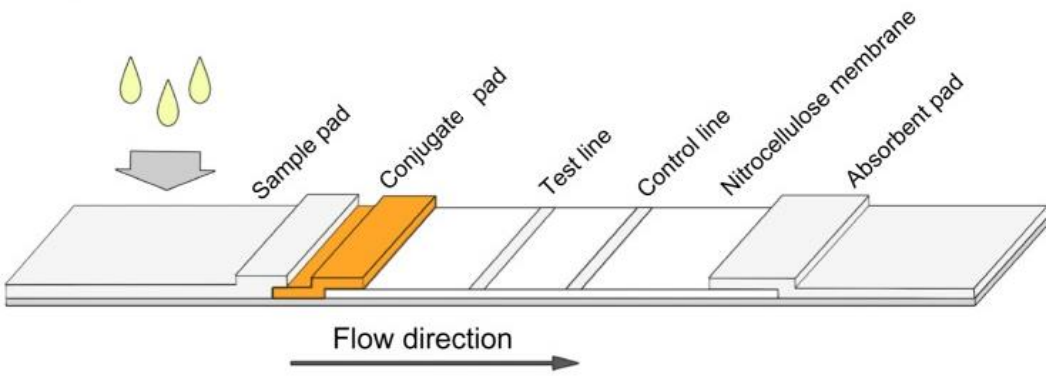

Figure 23: **Schematic showing various components of a general LFIA (**173).

4.1.3 Lateral flow test format

Lateral flow assays can be constructed in either sandwich or competitive formats (177). Sandwich formats are typically used when testing for high molecular weight molecules with multiple antigenic sites or antibodies to infectious agents (176, 177). In this format a positive result is indicated by the presence of a visible test line. In this case excess conjugated particles that aren't captured at the test line will continue to flow towards the control line to be captured by immobilized antibodies (176). This control line typically comprises a species-specific anti-immunoglobulin antibody, specific for the conjugate antibody on the conjugate. Competitive assay formats are typically used to detect low-molecular-weight analyte molecules or analytes with single antigen epitopes such as mycotoxins and antibiotics, which cannot bind to two antibodies simultaneously (176, 177). In this format, a positive result is indicated by the absence of a test line. A control line should still form, irrespective of the result on the test line (176). The two formats are illustrated schematically in Fig 24 (A and B) (176). The competitive format most closely resembles the format for the proposed diagnostic of this study.

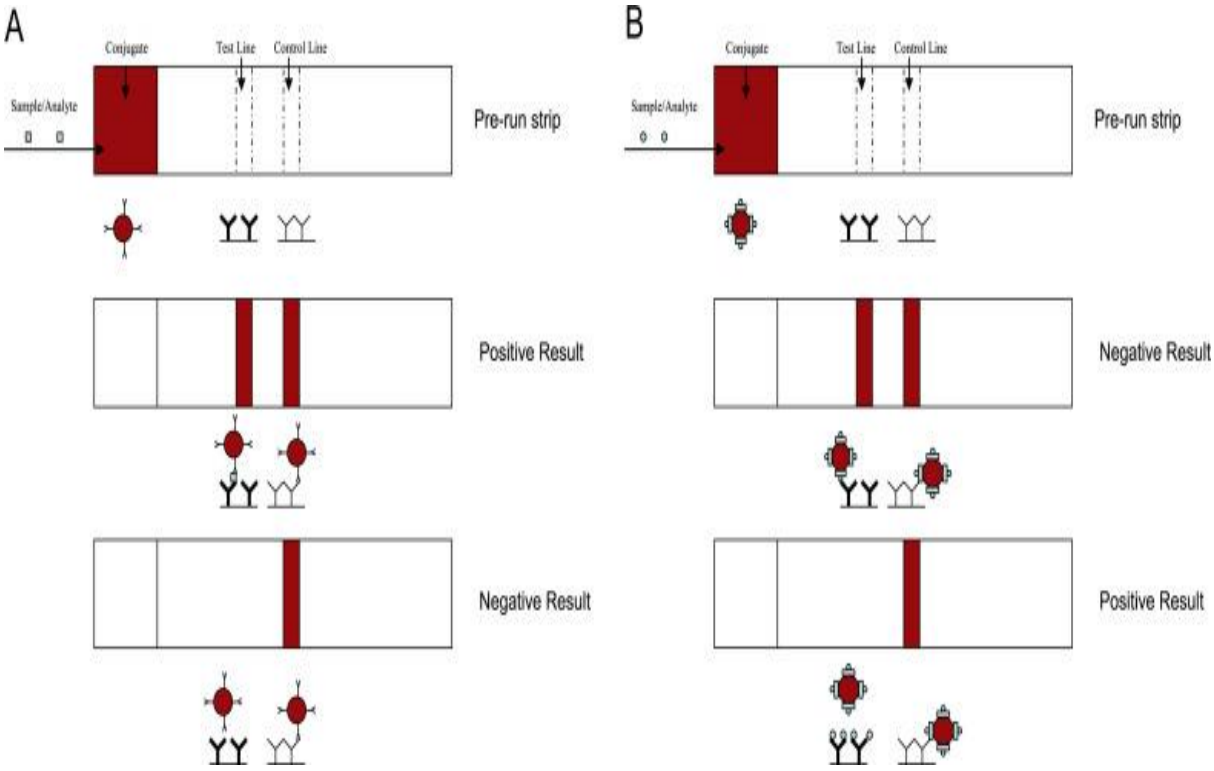

Figure 24: **Mode of action of the sandwich (A) and competitive (B) formats of LFIA** (176).

4.1.4 Use of lateral flow immunoassays in diagnostics

Home pregnancy test strips have been one of the most successful diagnostic immunoassays so far. It measures the human chorionic gonadotropin hormone (hCG) in urine from pregnant women and makes use of three kinds of antibodies i.e., a monoclonal anti-hCG antibody and an anti-immunoglobin G (IgG) (178). The hCG test is an example of a sandwich-based assay where the presence of visible test line indicates a positive result. In this case, anti-hCG antibody, conjugated with labelled particles that can specifically recognize and bond with hCG in the sample. These reactions require a signal molecule to indicate whether the reactions occur or not. The idea of using signal molecules has been used to measure tumour markers such as hepatic carcinoma (178, 179) and to diagnose infectious diseases like AIDS (178).

Examples of current commercial serological assays in the LFIA format include tests for HIV-1/2 or hepatitis C virus (180). These tests have received Clinical Laboratory Improvement Amendments (CLIA) waivers that enable their POC use (180,181). CLIA-waived tests are typically simple and have a low risk for an incorrect result. Several LFIAs have been CLIA approved for the detection of HIV antibodies in blood samples obtained by fingerstick or venipuncture. These tests do not require electricity or skilled technicians and use non-invasive patient sampling (182). A positive rapid HIV screening test can be confirmed by a more accurate laboratory assay, based on similar, but more sophisticated antigen/antibody detection principles compared to the rapid tests (182).

LFIAs for HIV antibodies have been developed for use with oral specimens as well, e.g., the OraQuick Advance rapid HIV-1/2 antibody test (182). OraQuick At-Home HIV test is an FDA approved POC HIV test that has a 92% sensitivity and a 99.98% specificity. In theory, it can cause one false negative in every 12 HIV-infected individuals. The major progress of the diagnostic has been in reducing the negative window period between infection and production of patient antibodies (182). The major advantage learnt from this test is that patients can know their results and start treatment immediately; thereby drastically reducing the number of patients lost for treatment and also preventing further transmission of the disease as positively diagnosed patients can immediately be put on therapy and advised on how to reduce the risk of transmission to partners and healthcare workers (183). Overall, the impact of early, rapid diagnosis of HIV has had an enormous impact on limiting the spread of

the disease. A similar test for TB could conceivably have a large impact to improve the management of the TB epidemic.

4.1.5 Lateral flow tests for TB

Due to the success of the rapid HIV diagnostic and the wide applicability and acceptability of the LFIA format, several TB diagnostics based on the same principles were developed and marketed. One prime example is commercially available lateral flow urine LAM assay (LF-LAM) available from Alere Hea (Alere Determine™ TB LAM Ag, Alere Inc, Waltham, MA, USA) (184). This test is designed to detect the *M. tb* cell wall component LAM in patients' urine samples. An anti-LAM monoclonal antibody labelled with gold is put in the conjugate pad of the test to capture and carry samples presenting the LAM antigen. The antigen-antibody complex then travels up the device substrate to the antibody laced on the test line, resulting in a colour change when a result is positive (138). The major drawback of this test is that it has been shown to have an extremely low sensitivity in patients that are not in an advanced stage of AIDS (185). It does not eliminate the need for other diagnostic tests such Xpert MTB/RIF, culture or sputum-smear microscopy, as these tests exceed LF-LAM in accuracy. It is suggested that a positive LF-LAM should always be followed up with a confirmation test such as Xpert MTB/RIF, line probe assay or bacteriological culture and drug-susceptibility testing (184).

The low sensitivity and specificity of the LFIA format for TB diagnosis influenced the World Health Organization (WHO) policy recommendation not to use them (186, 188). Despite this evidence, these tests were widely used in developing countries (187,188). As mentioned above, a comprehensive WHO/TDR report described the use of 355 well-characterized archived serum samples to evaluate 19 rapid TB tests (168). These tests were conducted at the Prince Leopold Institute of Tropical Medicine's Mycobacteriology Unit in Belgium. Results showed that the sensitivity of these rapid tests ranged from 0.97% to 59.7% and specificity ranged from 53% to 98.7%, compared to a combined reference standard of mycobacterial culture and clinical follow-up (168). The results of the evaluation indicated that none of the assays performed well enough to replace the more established laboratory tests, such as smear microscopy. However, smear microscopy combined with most rapid tests

improved overall diagnostic sensitivity from 75% up to 89% (168). A possible reason for this poor performance may be because TB antigens resemble those of many other human pathogens and the antigenic targets of antibodies generated toward the bacteria vary widely among patients (189). These factors would limit the sensitivity and so the overall performance of the tests. The WHO evaluation, however, did not permit an analysis of how the individual antigen or antigen combinations performed. The WHO suggests that the way forward clearly needs to include a review of the literature as well as a systems approach to identify specific test antigens with immunodiagnostic potential (168).

4.1.6 MALIA

As mentioned in chapter 1, efforts for the diagnosis of active TB by means of biomarker anti-MA antibody detection using ELISA (79), evanescent field biosensors by Thanyani *et al.* (153), electro impedance spectroscopy by Mathebula *et al.* (83) and development of monoclonal antibodies by Ranchod *et al.* (86) and the standardisation of the MA antigen for immunoassay by Ndlandla *et al.* (123) have all paved the way for an eventual lateral flow test for POC screening of active TB. The most advanced development in this field to date is the Mycolic acid Antibody Real Time Inhibition (MARTI) assay concept (84). The MARTI test has the ability to accurately detect patient low affinity anti-mycolic acids antibodies as biomarker for active tuberculosis and was patented in 2005 by University of Pretoria (190). Although seemingly successful with a limited number of TB patients and controls, it only has potential implementation in reference laboratories; therefore, not yet suitable to be utilized as a point-of-care device. This challenge led to the conception of a lateral-flow based test named the Mycolic Acid Lateral-flow Immuno-Assay (MALIA). The principles of MARTI must therefore be incorporated to create this POC device for screening of TB in rural HIV burdened areas.

As the name MALIA suggests, MA antigen is used in the test to detect antibodies that indicate active TB in a patient, with the aid of monoclonal labelled anti-MA antibodies. The principle of the test is based on a competition assay, whereby patient serum antibodies will compete with a gold labelled monoclonal antibody/gallibody displacement probe for binding to MA. Figure 25 illustrates the proposed MALIA layout. Patient antibodies added to the sample pad will travel along the strip from the

start point in the sample pad through to the wick. As the patient serum antibodies travel through the conjugate pad, they will come into contact with the gold labelled gallibodies. The patient serum anti-MA antibodies and the gallibodies are then to compete for binding to the MA immobilized at the test line. In addition to the test line, a control line will have immobilized anti-chicken IgG antibodies to capture the unbound gallibodies. The results can be interpreted by the colour change taking place on the test and control lines. A TB positive case will be represented by a colour development occurring at the control line only. This will indicate that the patient serum anti-MA antibodies were able to outcompete the gold labelled gallibody displacement probe in binding to the MA. Thus, no signal or only a weak signal will be present at the test line. In contrast a colour change taking place at both the test and control line will indicate a negative result illustrating the ability of the gold labelled gallibody displacement probe to bind to the MA on the test line without any competition from the patient serum antibodies (140).

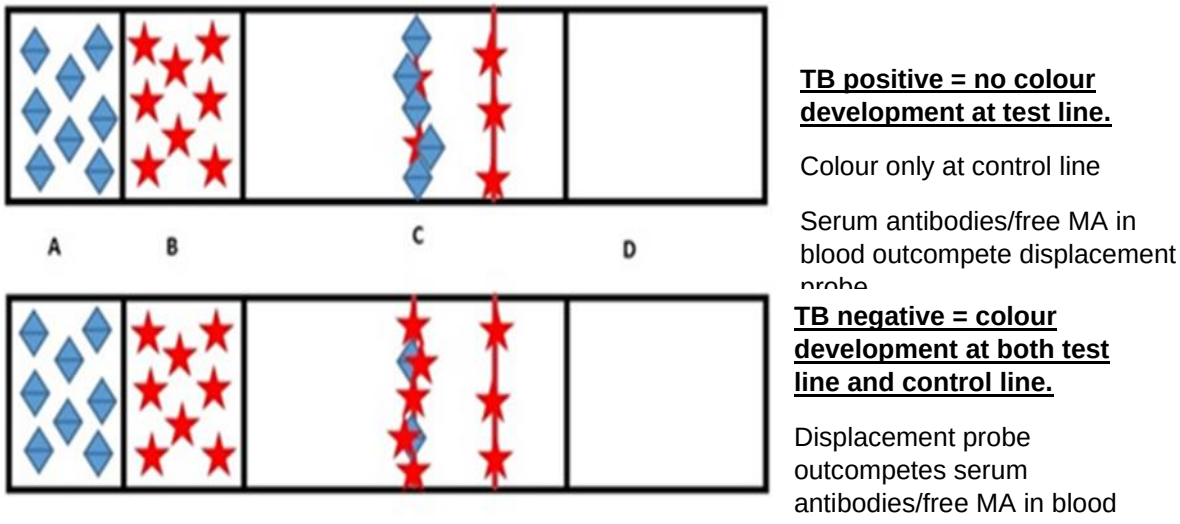

Figure 25: Diagram of the MALIA lateral flow test as described by *Ranchod* (140). A - Sample pad with patient antibodies (blue diamonds), B - Conjugate pad containing gold labelled displacement probe (red stars), C – Nitrocellulose membrane with test line and control line, D – Wick.

4.1.7 Challenges of MALIA

A major advantage of a LFIA, to benefit the POC nature of the technology, is its ease of use and cost effectiveness (191). Because of this ease of use, it is widely believed

that it is simple to develop. However, the challenges to overcome for each particular application are numerous in terms of the optimization required to make the test sensitive, rapid and easy to use (192).

The application of the MA antigen on the test line and immunoglobulin capture antibody (anti-chicken antibody) on the control line was explored by Alma Truyts in her MSc dissertation (147). The functionality of the MALIA test centres around the assumption that TB patient antibodies will have a stronger avidity for binding the MA antigen on the test line than the labelled gallibodies, thereby out-competing them for binding on the test line, thus preventing or reducing the colour signal. This indicates a positive result.

The interaction between gold labelled anti-MA gallibodies with the MA on the test line and with anti-chicken antibodies on the control line was investigated and reported by Alma Truyts. Results of her study indicated that no MA/gallibody binding was visualised on the test line or spot (147). It was subsequently shown that the biological activity of the gallibodies is adversely affected by labelling with gold nanoparticles (147). This loss of biological activity may be because the MA/gallibody binding already has a low antigen binding affinity, unlike the interaction of the anti-chicken antibody with a gallibody.

The immobilisation of the MA on the nitrocellulose was achieved by spotting of MA dissolved in freshly distilled hexane, but presented a unique problem of lack of wettability with the aqueous buffers used in LFIA. The alternative membrane-substrates tested did not allow for the formation of an anti-MA gallibody signal. Three substrates were investigated by Alma Truyts using a flow through test format (147). These substrates were: Fusion 5, a glass fibre, Chromatography number 1, a commonly used paper type in paper microfluidics and CF3, a cotton linter paper (147). While eventual success was achieved by immersing MA spotted nitrocellulose papers in ELISA plates and developing the immunoassay further with standard ELISA protocol, hexane is not compatible with the printing machinery commonly used for antigen printing in larger scale manufacturing of LFIA devices. The BioDot system is an instrument that is used for antigen printing on surfaces used for rapid tests development. It can dispense solutions onto a surface either by vapour spray or liquid ink jet. Aqueous solvents in general are compatible with the BioDot dispensing

technology (193). Buffers with a pH range from 3 to 10 are suitable. Extremes in pH may cause corrosion of the stainless steel or glass materials (193). Polar organic solvents are compatible with the dispensing system. Although not all polar organic solvents have been tested under long-term conditions, the following have shown good chemical compatibility; dimethyl sulfoxide, acetone, methylether ketone and ethyl acetate (193). Most non-polar organic solvents are incompatible with the BioDot dispensing technology. These would include benzene, diethyl ether, hexane and methylene chloride (193), which cause swelling and/or degradation of tubings, vessels and fittings. An ideal solvent for the bio-printing machinery would therefore be a polar organic solvent such as acetone.

The above challenges imply that the standard approach to a LFIA does not work for MALIA development. The following challenges needed to be overcome, according to Truyts (147):

- The low avidity of gallibodies for binding MA precludes their direct labelling with colloidal gold.
- Limited or no solubility of MA in solvents that are compatible with antigen printing instruments
- Incompatibility of nitrocellulose substrates with acetone for MA antigen printing

This chapter attempts to demonstrate a workable model of MALIA by making use of the discovery that MA is at least partially dissolved in acetone. The incompatibility of acetone for spotting solutions on nitrocellulose was thought to be overcome by the use of silica TLC plates as LFIA substrate. From chapter 3 it was discovery that MA in acetone is antigenic on silica and produces a visible binding spot. The discovery of acetone soluble MA in chapter 3 may overcome the challenges in automated MA immobilisation for a lateral flow device.

4.1.8 Hypothesis

The application of newly discovered acetone soluble MA on TLC silica plates may overcome the challenges in automated MA immobilisation and substrate compatibility to improve diagnosis of TB by MALIA.

4.2 Materials and Method

4.2.1 Materials

Silica plates: Thin layer chromatography (TLC) silica gel 60 F_{254} 20 x 20 cm plates (Merck, Kenilworth, New Jersey, USA).

Petri dishes: Polystyrene petri dish, 60 x 15 mm (Sigma-Aldrich, Missouri, USA).

Tank: Rectangular TLC developing tank (Sigma-Aldrich, Missouri, USA).

4.2.2 Reagents

Acetone: (purity 99.5%, Sigma-Aldrich, Missouri, USA).

Stearic acid: (purity 99%, Sigma-Aldrich, Missouri, USA).

Phosphate buffered saline (PBS) 20X, pH 7.4: Prepared by dissolving 160 g of sodium chloride (NaCl), potassium chloride (KCl, 4 g), di-hydrogen potassium phosphate (KH_2PO_4, 4 g) and di-sodium hydrogen phosphate (Na_2HP0_4, 28 g) in a total of 800 ml of autoclaved double distilled deionized (ddd) water (ddd H_2O) while stirring. The volume was brought up to 1 L and filtered through 0.2 µm cellulose acetate filters (Sigma-Aldrich, Missouri, USA)

PBS (1 X) was prepared by adding 50 ml of 20 X PBS to 900 ml of autoclaved ddd H_2O. The pH was adjusted to 7.4 with 1 M HCl, after which the volume was made up to 1000 ml with ddd H_2O.

Block buffer pH 7.4: Casein hydrolysate (4% m/v, Oxoid, United Kingdom) dissolved in 1 X PBS pH 7.4.

Dilution buffer pH 7.4: Casein hydrolysate (4% m/v) dissolved in 1 X PBS pH 7.4 and 0.1% (v/v) Tween20 (Sigma-Aldrich, Missouri, USA).

Wash buffer pH 7.4: PBS 1X, pH 7.4 and 0.1% (v/v) Tween20.

Borate Buffer 0.1 M pH 7.4: Sodium tetraborate ($Na_2B_4O_7$ 0.1 M) and 0.1 M Boric acid (H_3BO_3) dissolved in triple distilled water (dddH_2O) (Sigma-Aldrich, Missouri, USA).

Secondary antibody: Goat anti-chicken Fc: HRP diluted 1:1000 in 4% Casein hydrolysate/1 X PBS -0.1% Tween 20, pH 7.4 (AbD Serotic, Kidlington, UK).

Blot test Tetramethyl Benzidine (TMB) HRP substrate solution: Life Technologies, California, USA.

Mycolic acids: Self purified (see chapter 2). Aliquots of 1 mg in tightly capped brown glass vials stored at 4°C and thawed when used.

Gallibody type 12CH1-4 purified from the 50 ml aliquots frozen culture media provided by Heena Ranchod (see chapter 2) and concentrated to 50 µl aliquots in 0.1 M Borate buffer pH 7.4. Stored at -20°C, thawed once only for use.

4.2.3 Immuno-blot test of acetone soluble MAs

A volume of 4 ml acetone was added to an aliquot of 1 mg MA and heated at 90ºC on a heating block (Reacti-Therm Thermo Scientific Pierce III, USA) for 5 min and shaken by hand to mix. The MA/acetone solution was left to cool for 1 hour before 10 µl was spotted using a Hamilton Syringe on a silica plate at a concentration of 0.25 mg/ml. Hexane (4 ml) was used to dissolve another aliquot of 1 mg MA and was further spotted as above. The silica plate with spotted MA was placed in a petri dish and was immersed in block buffer such that the entire plate was covered in solution. It was then incubated for 2 hours at room temperature. After 2 hours, the block buffer was tipped out of petri dish making sure not to tip out the silica plate, which was then washed three times with wash buffer by gently shaking the buffer solution side to side in the petri dish without removing the silica plate. The wash buffer was tipped out and excess buffer was removed with a disposable plastic dropper. The silica plate was then immersed in gallibody type 12CH1-4 in dilution buffer at a concentration of 0.031 mg/ml and incubated for 1 hour at room temperature. Secondary antibody solution of goat anti-chicken IgG HRP at a 1:1000 volume ratio was added to the reaction after another wash step and incubated for 1 hour at room temperature. The plate was then washed three times with wash buffer to remove unbound secondary antibody before 5 ml of TMB blot solution was added to develop the colour for 3 minutes, after which the colour signals on the plate were analyzed by eye and recorded by taking a photograph using a mobile phone camera Because TMB oxidation is fast, colour development must be recorded within 5 minutes, after which precipitation of the coloured stain occurs that destroys the resolution.

4.2.4 Adaption of lateral flow paper substrate with immobilized silica

The principle of a silica based LFIA follows the immunoblot test protocol with the following changes: Incubation in block buffer and dilution buffer is replaced by lateral flow of dilution buffer with primary antibody (gallibody) at a concentration of 0.031 mg/ml. Gallibody solution is transported rapidly over the spotted antigen on the silica plate by capillary action as would be expected for an LFIA. The capillary flow set-up to bring the gallibody solution over the spotted MA is shown in Figure 26A. Further development of the plate in a normal immunoblot blot test was then done as described in section 3.2.6 in a petri dish shown in figure 26B.

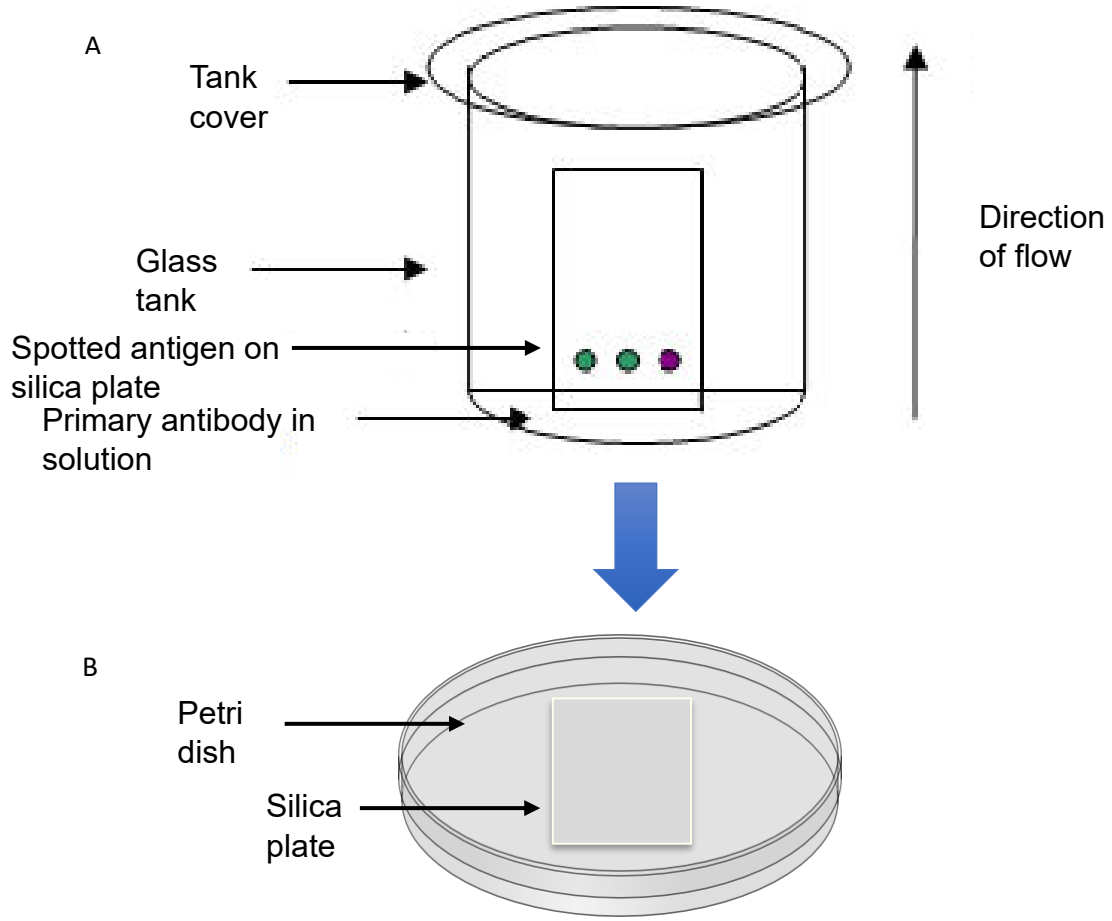

Figure 26: Schematic illustration of the methodology of the adapted silica based lateral flow mechanism. (A) - Monoclonal gallibodies, in dilution buffer poured in a TLC tank to reach a level of 0.5 cm. Silica plate with spotted MA antigen is placed in buffer solution, which then proceeds to move up the plate by capillary force. Vertical direction of capillary flow is shown by the arrow. (B) – After gallibody solution reached

1 cm from the top of the plate in (A), the plate is removed from the tank and placed in the petri dish where the immunoblot protocol is followed, starting with washing 3 times in wash buffer, then incubation in secondary antibody HRP conjugate for an hour and finally colour development in TMB substrate solution.

A volume of 4 ml acetone was added to an aliquot of 1 mg MA and heated at 90^{o}C on a heating block (Reacti-Therm Thermo Scientific Pierce III, USA) for 5min and shaken by hand to mix. The MA/acetone solution was left to cool for 1 hr before 10 µl was spotted on a silica plate in an increasing two-fold concentration range from 0.25 mg/ml (one spot of 10 µl) to an eventual equivalent of 1 mg/ml (four spots of 10 µl). A volume of 2 ml of gallibody type 12CH1-4 at a concentration of 0.031 mg/ml dissolved in dilution buffer was poured into the TLC tank. The silica plate was then placed upright in the gallibody buffer solution in the TLC tank. The gallibody buffer solution moved up the silica plate by capillary action. The plate was taken out when the gallibody solution reached 1 cm from the top of the plate and placed in a petri dish to be washed three times with wash buffer by gently shaking the buffer solution side to side without removing the silica plate. The wash buffer was tipped out and excess buffer was removed with a disposable plastic dropper. The steps of secondary antibody conjugate exposure followed by colour development with TMB was carried out as described in Section 4.2.3.

4.3 Results

4.3.1 Immuno-blot test of acetone soluble MAs

A 10 µl aliquot of MA in acetone at 0.25 mg/ml was blotted in duplicate on nitrocellulose to demonstrate the effect of incompatibility with acetone. Similarly, MA in hexane at the same concentration was blotted in duplicate on the same substrate. It was compared to two different substrate types, i.e. Whatman no 1 paper and a silica TLC plate that were blotted with MA in the same way as the nitrocellulose substrate. Hexane and acetone alone were spotted as negative controls. The blotted and dried substrates were incubated in gallibody type 12CH1-4 at a concentration of 0.031 mg/ml as shown in figure 27. Immunoblot development with secondary antibody-HRP

conjugate was done as described in Section 4.2.2.1. Blue spots indication positive binding of gallibody to the MA spots.

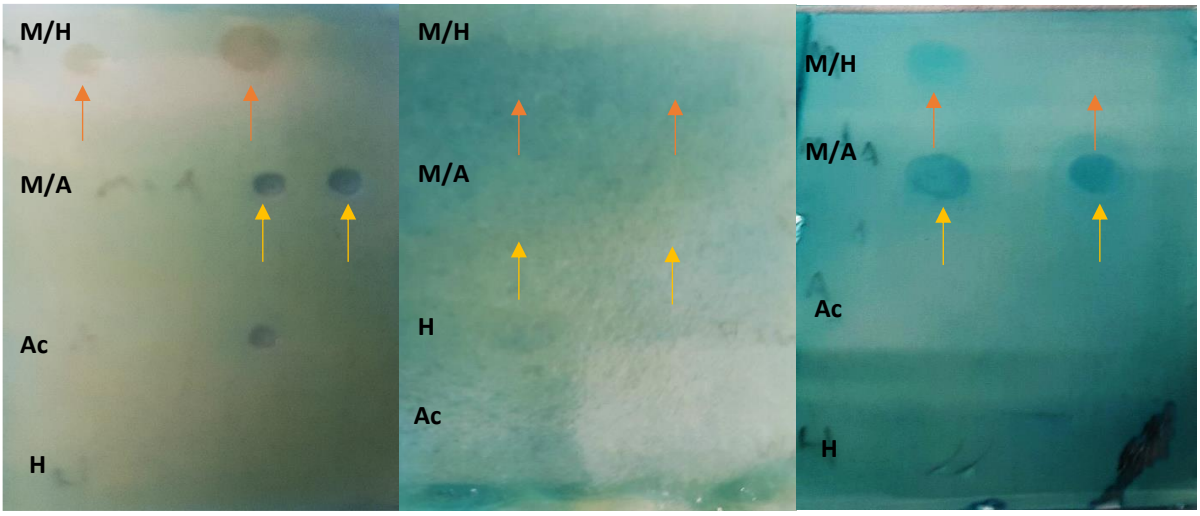

A Nitrocellulose **B** Whatman no1 **C** Silica

Figure 27: Immunoblot test to determine the feasibility of spotting of MA in acetone (M/A) compared to MA in hexane (M/H) on 3 substrate types. MA in acetone (0.25 mg/ml) and MA in hexane (0.25 mg/ml) were spotted at room temperature on paper type (A) Nitrocellulose, (B) Whatman no1, (C) Silica. Hexane (H) and acetone (Ac) were spotted as negative antigen controls. The plates were incubated in gallibody type 12 CH1-4 at a concentration of 0.031 mg/ml and developed with TMB enzyme substrate solution. Spots for MA in hexane are indicated by red arrow and spots for MA in acetone indicated by yellow arrow. Darker spots on (A) nitrocellulose indicate holes.

The results of the immunoblot test (Fig 27) showed that where MA in acetone was spotted on nitrocellulose, the nitrocellulose was dissolved at the area of spotting, confirming incompatibility, in contrast to where MA was spotted from hexane solution (Fig 27A). The Whatman no 1 substrate, most commonly used as filter paper, was not usable as it has a high-water wettability and no spots were visible (Fig 27B). Whatman no. 1 was therefore ruled out as a possible substrate for a lateral flow test. Results of blot test on silica TLC plate showed spots for MA in acetone and MA in hexane (Fig 27C), however only one spot of MA in hexane was visible were as both spots were visible for MA in acetone. The positive visible signal is far stronger for MA in acetone

than MA in hexane. The negative controls (hexane and acetone only) showed no detectable signal.

The MA signals in Figure 27C indicate that MA is antigenic when spotted onto silica and that MA in acetone remains antigenic, even to a better degree than when spotted from hexane solution. To further investigate the antigenicity of MA in acetone compared to MA in hexane on silica a dilution range was done at spotting concentrations of 0.25; 0.05 and 0.01 mg/ml. Results of blot test of MA in acetone and MA in hexane spotted at a decreasing concentration range is shown in figure 28.

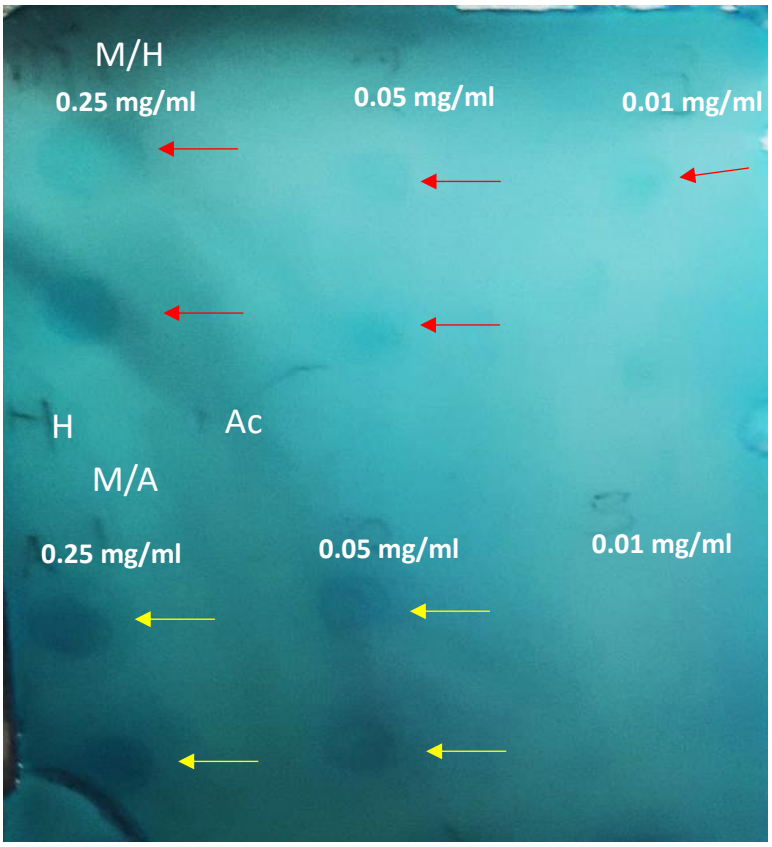

Figure 28: Immunoblot test to determine antigenicity of MA in acetone (M/A) compared to MA in hexane (M/H) spotted on silica TLC plate. MA in acetone, MA in hexane spotted on silica at dilution range of 0.25 - 0.01mg/ml. Hexane (H) and acetone (Ac) only spotted as negative control. The plates were incubated in gallibody type 12 CH1-4 at a concentration of 0.031 mg/ml and developed with TMB enzyme substrate solution. Spots for MA in hexane are indicated by red arrow and spots for MA in acetone indicated by yellow arrow.

MA concentration dependent blue positive antibody binding spots were visible for MA spotted in acetone and hexane at concentrations of 0.25 mg/ml and 0.05 mg/ml, but significantly weaker for spots from MA in hexane, indicated by red arrows. The duplicate spots for MA in acetone (yellow arrows) showed clear blue duplicate spots, which decreased in intensity with lower concentration, but were much better visible at concentration of 0.05 mg/ml compared to that coated with MA in hexane. The reproducibility of spotting MA in acetone on silica was also better than the case for MA in hexane. The negative controls (hexane and acetone only as spotting reagents) showed no detectable signal, testifying to the success of washing away the background in the immunoblotting process.

These results suggest that aluminum backed silica plates may work as substrate for a lateral flow immunoassay to detect anti-MA antibodies. Clear antibody binding spots were obtained where MA was spotted from acetone solution, while the background of unspotted silica could be washed clear with aqueous buffer, indicating no non-specific binding of antibodies to silica. In addition, the silica plate was not damaged after extensive washing with aqueous buffer. Should it work, then the solvent incompatibilities for both MA in automated antigen printing machinery and spotting or striping on lateral flow substrates will have been solved, leaving only the susceptibility of anti-MA gallibodies to loss of antigen binding activity by labelling as a problem to be solved towards the development of a MALIA test that will be suitable for validation with human patient sera.

4.2.3 Towards lateral flow immunodetection of anti-MA antibodies on silica substrate

In order to mimic a lateral flow test, an MA and stearic acid antigen spotted silica plate was vertically placed in a small volume gallibody dilution buffer in a TLC tank, much as one would position a TLC plate in a tank to prepare for TLC separation of the spotted samples. This is shown in Fig 26, where the buffer is then taken up from the bottom of the plate to flow upwards due to capillary force. Figure 29A shows the buffer flow dynamics over 3 mins, resulting in a flow speed that compared very well with that of commercial lateral flow immunoassays. Besides flow speed, the aqueous wettability

of the lipid coated spot can also be a problem, as mentioned by Truyts (147). Poor wettability would be characterised by indentation of the front of the moving buffer in the silica plate when it comes into contact with the lipid MA and stearic acid spots. Stearic acid provides a hydrophobic, non-specific negative antigen control. Figure 7A shows the buffer flow front between 1 and 2 minutes, during which time contact is made with the spotted lipid antigens. No indentation of the front was observed, testifying to the fact that the MA (and stearic acid) remained perfectly wettable after antigen spotting. Results of the subsequent secondary antibody immunoblot of the LFIA plate that was developed with primary antibody under lateral flow conditions is shown in figure 29B. Blue spots indicate positive binding of gallibody to MA antigen.

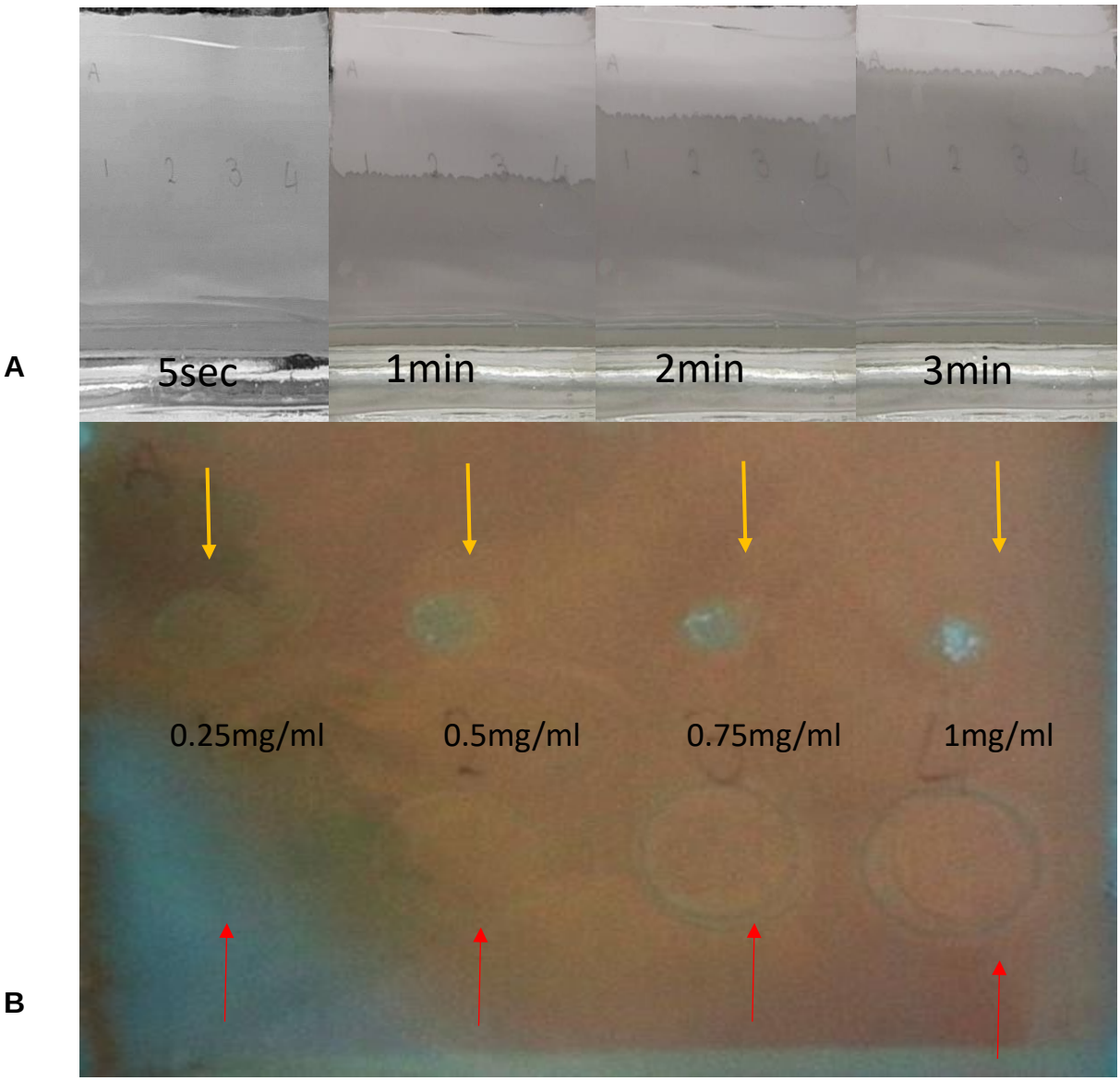

Figure 29: Lateral flow of primary anti-MA gallibody on silica substrate spotted with MA and a non-relevant lipid antigen control on the test zone. (A) rate of flow of primary antibody (gallibody type 12CH1-4 in buffer solution at a concentration of 0.031 mg/ml) over spotted MA and non-relevant stearic acid lipid antigen. (B) Visualisation of the lateral flow immunoassay result after immunoblotting with secondary anti-chicken immunoglobulin HRP conjugate. MA spots are indicated with yellow arrows and stearic acid with red arrows. Both antigens were spotted from acetone solutions in a dilution range from 0,25 -1 mg/ml.

Figure 29A demonstrates the rate at which the gallibody solution moved up the silica plate by capillary force. It took 3 min from the moment it was dipped in the gallibody solution to reach 1 cm from the top of the plate. This indicates an adequately fast flow

for LFIA. Figure 29B shows blue spots for MA, which indicate positive binding. The blue spots become more pronounced as the concentration increased from 0.25 mg/mL to 1 mg/ml. At concentrations exceeding 0.5 mg/ml, white waxy deposits can be seen on the spots indicating antigen overload during spotting. The stearic acid (negative control) spots produced a whitish ring around the area where it was spotted, indicating absence of antibody binding of to the stearic acid. The ring shows darker discoloration as the concentration increased. Overall, these results indicate that for a LFIA in this format MA in acetone spotted at 0.5 mg/ml gives the best results as the spot is more visible than when spotted at a concentration 0.25 mg/ml, while showing the least amount of waxy MA deposits. The experiment was repeated as described in section 4.2.4 with antigen spotting only at 0.5 mg/ml to ensure that the method was reproducible. This was found to be the case (Fig 30), as long as one was alert to the fact that result recording had to be done within 3 minutes after TMB exposure, after which the blue spots lost their contrast with the discolouring background.

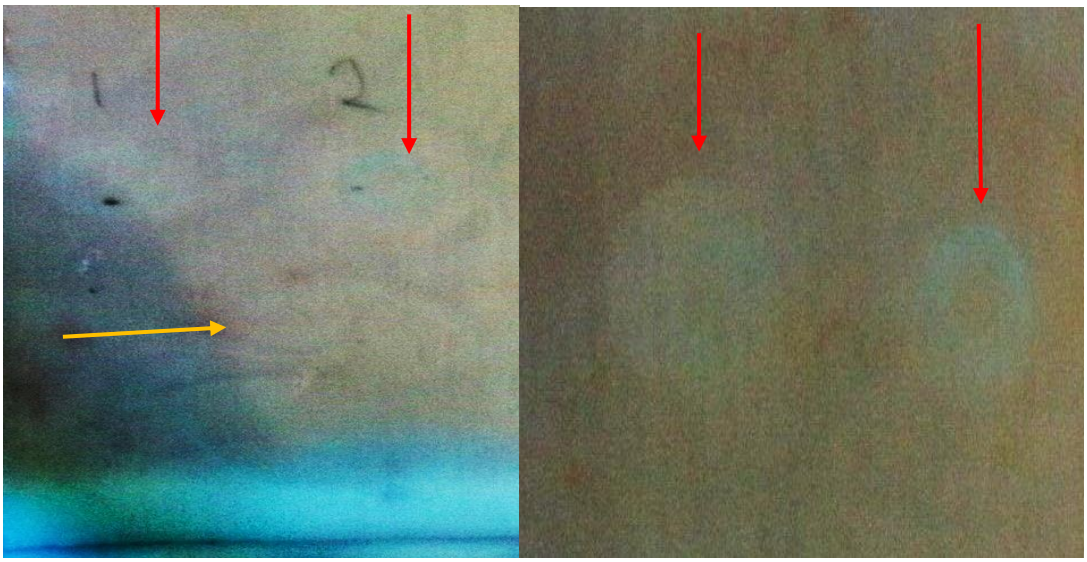

Figure 30: Repeats of lateral flow immunoassay of MA (red arrows) and stearic acid (yellow arrow) in acetone spotted at 0.5 mg/ml. The two plates represent two repeats, of which only the first (left) also had stearic acid spotted.

Results of figure 30 indicate that the silica based LFIA with MA as antigen and gallibody 12CH1-4 is reproducible. Blue spots are seen where MA in acetone was spotted at a concentration of 0.5 mg/ml, shown by red arrows, indicating positive binding and the stearic acid, shown by the yellow arrow, which again produced only a whitish ring around the area where it was spotted.

4.4 Discussion

The unique and remarkable properties of LFAs have contributed to the detection of disease biomarkers for rapid and affordable screening of health conditions in man and animals. Although the principle of the method has remained unchanged for decades, there have been continuous improvements of LFA techniques leading to increased sensitivity and reproducibility and the simultaneous detection of several analytes.

This chapter aimed to demonstrate a workable model of MALIA by overcoming two critical challenges of antigen solvent incompatibilities on lateral flow substrates and antigen printing machines. This model took the form of an aluminium backed silica substrate (intended originally for use in TLC) for LFIA. While MAs have been successfully immobilized on nitrocellulose in an antigenic conformation, the commonly used MA dissolution solvent hexane is not compatible with the bio-printing machinery used for large-scale manufacture of LFIA test assemblies. The discovery of the solubility of MAs in acetone was covered in chapter 3, which is a compatible solvent for automated antigen printing on lateral flow substrates. Acetone is, however, incompatible with printing on nitrocellulose which is seen from figure 27A, where nitrocellulose was damaged by dissolution in the area spotted. instead, TLC silica plates were found to be the suitable substrate to spot MA antigen on from acetone solution as seen in figure 27C by the blue spots, also confirming MA antigenicity after spotting and immunoblotting. In figure 28 the superiority of acetone over hexane as MA solvents is proven, with stronger stained spots developing on the MA-acetone spots compared to the MA-hexane spots. it appeared that MA spotted from acetone is presented as a better antigen on silica than can be achieved with MA-hexane solutions. A possible explanation for this is the micellar nature of acetone solutions of MA, observed by the homogeneous opaqueness of the solutions, which gradually increased within four hours after heating. Hexane solutions of MA remained stably clear. It is believed that the micellar packing of MA assists their folding into an antigenic conformation before and during adsorption onto silica.

Additionally, the TLC silica plates allowed for efficient lateral flow of aqueous antibody and protein containing solutions. The lateral flow set-up is shown in the schematic diagram (Fig 26 A), which is followed by immunoblotting with secondary antibody (Fig 26 B). The results in Figure 29, demonstrated how well this model worked. No attempt was made to label the primary gallibodies, as Alma Truyts clearly proved that this was

not feasible option with the given anti-MA gallibodies (147). The aqueous antibody/casein hydrolysate buffer solution flowed up the plate by capillary force at an adequate speed typical of existing commercial LFIAs. Literature suggests LFIA substrates with a faster flow speed during running affect the amount of reaction time for the antibody (147,194) and that a slower flow rates improves sensitivity. As seen in figure 29B, fast flow rate did not abolish the reaction of gallibody to spotted MA antigen, because a positive binding signal was observed by the blue spots of which the intensity increased with increasing concentration of MA. It was concluded that the best concentration to spot MA from acetone in this format is 0.5 mg/ml. This was further proven by figure 30 where MA in acetone was spotted 4 times to assess the reproducibility of the reaction. Wettability of the spotted MA to ensure proper contact with primary anti-MA gallibody was achieved nicely, evidenced by a homogeneously blue stained MA spot, as compared to peripheral half-moon stains obtained by Truyts for MA-hexane spots on nitrocellulose (147). The ability of the gallibodies to specifically recognize MAs in a LFIA test demonstrates the feasibility of developing the test further into a competitive LFIA test.

Further challenges of MALIA exist due to the cholesteroid nature of MA and the presence of anti-cholesterol antibodies in patient sera that may cross-react. The gallibodies then need to outcompete the serum anti-cholesterol antibodies for binding to MA but not the anti-MA antibodies. This then also serves to limit the cross-reactivity of the test that would occur in the case of direct detection. The fast rate of flow towards and over MA may overcome binding of low avidity cross-reactive anti-cholesterol antibodies. Thus, a preliminary MALIA proof of principle was achieved by demonstration of a fast rate of movement of sample buffer and gallibody mixture through silica substrate to give a homogeneous antibody binding signal on the test spot.

This is the first study where the principle of MALIA on silica based lateral flow substrate was demonstrated.

Chapter 5: Concluding Summary

Tuberculosis (TB) remains the leading infectious cause of death worldwide. It is estimated that 1.7 billion of the global population is living with latent TB (17) of which ~10% are likely to develop active TB within 2 years after initial exposure (195,196). The risk of reactivation of latent TB is remarkably high among individuals infected with the human immunodeficiency virus (HIV). The World Health Organization (WHO) aims to reduce TB-related mortality by 95% and incidence by 90% between 2015 and 2035 through its End TB strategy (29,66). This goal is to be achieved with more effective vaccines and treatment regimens and improved diagnostic tests. Current diagnostic tools in routine clinical use today rely on sputum-based testing, which has consistently demonstrated poor sensitivity, especially in immune compromised individuals and children who are unable to produce sputum of the desired consistency(197,198) There have been tremendous improvements in diagnostic tests for TB over the last few years (66). Despite these advances, no test is able to meet all the required specifications in terms of performance (sensitivity and specificity), ease of use, cost, rapidity of diagnosis, and the ability to generate same-day results at point of care (POC). The most important contribution to the End TB strategy will be the POC platforms which will make TB diagnosis more accurate, affordable and widely available for patients and care providers (29).

Proper and rapid diagnosis is key to control TB. However, an accurate and rapid POC test that is usable in field conditions is still elusive. POC diagnostics for TB are critical in resource-limited settings, where the largest burden of TB lies. The goal of POC testing remains to provide immediate and convenient rapid diagnostic testing at or near the site of patient care. Lateral flow or Lateral Flow Immunoassay (LFIA) technology is one of the most successful and simple rapid diagnostic testing systems. The current global challenge is to develop and process already identified biomarkers into diagnostics with a POC format.

This study investigated the use of mycolic acid (MA) to detect TB patient anti-mycolic acid antibody biomarkers towards a workable LFIA model for diagnosis in a POC environment, which would fulfil a great need in the management and control of the TB epidemic.

The use of MA antigens to detect antibodies as surrogate markers for TB diagnosis was shown to be feasible in ELISA assays, albeit of limited accuracy (79, 122). Mycolic Acid Real Time Inhibition assay (MARTI) makes use of MA and antibodies against mycolic acid for the detection of TB with evanescent field biosensors (81,140). Although this method has been successful in the serological diagnosis of TB, this system remains highly impractical in resource-limited settings as the biosensor equipment requires highly skilled personnel for operation and costs included are extremely high (140). While developments have been made in converting the biosensor method into a more user-friendly process using electro-impedance spectroscopy (EIS), challenges remain on containing the cost and making it independent of a laboratory environment to serve as a point of care device. As a result, a new device needs to be developed employing the use of mycolic acids and labelled monoclonal anti-mycolic acid antibodies in a simple process that can be used in a POC set up. This gave rise to a research programme aiming towards developing a Mycolic Acid Lateral-flow Immunoassay Assay (MALIA).

In performing the MALIA test, MAs are used to indicate the presence of active TB in a patient with the use of monoclonal anti-mycolic acids antibodies. However, it was found that MA can fold in such a way as to assume a structure that relates to cholesterol (86). This leads to cross-reactivity occurring between anti-cholesterol antibodies and anti-mycolic acid antibodies. One way to overcome this problem is by using monoclonal antibodies that are monospecific to MAs. Work done by Ndlandla *et al*, (123) selected and established stably expressing recombinant phage antibodies to mycobacterial mycolates from a chicken antibody gene library. These were converted to divalent IgY-type chicken antibodies (gallibodies) by Ranchod *et al*. (86). Recombinant, monoclonal anti-MA gallibodies can be applied in a lateral flow immunoassay as a basis for the development of a MALIA point of care TB diagnostic.

This study set out to demonstrate a workable model of MALIA, using MA isolated from self-cultured *M. tuberculosis* according to conditions established by Ndlandla *et al.* (123). Purification of the MA was done according to the protocol of Goodrum *et al.* (92), but the process was upscaled to yield a larger amount of pure MA per run by loading more concentrated MA crude extract for CCD purification. MA from crude

extracts was successfully purified using CCD purification followed by acetone precipitation yielding pure MA.

In chapter 2, thin layer chromatography (TLC) was used for the analytical tracking of MAs from the crude extract to post purification state. Acetone precipitation should ideally remove all contaminants that the CCD could not eliminate and leave pure uncontaminated MA. The TLC done post acetone precipitation confirmed this fact, but the MA yield obtained was only 4.8%. When this is compared to the maximum potential yield of MA crude mycobacterial extract that was determined by Goodrum *et al*. (92), then the upscaled purification caused a 37% loss of MA. It was then deemed imperative to re-assess the acetone waste after the last step of acetone precipitation for the presence of any acetone soluble MA. Due to the fact that the purification procedure was run with more concentrated MA than ever done before, the possibility some of the MA could have been filtered with the acetone during the acetone precipitation procedure, accounting for the loss of yield. This study was the first attempt at upscaling the CCD purification process. It was never before explored whether any MA was retained in the acetone filtrate (AcF) fraction after acetone precipitation of the CCD purified MAs as it was thought that MA is not soluble in acetone, a fact that is based on the observation that MA does not dissolve at all in acetone at room temperature.

In chapter 3 the presence of antigenic MAs in AcF was investigated through the probing of the AcF with gallibodies for binding and signal detection by means of ELISA. The ELISA results led to the discovery that the AcF did in fact contain antigenic MAs. Probing of the TLC chromatogram directly with the gallibodies affirmed that the MAs in AcF lose antigenicity when the components of the complex are separated from one another with TLC. It was hypothesized that the MA in AcF could possibly exist in a non-covalent antigenic complex. This complex could be a mycolate bound to its organic counter-ion. This was further investigated by introducing alanine as an organic counter-ion. Exposing MA to alanine at high temperatures did not influence the acetone solubility of the MA. This work did, however brought to light the fact that the AcF fraction, that is normally regarded as waste could contain antigenic MA.

Although the attempt of complexing mycolate and an amino acid counter-ion did not succeed, the results brough to light the solubility of MA in acetone by first heating the solution and then allowing it to cool. Observations lead to the discovery that MA remains in solution of acetone to a maximum solubility of 0.25mg/ml for up to four hours at room temperature after heating, after which it coagulates in sizes that cause its sedimentation out of solution. It can be hypothesized that once heated, MA becomes soluble as a micellar suspension that coagulates into growing micelles until it sediments after several hours of cooling. This is an interesting idea to pursue in future research. Regardless, the important discovery of solubility of MAs in acetone may overcome challenges in development of lateral flow test such as low avidity of binding, compatibility of antigen solutions for antigen printing instruments and substrates used in the development of a workable model of MALIA

The hypothesis tested in this study is that use of recombinant, monoclonal anti-MA gallibodies in a LFIA can be applied as a basis for the development of a MALIA point of care TB diagnostic. Previous work showed that the application of the gallibodies in a MALIA test faced several challenges, mainly due to incorporation of lipid antigens such as MA (140). This is due to the fact that most lateral flow immunoassays make use of protein antigens, for which the nitrocellulose substrates have a high protein binding capacity, thus making them suitable for tests with protein antigens and antibodies (140). Lipid immobilisation on nitrocellulose did not work, while the typical low avidity of anti-lipid antibodies presented an almost unsurmountable problem of labelling.

Previous work done in our research group successfully immobilized MA from hexane on nitrocellulose in an antigenic conformation. Even though this was a success, hexane is not compatible with the bio-printing machinery used for LFIA. The dissolution of MAs in acetone solves this problem. In chapter 4, spotting of MA in acetone on possible LFIA substrates was explored. Acetone is, however, incompatible with nitrocellulose. Instead, TLC silica plates were found to be suitable as substrate to immobilize MA antigen on from acetone solution. It appeared that MA is presented as a better antigen in acetone than hexane on silica, due to the stronger indicator colour that developed on spots from acetone solutions of MA. Additionally, the TLC silica plates allowed for rapid lateral flow of aqueous antibody solutions. In the LFIA test, the solution of gallibodies move by capillary flow to approach the MA-coated spot. The

binding of the gallibodies to the MAs was then confirmed using an HRP-conjugated secondary antibody, providing a visual colour. The lateral flow immunoassay substrate nitrocellulose can therefore be replaced by immobilised silica. The rapid capillary flow may also overcome binding of low avidity cross-reactive anti-cholesterol antibodies, thereby limiting any effect of false positive testing in this application of MALIA.

The proof of the MALIA principle was therefore achieved, in support of the stated hypothesis to this effect. The fast rate of movement of sample buffer and gallibody mixture over silica substrate to give visual colour signal with secondary antibody binding all contributed to this proof of principle. Direct labelling of the indicator recombinant monoclonal gallibody was not attempted, after Truyts convincingly demonstrated the poor feasibility of that (147). Direct labelling of the indicator antibodies would have provided a more ideal demonstration of a workable MALIA. My fellow MSc student, Mosa Molatseli, has been investigating this possibility in parallel by attempting the multimerisation of recombinant anti-MA chicken scFv's to provide indicator antibody molecules of higher binding avidity and more resistance to chemical modification by labelling (199).

This is the first study where the principle of MALIA on silica based lateral flow substrate was demonstrated. The potential impact of MALIA as a POC test would be of enormous public health benefit in South Africa, but also the developing world burdened by the TB epidemic. Access to rapid, simple, affordable and reliable TB diagnostics at POC is crucial to the TB epidemic eradication and reducing the burden of disease. This now seems to be feasible to achieve. The need for simpler methods to accurately diagnose TB in high risk populations including children and people with immune suppression such as HIV cannot be overstated—the faster a patient is screened, the quicker treatment can be initiated, ultimately reducing morbidity and reducing the spread of TB. This work has made a critical contribution to the technical development of the MALIA POC TB diagnostic test.

References

1. Fogel, N. (2015). Tuberculosis: A disease without boundaries. *Tuberculosis.* 95 (5): 527-531.

2. Farmer, K.P. (2012) Tuberculosis, drug, resistance, and the history of modern medicine *N Engl J. Med*. 367 (10): 931-936

3. Van den Brande, P. (2005) Revised Guidelines for the Diagnosis and Control of Tuberculosis. *Drugs & Aging*. 22 (8): 663-686.

4. Brosch, R., Gordon, S.V., Marmiesse, M., Brodin, P., Buchrieser, C., Eiglmeier, K., Garnier, T., Gutierrez, C., Hewinson, G., Kremer, K., Parsons, L.M., Pym, A.S., Samper, S., van Soolingen, D., Cole, S.T. (2002). A new evolutionary scenario for the Mycobacterium tuberculosis complex. *Proc. Natl. Acad Sci*. 99 (6): 3684-999

5. Wirth T., Hildebrand F., Allix-Béguec C., Wölbeling F., Kubica T., Kremer K., van Soolingen, D., Rüsch-Gerdes, S., Locht, C., Brisse, S., Meyer, S., Supply, P., Niemann,S. (2008). Origin, Spread and Demography of the *Mycobacterium tuberculosis* Complex. *PLoS Pathog.* 4(9): e1000160

6. Barberis, I., Bragazzi, N. L., Galluzzo, L., & Martini, M. (2017). The history of tuberculosis: from the first historical records to the isolation of Koch's bacillus. *J Prev. Med. Hyg*. *58*(1), E9–E12.

7. Sakamoto, K. (2012). The Pathology of Mycobacterium tuberculosis Infection. *Vet Pathol*. *49*(3): 423–439.

8. Daffe, M., Draper, P. (1998). The envelope layers of mycobacteria with reference to their pathogenicity. *Adv. Microb. Physiol*. 39: 131–203.

9. Tang, J., Yam, W., Chen, Z. (2016). Mycobacterium tuberculosis infection and vaccine development. *Tuberculosis* 98: 30-41.

10. A Tuberculosis Refresher Course for Physicians (2007). The World Medical Association, B.P. 63, 01212 Ferney Voltaire Cedex, France. Availablefrom:http://www.wma.net/en/70education/10onlinecourses/40tb_refresher/TB_refresher_Course_final_lowversion.pdf. Accessed: 14 April 2016.

11. Nunes-Alves, C., Booty, M. G., Carpenter, S. M., Jayaraman, P., Rothchild, A. C., & Behar, S. M. (2014). In search of a new paradigm for protective immunity to TB. *Nat*. *Rev. Microbiol*.12(4): 289–299.

12. Cooper, A.M., Mayer-Barber, K.D., Sher, A. (2012). Role of innate cytokines in mycobacterial infection. *Mucosal Immunol*. 4:252–60

13. Russell, D.G. (2001) Mycobacterium tuberculosis: here today, and here tomorrow. *Nat Rev. Mo.l Cell Biol.* 2: 569-586.

14. Davies, P.D.O., 2005. Risk factors for tuberculosis. *Monaldi Arch. Chest Disease – Pulm. Ser*. 63 (1): 37–46

15. Loxton, A.G. (2019). B cells and their regulatory functions during tuberculosis: Latency and active disease, *Mol. Immunol*.111: 145-151.

16. Tang, J., Yam, W., Chen, Z. (2016). Mycobacterium tuberculosis infection and vaccine development. *Tuberculosis* 98: 30-41.

17. WHO. (2018). Global tuberculosis report. Geneva, Switzerland.

18. Abdool Karim, S.S., Churchyard, G.J., Abdool Karim, Q, Lawn, S.D. (2019). HIV infection and tuberculosis in South Africa: an urgent need to escalate the public health response. *Lancet*. 374 (9693): 921-933.

19. Basu S., Friedland, G., Medlock, J.J.R., Andrews, J.R., Shah, S.N., Gandhi, N.R., Anthony, M.A., Moodley P, Sturm, A.W., Galvania, A.P. (2009). Averting epidemics of extensively drug-resistant tuberculosis. *PNAS USA.* 106:7672-7677.

20. Foster, N., Vassall, A., Cleary, S., Cunnama L., Churchyard, G., Sinanovic, E. (2016). The economic burden of TB diagnosis and treatment in South Africa. *Soc. Sci. Med*. 130: 42–50.

21. Grobler, L., Mehtar, S., Dheda, K., Adams, S., Babatunde, S., van der Walt, M & Osman, M. (2016).The epidemiology of tuberculosis in health care workers in South Africa: a systematic review *BMC Health Ser. Res*. 16: 416.

22. Kranzer, K., Bekker, L.G., van Schaik, N., Thebus, L., Dawson, M., Caldwell, J., Hausler, H., Grant, R., Wood, R. (2010). Community health care workers in South Africa are at increased risk for tuberculosis*. S. Afr. Med*. *J*. 100(4):224–6.

23. Connelly, D., Veriava, Y., Roberts, S., Tsotetsi, J., Jordan, A., DeSilva, E. (2007). Prevalence of HIV infection and median CD4 counts among health care workers in South Africa. *S. Afr. Med. J*. 97(2):115–20.

24. Shisana, O., Hall, E.J., Maluleke, R., Chauveau, J., Schwabe, C. (2004). HIV/AIDS prevalence among South African health workers*. S. Afr. Med. J*. 94(10):846–50.

25. Ndlandla, F. L (2017). Diagnostic antibody biomarkers of tuberculosis characterized by natural and chemically synthetic mycolic acid antigens. PhD thesis, Faculty of Natural and Agricultural Sciences, University or Pretoria.

26. O'Donnell, M.R., Jarand, J., Loveday, M., Padayatchi, N., Zelnick, J., Werner, L., Naidoo, K., Master, I., Osburn, G., Kvasnovsky, C., Shean, K., Pai, M., Van der Walt, M., Horsburgh, C.R., Dheda, K. (2010). High incidence of hospital admissions with multidrug-resistant and extensively drug-resistant tuberculosis among South African health care workers. *Ann. Intern Med*. 153 (8): 516-522.

27. Van den Brande*, P. (2005).* Revised Guidelines for the diagnosis and control of Tuberculosis impact on management in the elderly. *Drugs Aging. 22 (8): 663-686.*

28. Trunz, B.B., Fine, P., Dye, C. (2006). Effect of BCG vaccination on childhood tuberculous meningitis and miliary tuberculosis worldwide: a meta-analysis and assessment of cost-effectiveness. *Lancet*. 367(9517): 1173–80.

29. World Health Organisation. WHO. (2015). Implementing the end TB strategy: the essentials. Geneva: World Health Organization. WHO policy framework.

30. Rabahi, M. F., Silva Júnior, J., Ferreira, A., Tannus-Silva, D., & Conde, M. B. (2017). Tuberculosis treatment. *Jornal brasileiro de pneumologia: publicacao oficial da Sociedade Brasileira de Pneumologia e Tisilogia*, *43*(6), 472–486. doi:10.1590/S1806-37562016000000388

31. Pascual-Pareja, J.F., Carrillo-Gómez, R., Hontañón-Antoñana, V., Martínez-Prieto, M. (2018). Treatment of pulmonary and extrapulmonary tuberculosis. *Enferm Infecc. Microbiol. Clin*. 36:507–516.

32. Caminero Lunaa, J.A. (2016). Update on the diagnosis and treatment of pulmonary tuberculosis. *Revista. Clínica. Española.* 216(2):76-84.

33. Collins S. (2010) HIV, Tuberculosis and Viral Hepatitis. TAG 2010 Pipeline Report: HIV, Tuberculosis, and Viral Hepatitis: Drugs, Diagnostics, Vaccines, Immune-Based Therapies, and Preventive Technologies in Development (Second Edition). New York: I-Base and Treatment Action Group, September 2010.

34. Wood, R. (2007). Challenges of TB diagnosis and treatment in South Africa. *Southern Afr. J. HIV Med*. 27: 44-48

35. Cheon, S.A., Cho, H.H., Kim, J., Lee, J., Kim, H.J., Park, T.J. (2016) Recent tuberculosis diagnosis toward the end TB strategy. *J. Microbiol. Methods. 123*:51-61.

36. Vermaak, Y. (2005). Properties of Anti-Mycolic Acid Antibodies in Human Tuberculosis Patients. MSc dissertation, Faculty of Natural and Agricultural Sciences, University or Pretoria.

37. Steingart, K.R., Henry, M., Ng, V., Hopewell, P.C., Ramsay, A., Cunningham J, Urbanczik, R., Perkins, M., Aziz, M.A., Pai, M. (2006a). Fluorescence versus conventional sputum smear microscopy for tuberculosis. *Lancet Infect. Dis.* 6(10):628.

38. Steingart, K.R., Ng, V., Henry, M., Hopewell, P.C., Ramsay, A., Cunningham, J., Urbanczik, R., Perkins Aziz, M.A., Pai, M. (2006b). Sputum processing methods to improve the sensitivity of smear microscopy for tuberculosis: a systematic review. *Lancet Infect. Dis*. 6: 664-674.

39. Mase, D., Aziz, M.A., Pai, M. (2007). Yield of serial sputum specimen examinations in the diagnosis of pulmonary tuberculosis: a systematic review. *Int. J. Tuberc. Lung Dis.* 10(1): 60-7.

40. American Thoracic Society. (1999). Diagnostic standards and classification of tuberculosis in adult and children, an official statement adopted by the ATS Board of Directors. *Am. J. Respir. Crit. Care Med.* 161: 1376-1395

41. Siddiqi, S. H., Rusch-Gerdes, S. (2006). *MGIT Procedure Manual for BACTEC MGIT 960 TB System*. Foundation for Innovative New Diagnostics.

42. Ogwang, S., Mubiri, P., Bark, C.M., M. Joloba, L.M., Boom, W.H., Johnson, J.H. (2015). Incubation time of Mycobacterium tuberculosis complex sputum cultures in BACTEC MGIT 960: 4weeks of negative culture is enough for physicians to consider alternative diagnoses. *Diagn. Microbiol. Infect. Dis*. 83(2):162–164.

43. Lee, J.-J., Suo, J. Lin, C.B., Wang, J.D., Lin, T.Y., Tsai, Y.C. (2003) Comparative evaluation of the BACTEC MGIT 960 system with solid medium for isolation of mycobacteria. *Int.J. Tuberc. Lung Dis*. 7(6): 569–574.

44. Hanna, B. A., Ebrahimzadeh, A., Elliott L. B., Morgan, M. A., Novak, S.M., Rüsch-Gerdes, S., Acio, M., Dunbar, D.F., Holmes, T.M., Rexer, C.H., Savthyakumar, C.,

Vannier, A.M. (1999). Multicenter evaluation of the BACTEC MGIT 960 system for recovery of mycobacteria. *J. Clin. Microbiol*. 37(3):748–752.

45. Peña, J.A., Ferraro, M.J., Hoffman, C.G., Branda, J. A. (2012). Growth detection failures by the nonradiometric Bactec MGIT 960 mycobacterial culture system. *J. Clin. Microbiol*, 50(6). 2092–2095.

46. Sharma, P., Sharma, K. Singh, D., Verma, S., Mahajan, S., Kanga, A. (2014). "Failure of the MGIT™ 960 culture system in the detection of Mycobacterium tuberculosis. *Int J. Tuberc. Lung D*. 18(12):1525.

47. World Health Organisation. WHO. (2015). Practical considerations. Geneva: World Health Organization; 2015: WHO policy framework.

48. Lighter, J. and Rigaud, M. (2009) Diagnosing childhood tuberculosis: traditional and innovative modalities. *Curr. Probl. Pediatr. Adolesc. Health Care*. 39: 61-88 World Health Organization.

49. Sohn, H., Aero, A.D., Menzies, D. (2014). Xpert MTB/RIF testing in a low tuberculosis incidence, high-resource setting: limitations in accuracy and clinical impact. *Clin. Infect. Dis.* 58:970-976.

50. Maynard-Smith, L., Larke, N., Peters, J.A., Lawn, S.D. (2014). Diagnostic accuracy of the Xpert MTB/RIF assay for extrapulmonary and pulmonary tuberculosis when testing non-respiratory samples: a systematic review. *BMC Infect Dis.* 14:709.

51. WHO (2016). Chest radiography in tuberculosis detection summary of current WHO recommendations and guidance on programmatic approaches. Geneva: World Health Organization; 2016.

52. Nyboe, J. (1968). Results of the international study on x-ray classification. *Bull. Int. Union Tuberc.* 41:115–124.

53. Chaturvedi, N., Cockcroft, A. (1992). Tuberculosis screening in health service employees: who needs chest X-rays? *Occup. Med (Lond).* 42:179-82.

54. Deysel, M.S.M. (2008). Structure-function relationships of mycolic acids in tuberculosis. PhD dissertation, Faculty of Natural and Agricultural Sciences, University of Pretoria.

55. Gomes, M.N. (2007). Mycolic acid as antigen or analyte in tuberculosis. MSc dissertation, Faculty of Natural and Agricultural Sciences, University of Pretoria.

56. WHO. (2009). Global tuberculosis control: epidemiology, strategy, financing. Geneva, World Health Organization.

57. Batz, H.G, Cooke, G.S, Reid,S.D .(2011). Towards lab-free tuberculosis diagnosis. Médecins Sans Frontières/Stop TB partnership TB/HIV Working Group/Treatment Action Group, Geneva/New York.

58. Global Laboratory Initiative (GLI). (2015) Guide for Providing Technical Support to TB Laboratories in Low- and Middle-Income Countries. Geneva: GLI; (a working group of the Stop TB Partnership).

59. Losina, E., Bassett, I.V., Giddy, J., Chetty, S., Regan, S., Walensky, R.P., Ross, D., Scott, C.A., Uhler, L.M., Katz, J.N. (2010). The “ART” of Linkage: Pre-Treatment Loss to Care after HIV Diagnosis at Two PEPFAR Sites in Durban, South Africa. *PLoS One*. 5(3): e9538.

60. Lessells R.J., Mutevedzi, P.C., Cooke, G.S., Newell, M-L. (2011). Retention in HIV Care for Individuals Not Yet Eligible for Antiretroviral Therapy: Rural KwaZulu-Natal, South Africa. *J. Acquir Immune Defic. Syndr.* (3):79-86.

61. Tayler-Smith, K., Zachariah, R., Massaquoi, M., Manzi, M., Pasulani, O., Bemelmans M, (2010). Unacceptable attrition among WHO stages 1 and 2 patients in a hospital-based setting in rural Malawi: can we retain such patients within the general health system? *Trans R. Soc. Trop. Med Hyg*. 104(5):313-319.

62. Aledort, J.E, Ronald, A., Rafael. M.E, Girosi, F., Vickerman, P., Le Blancq, S.M., Landay, A., Holmes, K., Ridzon, R., Hellmann, N., Shea, M.V., Peeling, R.W. (2006). Reducing the burden of sexually transmitted infections in resource-limited settings: the role of improved diagnostics. *Nature*. 444:59–72.

63. Keeler, E., Perkins, M.D., Small, P., Hanson, C., Reed, S., Cunningham, J., Aledort, J.E., Hillborne, L., Rafael, M.E., Girosi, F. (2006). Reducing the global burden of tuberculosis: the contribution of improved diagnostics. *Nature*. 444: 49-57.

64. Urdea, M., Penny. L.A., Olmsted, S.S., Giovanni, M.Y., Kaspar, P., Shepherd, A., Wilson, P., Dahl, C.A., Buchsbaum, S., Moeller, G., Hay Burgess, D.C. (2006). Requirements for high impact diagnostics in the developing world. *Nature*. 444: 73-79.

65. Yager, P., Domingo, G.J., Gerdes, J. (2018). Point-of-care diagnostics for global health. *Annu. Rev. Biomed. Eng*, 10:107-144

66. Garcia-Basteiro, A.L, DiNardo, A. Saavedra, B, Silva, D.R, Palmero, D, Gegia, M, Migliori, G.B, Duarte, R, Mambuque, E, Centis, R, Cuevas, L.E, Izco, S, Theron, G. (2018). Point of care diagnostics for tuberculosis. *Pulmonology*, 24 (2): 73-8585.

67. Pai, N.P., Pai, M. (2012). Point-of-care diagnostics for HIV and tuberculosis: landscape, pipeline, and unmet needs. *Discov. Med*. 13:35–45.

68. Wang, S., Inci, F., De Libero, G., Singhal, A., Demirci, U. (2013). Point-of-care assays for tuberculosis: role of nanotechnology/microfluidics. *Biotechnol. Adv*. 31(4), 438–449.

69. Steingart, K.R., Henry, M., Laal, S., Hopewell, P.C., Ramsay, A., Menzies, D., Cunningham, J., Weldingh, K., Pai, M. (2007) Correction: Commercial Serological Antibody Detection Tests for the Diagnosis of Pulmonary Tuberculosis: A Systematic Review. *PLOS Medicine.* 4(8): e254.

70. Ejoh, V.E. (2014). Requirements for accurate biosensor detection of anti-lipid biomarker antibodies in active TB. MSc dissertation, Faculty of Natural and Agricultural Sciences, University of Pretoria.

71. Daniel, T.M., and Debanne, S.M. (1987). The serodiagnosis of tuberculosis and othermycobacterial diseases by enzyme-linked immunosorbent assay. *Am. Rev. Respi. Dis*. 135(5): 1137 – 1151.

72. Starvi, H., Moldovan, O., Mihaltan, F., Banica, D., and Doyle, R.J. (2003). Rapid dot sputum and serum assay in pulmonary tuberculosis. *J. Microbiol. Methods.* 52: 285 –296.

73. Litman, G.W., Rast, J.P., Shamblott, M.J., Haire, R.N., Hulst, M., Roess, W., Litman, J.T., Hinds-Frey, K.R., Zilch, A., and Amemiyag, C.T (1993). Phylogenetic diversification of immunoglobulin genes and the antibody repertoire. *Mol. Biol. Evol*. 10(1):60-72.

74. Okeke, I.E. (2015). Core elements for “point of care” tuberculosis diagnosis by electrochemical detection of patient antibodies to mycolic acids. MSc dissertation, Faculty of Natural and Agricultural Sciences, University of Pretoria.

75. Druszczynska, M., Wawrocki, S., Szewczyk, R., & Rudnicka, W. (2017). Mycobacteria-derived biomarkers for tuberculosis diagnosis. *Indian J. Med. Res.* 146(6): 700–707.

76. Kunnath-Velayudhan, S., and Gennaro, M.L. (2011). Immunodiagnosis of Tuberculosis: A Dynamic View of Biomarker Discovery. *Clin. Microbiol. Rev*. 24 (4): 792–805.

77. Weiner, J., Kaufmann, S.H.E. (2017). High-throughput and computational approaches for diagnostic and prognostic host tuberculosis biomarkers. *Intl. J. Infect. Dis.* 56, 258-262.

78. Baumeister, C.R (2012). Electrochemical impedance spectroscopy and surface plasmon resonance for diagnostic antibody detection. MSc dissertation. Faculty of Natural and Agricultural Sciences, University of Pretoria.

79. Schleicher, G.K., Feldman, C., Vermaak, Y., Verschoor, J.A. (2002). Prevalence of anti-mycolic acid antibodies in patients with pulmonary tuberculosis coinfected with HIV. *Clin. Chem. Lab. Med*. 40 (9): 882–887.

80. Thanyani, S.T. (2003). A novel application of affinity biosensor technology to detect antibodies to mycolic acids in tuberculosis patients. MSc dissertation, Faculty of Natural and Agricultural Sciences, University of Pretoria.

81. Thanyani, S. T. (2008). An assessment of two evanescent field biosensors in the development of an immunoassay for tuberculosis. PhD thesis, Faculty of Natural and Agricultural Sciences, University of Pretoria.

82. Lemmer, Y., Thanyani, S.T., Vrey, P.J., Driver, C.H.S., Venter, L., van Wyngaardt, S., ten Bokum, A.M.C., Ozoemena, K.I., Pilcher, L.A., Fernig, D.G., Stoltz, A.C., Swai, H.S., Verschoor, J.A., Nejat, D. (2009). Chapter 5 Detection of antimycolic acid antibodies by liposomal biosensors. *Method Enzymol*. Academic Press, 79-104.

83. Mathebula, N.S., Pillay, J., Toschi, G., Verschoor, J.A., Ozoemena, K.I., (2009). Recognition of anti-mycolic acid antibody at self-assembled mycolic acid antigens on a gold electrode: A potential impedimetric immunosensing platform for active tuberculosis. *Chem. Commun.* 23: 3345-3347.

84. Verschoor, J. A., and M. Beukes. (2011). A method of detecting surrogate markers in a serum sample. International Patent Application no. PCT/IB2011/053108 (12 July 2011). Published as “Immunodiagnostic test for tuberculosis”: WO 2012/007903 (19 January 2012).

85. Beukes, M., Lemmer, Y., Deysel, M., Al Dulayymi, J.R., Baird, M.S., Koza, G., Iglesias, M.M., Rowles, R.R., Theunissen, C., Grooten, J., Toschi, G., Roberts, V.V., Van Wyngaardt, S, Mathebula, N., Balogun, M, Stoltz, A.C., Verschoor, J.A. (2010). Structure-function relationships of the antigenicity of mycolic acids in tuberculosis patients. *Chem. Phys. Lipids*. 163:800-808.

86. Ranchod, H.; Ndlandla, F.; Lemmer, Y.; Beukes, M.; Niebuhr, J.; Al Dulayymi, J. R.; Wemmer, S.; Fehrsen, J.; Baird, M. S.; Verschoor, J. A. (2018). The Antigenicity and Cholesteroid Nature of Mycolic Acids Determined by Recombinant Chicken Antibodies. *PLoS One.* 13 (8): e02002984.

87. Jackson, M. (2014). The mycobacterial cell envelope-lipids. *Cold Spring Harb. Perspecs. Med.* 4(10): a021105.

88. Fenton, M. J. and Vermeulen, M.W. (1996). Immunopathology of tuberculosis: Roles of Macrophages and Monocytes. *Infect Immun*. 64: 683-690.

89. Smith J. P. (2011). Nanoparticle delivery of anti-tuberculosis chemotherapy as a potential mediator against drug-resistant tuberculosis. *Yale J. Biol. Med.* 84(4): 361–369.

90. Goren, M.B and Brennan, P.J (1979). Mycobacterial lipids: Chemistry and biologic activities. *Tuberculosis*. 63-193

91. Minnikin, D.E (1982). The biology of the mycobacteria. Physiology, idendification and classification. *Physiology, Identification and Classification Academic Press London*. 1: 95-184.

92. Goodrum, M.A., Siko, D.G., Niehues, T., Eichelbauer, D. and Verschoor, J.A. (2001). Mycolic acids from Mycobacterium tuberculosis: purification by countercurrent distribution and T-cell stimulation. *Microbios*.106: 55-67.

93. Dubnau, E., Chan, J., Raynaud, C., Mohan, V.P., Lanéelle, M.A., Yu K, et al. (2000). Oxygenated mycolic acids are necessary for virulence of Mycobacterium tuberculosis in mice. *Mol. Microbiol*. 36:630–7.

94. Ghazaei, C. (2018). Mycobacterium tuberculosis and lipids: Insights into molecular mechanisms from persistence to virulence. *J. Res. Med. Sci*. 23:63.

95. Collins, F. M. (1994). The immune response to mycobacterial infection—development of new vaccines. *Vet Microbiol*.40: 95-110.

96. Verschoor, J.A. (2001). Method for the isolation and purification of lipid cell-wall components. Patent application no. PCT/GB96/00416 (22 Feburary 1996). Publication no WO 96/26288 (29 August 1996)

97. Ojha, AK., Baughn, A.D., Sambandan, D., Hsu, T., Trivelli, X., Guerardel, Y., Alahari, A., Kremer, L., Jacobs, W.R Jr., Hatfull, G.F. (2008). Growth of *Mycobacterium tuberculosis* biofilms containing free mycolic acids and harbouring drug-tolerant bacteria. *Mol. Microbiol.* 69:164-174.

98. Cantrell, S.A., Leavell, D.M., Marjanovic, O., Iavarone, A.T., Leary, J.A., Riley, L.W., (2013). Free mycolic acid accumulation in the cell wall of the mce1 operon mutant strain of Mycobacterium tuberculosis. *J. Microbiol*. 51: 619–626.

99. Cooper, A.M. (2009) T cells in mycobacterial infection and disease. *Curr Opin Immunol*. 21: 378–384.

100. Pawlowski, A., Jansson. M., Sko¨ld. M., Rottenberg, M.E., Ka¨llenius, G. (2012). Tuberculosis and HIV co-infection. *PLoS Pathog*. 8(2): e1002464.

101. Arloing, S. (1898). Agglutination de bacille de la tuberculose vrate. *C. R. Acad. Sci*. 126:1398-1400.

102. Engvall, E., Perlmann, P. (1972). Enzyme-linked immunosorbent assay, ELISA, III: Quantitation of specific antibodies by enzyme-labeled anti-immunoglobulin in antigen-coated tubes. *J. Immunol*. 109(1):129–135.

103. Tandon, A., Saxena, R. P., Saxena, K. C., Jamil, Z., Gupta, A. K. (1980). Diagnostic potentialities of enzyme-linked immunosorbent assay in tuberculosis using purified tuberculin antigen. *Tubercle*. 61(2):87-9.

104. Zeiss, C. R., Kalish, S. B., Erlich, K. S., Levitz, D., Metzge,r E., Radin, R., Phair, J. P. (1984). IgG antibody to purified protein derivative by enzyme-linked immunosorbent assay in the diagnosis of pulmonary tuberculosis. *Am. Rev. Respir. Dis*. 130(5):845-8.

105. Chiang, H., Suo, J., Bia, K.-J., Lin, T.-P. (1997). Serodiagnosis of tuberculosis. A study comparing three specific mycobacterial antigens. *Am. J. Respir. Crit. Care Med*. 6:906–911.

106. Hunter, S.W., Gaylord, H & Brennan, P.J. (1986) Structure and antigenicity of the phosphorylated lipopolysaccharide antigens from the leprosy and tubercle bacilli. *J. Biol. Chem*. 261:12345–12351.

107. Levis, W.R., Meeker, H.C., Schuller-Levis, G., Sersen, E., Brennan P.J & Fried, P. (1987) Mycobacterial carbohydrate antigens for serological testing of patients with leprosy. *J. Infect. Dis*.156: 763–769.

108. Sada, E., Brennan, P.J., Herrera, T., Torres, M. (1990). Evaluation of lipoarabinomannan for the serological diagnosis of tuberculosis. *J. Clin. Microbiol*. 28: 2587–2590.

109. Verma, R.J., Jain, A. (2007). Retracted: Antibodies to mycobacterial antigens for diagnosis of tuberculosis. *FEMS Immunol. Med. Microbiol*. 51(3):453–461.

110. Boggian, K., Fierz, W., Vernazza, P.L. (1996). Infrequent detection of lipoarabinomannan antibodies in human immunodeficiency virus-associated mycobacterial disease. Swiss HIV Cohort Study. *J. Clin. Microbiol*. 34: 1854–1855.

111. Julian, E., Matas, L., Ausina, V., Luquin, M. (1997). Detection of lipoarabinomannan antibodies in patients with newly acquired tuberculosis and patients with relapse tuberculosis. *J. Clin. Microbiol*. 35: 2663–2664.

112. Lawn, S.D., Frimpong, E.H., Nyarko, E. (1997). Evaluation of a commercial immunodiagnostic kit incorporating lipoarabinomannan in the serodiagnosis of pulmonary tuberculosis in Ghana. *Trop. Med. Int. Health*. 2: 978–981.

113. Del Prete, R., Picca, V., Mosca, A., D'Alagni, M., Miragliotta, G. (1998). Detection of anti-lipoarabinomannan antibodies for the diagnosis of active tuberculosis. *Int. J. Tuberc. Lung Dis*. 2: 160–163.

114. Somi, G.R., O'Brien, R.J., Mfinanga, G.S., Ipuge, Y.A., (1999). Evaluation of the MycoDot test in patients with suspected tuberculosis in a field setting in Tanzania. *Int. J. Tuberc. Lung Dis*. 3: 231–238.

115. Munoz, M., Laneelle, M., Luquin, M., Torrelles, J.E., Ausina, V., Daffe, M., (1997). Occurrence of an antigenic triacyl trehalose in clinical isolates and reference strains of Mycobacterium tuberculosis, *FEMS Microbiol. Let*. 157(2):251-259.

116. Bisen, P.S., & Prasad, G.B.K.S., Nitesh, J., Dubey, R., Zacharia, A., Tiwari, R.P. (2010). Liposomes in diagnosis of tuberculosis. *J. Adv. Med Biomed Res.*381-40.

117. Tiwari, R.P., Garg S.K., Bharmal, R.N., Kartikeyan, S., Bisen, P.S. (2007). Rapid liposomal agglutination card test for the detection of antigens in patients with active tuberculosis, *J. Tuberc. Lung Dis*. 10(11): 1143–1151.

118. Stodola, F. H., Lesuk, A., Anderson, R.J. (1938). The chemistry of the lipids of tubercle bacilli. *J. Biol. Chem*. 54: 505-513.

119. Brennan, P. J. (1995). "The envelope of mycobacteria." *Annu. Rev. Biochem.* 64: 29-63.

120. Asselineau, J. and E, Lederer. (1950). Structure of the mycolic acids of mycobacteria. *Nature*. 166: 782-3.

121. The Merck Index, 1989. Editors: S. Budavari, M. J. O'Neil, A. Smith and P. E. Heckelman, Eleventh Edition, p 6236.

122. Fujiwara, N., Pan, J., Enomoto, K., Terano, Y., Honda, T. and Yano, I. (1999). Production and partial characterization of anti-cord factor (trehalose-6,6P-dimycolate) IgG antibody in rabbits recognizing mycolic acid subclasses of Mycobacterium tuberculosis or *Mycobacterium avium*. *FEMS Immunol. Med Microbiol*. 24: 141-149.

123. Ndlandla, F., Ejoh, V., Stoltz, A., Naicker, B., Cromarty, A., van Wyngaardt, S.; Khti, M., Rotherham, L., Lemmer, Y., Niebuhr, J., Baumeister, C., Al Dulayymi, J.R., Swai, H., Baird, M.S., Verschoor, J.A. (2016). Standardization of natural mycolic acid antigen composition and production for use in biomarker antibody detection to diagnose active tuberculosis. *J. Immunol. Methods*. 435: 50–59.

124. Verschoor, J., Baird, M., & Grooten, J. (2012). Towards understanding the functional diversity of cell wall mycolic acids of *Mycobacterium tuberculosis*. *Prog. Lipid Res*. 51: 325-39.

125. Watanabe, M., Aoyagi, Y., Ridell, M., and Minniken, D. E. (2001). Separation and characterization of Individual mycolic acids in representative mycobacteria. *Microbiology*. 147: 1825–1837.

126. Watanabe, M., Aoyagi, Y., Mitome, H., Fujita, T., Naoki, H., Ridell, M., and Minniken D. E. (2002). Location of functional groups in mycobacterial

meromycolate chains; the recognition of new structural principles in mycolic acids. *Microbiology*. 148: 1881–1902.

127. Glickman, M.S., Cox, J., S., Jacobs, W. R. Jr. (2000). A Novel Mycolic Acid Cyclopropane Synthetase Is Required for Cording, Persistence, and Virulence of Mycobacterium tuberculosis. *Mol. cell*. 5:717-727.

128. De Libero, G., Mori, L. (2005). Recognition of lipid antigens by T cells. *Nat. Rev. Immunol.* 5: 485-496.

129. Chan, C.E., Zhao, B.Z., Cazenave-Gassiot, A., Pang, S., Bendt, A.K., Wenk, M.R., MacAry, P.A., Hanson, B.J. (2013). Novel phage display-derived mycolic acid-specific antibodies with potential for tuberculosis diagnosis. *J. Lipid. Res.* 4:2924.

130. Lemmer, Y., Thanyani, S.T., Vrey, P., Driver, C.H., van Wyngaardt, S., ten Bokum, A.M., Ozoemena, K.I., Pilcher, L.A., Fernig, D.G., Stoltz, AC., Swai, H.S. and Verschoor, J.A. (2009). Chapter 5 – Detection of antimycolic acid antibodies by liposomal biosensors. *Method Enzymol.* 64: 79-104.

131. Baumeister, C.R (2012). Electrochemical impedance spectroscopy and surface plasmon resonance for diagnostic antibody detection. MSc dissertation. Faculty of Natural and Agricultural Sciences, University of Pretoria.

132. Butler, W.R. (1985). Reverse phase High performance liquid chromatography separation of mycolic acids as para – bromophencyl esters as an acid in mycobacterial classification. MSc Dissertation. Georgia state University.

133. Glick, D. (1962). Methods of biochemical analysis. *Interscience, New York*. 9: 139.

134. Siko, D.G.R. (1999). The effects of mycobacterial mycolic acids on rodent tuberculosis and adjuvant arthritis. MSc Dissertation. Faculty of Natural and Agricultural Sciences, University of Pretoria.

135. Goodruam, M.A. (1998). Mycolic acid antigens in tuberculosis. MSc thesis, Faculty of Natural and Agricultural Sciences, University or Pretoria.

136. Beckman, E. M., Porcelli, S. A., Morita, C. T., Behar, S. M., Furlong, S. T., Brenner, M. B. (1994). Recognition of a Lipid Antigen by CD1-Restricted (Alpha)(Beta)(Positive) T Cells. *Nature*. 372 (6507):691–694.

137. F. Poole, C. & Poole, S. K. (1994). Instrumental thin-layer chromatography. *Analytical Chemistry*. 66, 27A-37A.

138. Benadie, Y., Deysel, M., Siko, D.G. (2008). Cholesteroid nature of free mycolic acids from M. tuberculosis. *Chem. Phys. Lipids* 152:95–103.

139. Alving, C.R., Wassef, N.M. (1999). Naturally occurring antibodies to cholesterol: a new theory of LDL cholesterol metabolism. *Immunol. Today.* 20:362-66.

140. Ranchod, H. (2018). Novel Recombinant Anti-Mycolic Acid Immunoglobulin Tools for Improved Understanding and Management of Tuberculosis. PhD thesis, Faculty of Natural and Agricultural Sciences, University of Pretoria.

141. Füst G, Beck Z, Bánhegyi D, Kocsis J, Bíró A, Prohászka Z. (2005) Antibodies against heat shock proteins and cholesterol in HIV infection. *Mol. Immunol*. 42:79–85.

142. Sekanka, G., Baird, M., Minnikin, D., Grooten, J. (2007). "Mycolic acids for the control of tuberculosis." *Expert Opin. Ther. Patents*. 17:315-331.

143. Villeneuve, M., Kawaia, M., Watanabe, M., Aoyagi, Y., Hitotsuyanagi, Y., Takeya, K., Gouda, H., Hirono, S., Minnikin, D. E., Nakaharaa, H. (2007). " Conformational behavior of oxygenated mycobacterial mycolic acids from Mycobacterium bovis BCG." *Biochim. Biophys. Acta*. 1768:1717-1726.

144. Groenewald, W., Baird, M.S., Verschoor, J.A., Minnikin, D.E., Croft, A.K. (2014) Differential spontaneous folding of mycolic acids from *Mycobacterium tuberculosis*. *Chem. Phys. Lipids*. 180:15-22.

145. Chan, C. E.; Zhao, B. Z.; Cazenave-Gassiot, A.; Pang, S.-W.; Bendt, A. K.; Wenk, M. R.; MacAry, P. A.; Hanson, B. J. (2013). Novel Phage Display-Derived Mycolic Acid-Specific Antibodies with Potential for Tuberculosis Diagnosis. *J. Lipid Res*. 54 (10), 2924–2932.

146. Engvall, E., and P. Perlmann. (1971). Enzyme-linked immunosorbent assay (ELISA) quantitative assay of immunoglobulin G. *Immunochemistry.* 8: 871-874.

147. Truyts, A. (2019). Towards paper-based micro bio-sensing of biomarker anti-mycolic acid antibodies for TB diagnosis. MSc dissertation, Faculty of Natural and Agricultural Sciences, University of Pretoria.

148. Jung, S., Honegger, A., Pluckthun, A. (1999). Selection for improved protein stability by phage display. *J. Mol. Biol*. 294: 163–180

149. Wemmer, S. (2008). Expression and engineering of recombinant antibodies against heat shock protein of *Mycobacterium bovis*. Veterinary Science. Pretoria, University of Pretoria. MSc.

150. Greunke K, Spillner E, Braren I, Seismann H, Kainz S, Hahn U, et al. (2006). Bivalent monoclonal IgY antibody formats by conversion of recombinant antibody fragments*. J. Biotechnol*. 124: 446–456.

151. Porcelli, S.A., Modlin, R.L. (1999). The CD1 system: Ag-presenting molecules for T cell recognition of lipids and glycolipids. *Ann. Rev. Immunol*. 17:297-329.

152. Liang, M., Klakamp, S.L., Funelas, C., Lu, H., Lam, B., Herl, C., Umble, A., Drake, A.W., Pak, M. Ageyeva, N., Pasumarthi, R., Roskos, L.K. (2007). Detection

of highand low-affinity antibodies against a human monoclonal antibody using various technology platforms. *Assay Drug Dev. Techn.* 5:655-662.

153. Thanyani, S. T., V. Roberts, D. G. Siko, P. Vrey, and J. A. Verschoor. (2008). A novel application of affinity biosensor technology to detect antibodies to mycolic acid in tuberculosis patients. *J. Immunol. Methods*. 332: 61-72.

154. Verschoor, J. A., and C. R. Baumeister. (2013). A method of diagnosing tuberculosis. Provisional SA patent application. International patent application no. PCT/IB2014/061468.

155. Verschoor, J. A., I. E. Okeke, L. Kalombo, and Y. Lemmer. (2016). Core elements for point of care TB diagnosis. International patent application no. PCT/IB2016/056643.

156. Verschoor, J.A., Siko, D.G.R. & Van Wyngaardt, S. (2005). A serodiagnostic method to detect antibodies to mycolic acid in tuberculosis patients as surrogate markers for infection. International patent application no. PCT/IB2005/051548.

157. Jones, A., M. Pitts, J. R. Al Dulayymi, J. Gibbons, A. Ramsay, D. Goletti, C. D. Gwenin, and M. S. Baird. (2017). New synthetic lipid antigens for rapid serological diagnosis of tuberculosis. *PloS One*. 12: e0181414.

158. Deidda, M., Piras, C., Bassareo, P. P., Cadeddu Dessalvi, C. & Mercuro, G (2015). Metabolomics, a promising approach to translational research in cardiology. *IJC Metabolic and Endocrine.* 9: 31–38.

159. Ozoemena, K., Mathebula, N.S., Jeseelan, P., Toschi, G., Verschoor, J.A. (2010). Electron transfer dynamics across self-assembled N-(2-mercaptoethyl) octadecanamide/mycolic acid layers: impedimetric insights into the structural integrity and interaction with anti-mycolic acid antibodies. *Phys. Chem. Chem. Phys*. 12: 345-357.

160. Peeling, R.W.; Mabey, D. (2010). Point-of-care tests for diagnosing infections in the developing world. *Clin. Microbiol. Infect.* 16: 1062–1069.

161. Sharma, S., Zapatero-Rodríguez, J., Estrela, P., O'Kennedy, R. (2015). Point-of-Care Diagnostics in Low Resource Settings: Present Status and Future Role of Microfluidics. *Biosensors* 5:577–601.

162. Gandham, P. (2015). POCT Tests - would they Meet the Goal of the Clinical Microbiology Laboratories? *Int. J. Curr. Microbiol. App. Sci*. 4(5): 508-524.

163. Singer, J.M., Plotz, C.M. (1956). The latex fixation test: I. Application to the serologic diagnosis of rheumatoid arthritis. *Am. J. Med.* 21: 888–892.

164. Connolly, R., Kennedy, R.O. (2017). Magnetic lateral flow immunoassay test strip development – Considerations for proof of concept evaluation. *Methods*. 116: 132-140.

165. Gubula V., Harris L.F., Ricco A.J., Tan M.X., Williams D.E. (2012). Point of care diagnostics: Status and future. *Anal. Chem*. 84:487–515.

166. St John, A., Price, C.P. (2014). Existing and emerging technologies for point-of-care testing. *Clin. Biochem. Rev*. 35 (3): 155–167.

167. Batz, H.G., Cooke, G.S., Reid, S.D. (2011). Towards lab-free tuberculosis diagnosis. Médecins Sans Frontières/Stop TB partnership TB/HIV Working Group/Treatment Action Group, Geneva/New York.

168. World Health Organization on behalf of the Special Program for Research and Training in Tropical Diseases. (2008). Laboratory-based evaluation of 19 commercially available rapid diagnostic tests for tuberculosis. Geneva, Switzerland. World Health Organization.

169. Koczula, K.M., Gallotta, A. (2016). Lateral flow assays. *Essays Biochem*. 60: 111–120.

170. Zhang, X., Wu, C., Wen, K., Jiang, H., Shen, J., Zhang, J., Wang, Z. (2015). Comparison of fluorescent microspheres and colloidal gold as labels in lateral flow immunochromatographic assays for the detection of T-2 toxin. *Molecules*. 21 (1): 27.

171. Mirasoli M., Buragina A., Dolci L.S., Guardigli M., Simoni P., Montoya A., et al. (2012). Development of a chemiluminescence-based quantitative lateral flow immunoassay for on-field detection of 2,4,6-trinitrotoluene. *Anal. Chim. Acta*. 721:167–172.

172. Yan, J., Liu, Y.Y., Wang, Y.L., Xu, X.W., Lu, Y., Pan, Y.J., Guo, F.F., Shi, D.L. (2014). Effect of Physiochemical Property of Fe_3O_4 Particle on Magnetic Lateral Flow Immunochromatographic Assay. *Sensor Actuators. B. Chem*. 197: 129–136.

173. Wang, Z., Zhi, D., Zhao, Y., Zhang, H., Wang, X., Ru, Y., Li, H. (2014). Lateral flow test strip based on colloidal selenium immunoassay for rapid detection of melamine in milk, milk powder, and animal feed. *Int. J. Nanomedicine.* 9: 1699-707.

174. Sajid M., Kawde A.-N., Daud M. (2015). Designs, formats and applications of lateral flow assay: A literature review. *J. Saudi Chem. Soc*. 19 (6): 689-705.

175. Anfossi, L., Di Nardo, F., Cavalera, S., Giovannoli, C., Baggiani, C. (2019). Multiplex Lateral Flow Immunoassay: An Overview of Strategies towards High-throughput Point-of-Need Testing. *Biosensors*. *9*: 2.

176. O'Farrell, B. (2015). Lateral Flow Technology for Field-Based Applications--Basics and Advanced Developments. *Top Companion Anim. Med*. *30*(4): 139.

177. Chen W., Huang Z., Hu S., Peng J., Liu D., Xiong Y., Xu H., Wei, H., Lai W. (2019). Invited review: Advancements in lateral flow immunoassays for screening hazardous substances in milk and milk powder. *J. Dairy Sci*. 102(3): 1887-1900.

178. Hu, J., Wang, S.Q., Wang, L., Li, F., Pingguan-Murphy, B., Lu, T.J., Xu, F. (2014). Advances in paper-based point-of-care diagnostics. *Biosens. Bioelectron*. 54: 585-597.

179. Yang, Q., Gong, X., Song, T., Yang, J., Zhu, S., Li, Y., Cui, Y., Li, Y., Zhang, B., Chang, J. (2011). Quantum dot-based immunochromatography test strip for rapid, quantitative and sensitive detection of alpha fetoprotein. *Biosens. Bioelectron*. 30:145–150.

180. Kozel, T.R., Burnham-Marusich, A.R. (2017). Point-of-care testing for infectious diseases: past, present, and future. *J. Clin. Microbiol*. 55:2313–2320.

181. Centers for Medicare and Medicaid Services. (2019). Tests waived granted status under CLIA. Centers for Medicare and Medicaid Services. U.S. Department of Health & Human Services. Baltimore, MD. https://www.cms.gov/Regulations-and-Guidance/Legislation/CLIA/ Downloads/waivetbl.pdf. (Accessed 09 November 2019).

182. World Health Organisation. WHO. (2015). HIV Assays: Laboratory Performance and Other Operational Characteristics: Rapid Diagnostic Tests (Combined Detection of HIV-1/2 Antibodies and Discriminatory Detection of HIV-1 and HIV-2 Antibodies). Geneva, Switzerland. World Health Organization.

183. Wu, G., Zaman, M. H. (2012). Low-Cost Tools for Diagnosing and Monitoring HIV Infection in Low-Resource Settings. *Bull. World Health Organ.*90 (12): 914–920.

184. World Health Organization. WHO. (2014). High-priority target product profiles for new tuberculosis diagnostics: report of a consensus meeting. 28-29 April 2014. Geneva, Switzerland. World Health Organization.

185. Dheda, K., V. Davids, L. Lenders, T. Roberts, R. Meldau, *et al*. (2010). Clinical utility of a commercial LAM-ELISA assay for TB diagnosis in HIV-infected patients using urine and sputum samples. *PloS One.* 5: e9848.

186. World Health Organisation. WHO. (2011). Commercial Serodiagnostic Tests for Diagnosis of Tuberculosis: Policy Statement. Geneva, Switzerland. World Health Organisation

187. Steingart, K.R., Ramsay, A., Dowdy, D.W., et al. (2012). Serological tests for the diagnosis of active tuberculosis: relevance for India. *Indian J. Med. Res*. 135:695-702.

188. Manga, S., Perales, R., Reaño, M., D'Ambrosio, L., Migliori, G., Amicosante, M. (2016). Performance of a lateral flow immunochromatography test for the rapid diagnosis of active tuberculosis in a large multicentre study in areas with different clinical settings and tuberculosis exposure levels. *J. Thorac.v Dis*. (11): 3307-3313.

189. Okuda, Y., Maekura, R., Hirotani, A., Kitada, S., Yoshimura, K., Hiraga, T., Yamamoto, Y., Itou, M., Ogura, T., Ogihara, T. (2004). Rapid Serodiagnosis of Active Pulmonary Mycobacterium Tuberculosis by Analysis of Results from Multiple Antigen-Specific Tests. *J. Clin. Microbiol. 42* (3):1136–1141.

190. Verschoor, J.A., Siko, D.G.R., Van Wyngaardt, S. (2005). Method for the detecting mycobacterial infection, International patent application no. PCT/B2OOS/OS 1548 (6 August 2007). Publication no. WO2005/116654 (8 December 2005)

191. Wong, R., Tse, H. Lateral flow immunoassay. New York: Humana Press; 2009.

192. Hsieh, H., Dantzler, J., Bernhard Weigl. (2017). Analytical Tools to Improve Optimization Procedures for Lateral Flow Assays. *Diagnostics. 7* (2): 29.

193. BIODOT. BIODOT AD6000 System Operating Manual Version 1.2. BIODOT September 2007.

194. Lee, J.-Y.; Kim, Y. A.; Kim, M. Y.; Lee, Y. T.; Hammock, B. D.; Lee, H.-S. (2012). Importance of Membrane Selection in the Development of Immunochromatographic Assays for Low-Molecular Weight Compounds. *Anal. Chim. Acta. 757*, 69–74

195. Lin, P.L., Flynn, J.L. (2010). Understanding latent tuberculosis: a moving target. *J. Immunol*. 185(1):15–22.

196. Burbelo, P.D., Keller, J., Wagner, J. *et al.* (2015). Serological diagnosis of pulmonary *Mycobacterium tuberculosis* infection by LIPS using a multiple antigen mixture. *BMC Microbiol*. 15: 205.

197. Drain, P.K., Heichman, K.A., Wilson, D. (2019). A new point-of-care test to diagnose tuberculosis. *Lancet Infect Dis. 19(8): 794-795*

198. Dunn JJ, Starke JR, Revell PA. (2016). Laboratory Diagnosis of Mycobacterium tuberculosis Infection and Disease in Children. *J. Clin. Microbiol*. 54(6):1434–1441.

199. Molatseli, M. (2020). Anti-mycolic acid gallibodies as labelling tools in tuberculosis related biological samples. MSc dissertation. Faculty of Natural and Agricultural Sciences, University of Pretoria.